UNIVERSITY OF LONDON THESIS

Degree *P h D*   Year *2006*   Name of Author *KA SHOFER*
Karl

COPYRIGHT

This is a thesis accepted for a Higher Degree of the University of London. It is an unpublished typescript and the copyright is held by the author. All persons consulting the thesis must read and abide by the Copyright Declaration below.

COPYRIGHT DECLARATION

I recognise that the copyright of the above-described thesis rests with the author and that no quotation from it or information derived from it may be published without the prior written consent of the author.

LOANS

Theses may not be lent to individuals, but the Senate House Library may lend a copy to approved libraries within the United Kingdom, for consultation solely on the premises of those libraries. Application should be made to: Inter-Library Loans, Senate House Library, Senate House, Malet Street, London WC1E 7HU.

REPRODUCTION

University of London theses may not be reproduced without explicit written permission from the Senate House Library. Enquiries should be addressed to the Theses Section of the Library. Regulations concerning reproduction vary according to the date of acceptance of the thesis and are listed below as guidelines.

A.   Before 1962. Permission granted only upon the prior written consent of the author. (The Senate House Library will provide addresses where possible).

B.   1962 - 1974.   In many cases the author has agreed to permit copying upon completion of a Copyright Declaration.

C.   1975 - 1988.   Most theses may be copied upon completion of a Copyright Declaration.

D.   1989 onwards. Most theses may be copied.

This thesis comes within category D.

☐   This copy has been deposited in the Library of ___ UCL ___

☐   This copy has been deposited in the Senate House Library, Senate House, Malet Street, London WC1E 7HU.

Developmental potential of human haematopoietic stem cells in the NOD/Scid xenotransplantation model

Karl Kashofer

A thesis submitted for the degree of

Doctor of Philosophy

2006

Institute of Immunology and Molecular Pathology

University College London

Haematopoietic Stem Cell Laboratory

Cancer Research UK

UMI Number: U592948

UMI U592948

ProQuest LLC
789 East Eisenhower Parkway
P.O. Box 1346
Ann Arbor, MI 48106-1346

Abstract

Early reports indicated cell engraftment from bone marrow transplants into non-hematopoietic tissues in mouse to mouse and in human allogeneic bone marrow transplants. To investigate the developmental potential of human stem cells I used xenotransplantation of stem cells purified from cord blood into a mouse model. Human stem cells introduced into the NOD/Scid mouse after partial myeloablation repopulate the bone marrow and contribute to the hematopoietic system of the mouse. Engraftment into the bone marrow was measured by FACS and human genetic material was found in the spleen, skin, lung and liver. Engraftment in the liver was studied with a variety of methods, ranging from PCR based assays to FISH analysis and immunohistochemistry. To allow better identification of human cells transduction with a lentivirus carrying the GFP gene was used. Liver damage has been suggested as one of the factors influencing homing of stem cells to the liver and transdifferentiation of bone marrow cells into hepatocytes. To assess the role of tissue damage a model of severe liver injury induced by CCl_4 was utilised. Two stages of damage might be important in this context, damage during the process of homing, and damage during transdifferentiation both of which were studied.

I demonstrate that stem cell homing to the liver is significantly increased upon liver injury. Human albumin and α-anti-trypsin messenger RNA is expressed in the livers of some animals by RT-PCR and large GFP positive hepatocytes and hepatocytes staining with HepPar-1, thought to be specific for human hepatocytes, are present.

However, transdifferentiation defined as the emergence of mature human hepatocytes after bone marrow transplantation could not be found. A variety of methods used to determine the genetic identity in GFP positive hepatocytes only identified remnants of the human genome. In addition to small amounts of human DNA the murine Y chromosome and the murine $TNF\alpha$ locus were readily detected in these hepatocytes.

I conclude that transdifferentiation of human stem cells to a mature hepatocyte phenotype does not occur in the NOD/Scid model of bone marrow transplantation even after severe CCl_4 induced liver damage. Instead human cells most probably of haematopoietic origin fuse with resident hepatocytes to give rise to mixed heterokaryons expressing some, but not all markers of human hepatocytes. To achieve true transdifferentiation a different, more chronic type of tissue damage, or a better defined stem cell population might be required.

Publications

Kashofer, K., E. K. Siapati, D. Bonnet (2005). "*In vivo* formation of unstable heterokaryons following liver damage and HSC/Progenitor transplantation."
Stem Cells 2005 Nov 10; [Epub ahead of print]

Kashofer, K. and D. Bonnet (2005). "Gene therapy progress and prospects: stem cell plasticity." Gene Ther 12(16): 1229-34.

E.K. Siapati, B.W. Bigger, K. Kashofer, M. Themis, A.J. Thrasher and D. Bonnet "Leukaemia formation after lentivirus gene therapy in hematopoietic stem cells is not due to vector insertional mutagenesis" Submitted to Gene Therapy

Acknowledgements

I would like to thank my supervisor Dominique Bonnet for her continuing support and encouragement throughout the four years of this study. I also want to thank my colleagues, Daniel Pearce, David Taussig, Chris Ridler, Elena Siapati and Fernando Afonso for the good working relationship and joyful environment in the lab. I want to thank Cancer Research UK for funding this study and express my gratitude to the multitude of service labs and supporting staff at CRUK. I also want to thank David Tosh and Huseyin Mehmet for being my PhD examiners.

At last I want to thank my family, especially my parents, for having faith in me and supporting me until this very day.

Table of Contents

List of Figures

List of Tables

Index of abbreviations

AAF	acetaminofluorene
AGM	aorta-gonad-mesonephros
BM	bone marrow
BMDC	bone marrow derived cells
BMP	bone morphogenetic protein
BrDU	Bromo-Deoxy-Uridine
CCl₄	Carbon-Tetra-Chloride
CFC	colony forming cell
CFU	colony forming unit
CRUK	cancer research UK
DMEM	dulbeccos modified eagles medium
DNA	deoxyribonucleic acid
E-LTC-IC	extended long term culture initiating cell
ES-cell	embryonic stem cell
FACS	fluorescence activated cell sorting
FAH	fumarat acetoacetate hydrolase
FCS	fetal calf serum
FGF	fibroblast growth factor
FISH	fluorescent in situ hybridisation
G-CSF	granulocyte colony stimulating factor
GFP	green fluorescence protein
HSA	hepatocyte specific antigen
HSC	haematopoietic stem cell
LDL	low density lipoprotein
LTC-IC	long term culture initiating cell
MAPC	multipotent adult progenitor cell
mRNA	messenger ribonucleic acid
MSC	mesenchymal stem cell
NBF	neutral buffered formalin
NK	natural killer
NOD	non obese diabetic

PCR	polymerase chain reaction
PEI	polyethylenimine
PH	partial hepatectomy
RT-PCR	reverse transcription polymerase chain reaction
Scid	severe combined immunodeficiency
SP	side population
TA	tibialis anterior
TNF	tumour necrosis factor
uPA	urokinase plasminogen activator

Introduction

The haematopoietic system

Overview

The haematopoietic system produces all cells of the blood lineage. To compensate for the finite lifespan of mature haematopoietic cells a constant replenishment of dying cells is necessary. The turnover of cells in the haematopoietic system in a human weighing 70 kg can be estimated to be close to 1 trillion cells per day, including 200 billion erythrocytes and 70 billion neutrophilic leukocytes. This remarkable cell renewal process is supported by a small population of bone marrow cells termed haematopoietic stem cells

Bone marrow is derived from the mesoderm (Zon 1995) and consists of a haematopoietic cellular component supported by a microenvironment composed of stromal cells embedded in a complex extracellular matrix. Two distinct but co-existing populations of stem cells have been identified in the bone marrow, the haematopoietic stem cell (HSC), and the mesenchymal stem cell (MSC).

Haematopoietic Stem Cells

The haematopoietic stem cell (HSC) is the only stem cell routinely used in the clinic. Through the successful use of HSC in bone marrow transplantation it became the most widely studied human stem cell population. As depicted in Figure 1 the HSC is the prototype of a lineage specific multipotent stem cell with well defined source and differentiation potential. The HSC is able to self renew, and to give rise to differentiated progenitors of the lymphoid and myeloid lineage. The lymphoid progenitor gives rise to B, T and NK cells whereas the myeloid lineage provides erythrocytes and platelets from the CFU-E/Mega, and monocytes, neutrophiles, eosinophiles and basophiles from the CFU-G/M. (Figure 1) HSC can be identified based on surface markers and self-renewal capacity. The HSC activity in bone marrow is contained within the lineage negative c-Kit+/Sca-1+ population (Uchida *et al.* 1992). When this subset of cells from the bone marrow was injected into lethally irradiated mice it gave rise to long-term multi-lineage engraftment (Smith *et al.* 1991). The characterization of human haematopoietic stem

cells was traditionally done *in vitro* due to the lack of a suitable experimental system and host organism. Much progress has been made after the introduction of the NOD/Scid mouse model (Larochelle *et al.* 1996) where the severe combined immunodeficiency gene was introduced into mice of the non obese diabetic strain giving rise to a severely immunocompromised mouse model capable of reliably engrafting human cells. Using this model it could be shown that HSC reside in the CD34$^+$ (Larochelle *et al.* 1996; Bhatia *et al.* 1997) and CD34$^-$(Bhatia *et al.* 1998) fraction of human bone marrow.
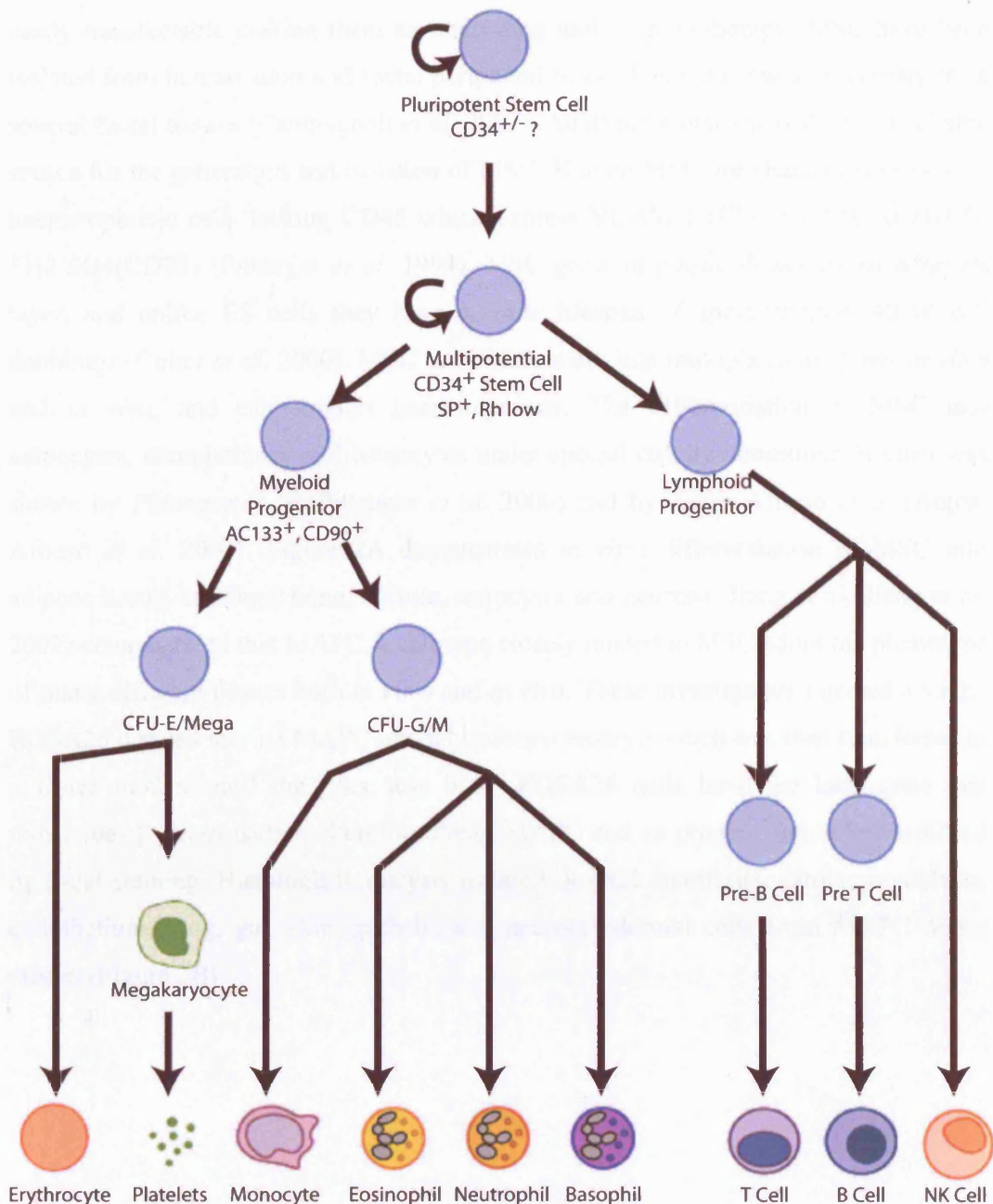
Figure 1 Schematic representation of human haematopoiesis

Mesenchymal stem cells

Mesenchymal stem cells (MSC) are clonogenic stromal cells of bone marrow origin and were first described by Friedenstein *et al* (Friedenstein *et al.* 1974). The inability to sustain and expand haematopoietic stem cells, and the ethical issues hampering the use of embryonic stem cells have created great interest in mesenchymal stem cells. MSC have the ability to self renew and differentiate into multiple tissue lineages. They are

easily transfectable making them an interesting tool in gene therapy. MSC have been isolated from human adult and foetal peripheral blood, bone marrow and recently from several foetal tissues (Campagnoli *et al.* 2001). Adult bone marrow is the most reliable source for the generation and isolation of MSC. Human MSC are characterised as non-haematopoietic cells lacking CD45 which express VCAM-1 (CD106), SH2 (CD105), SH3/SH4(CD73) (Pittenger *et al.* 1999). MSC grow in plastic dishes as an adherent layer, and unlike ES cells they have a finite lifespan of approximately 40-50 cell doublings (Colter *et al.* 2000). MSC can differentiate into multiple tissue types *in vitro* and *in vivo*, and can support haematopoiesis. The differentiation of MSC into adipocytes, chondrocytes and osteocytes under special culture conditions *in vitro* was shown by Pittenger *et al* (Pittenger *et al.* 2000) and by Anjos-Afonso *et al* (Anjos-Afonso *et al.* 2004). Figure 2A demonstrates *in vitro* differentiation of MSC into adipose tissue, cartilage, bone, muscle, astrocytes and neurons. Jiang *et al* (Jiang *et al.* 2002) demonstrated that MAPC, a cell type closely related to MSC adopt the phenotype of many different tissues both *in vitro* and *in vivo*. These investigators injected a single ROSA26 derived murine MAPC into a blastocyst embryo which was then transferred to a foster mother until the litter was born. ROSA26 cells have the lacZ gene that transcribes β-galactosidase, therefore donor MAPC and its progeny could be identified by β-gal staining. Histological analysis isolated skeletal myoblasts, cardiac myoblasts, endothelium, lung, gut, skin epithelia and neuroectodermal cells from MAPC donor origin. (Figure 2B)
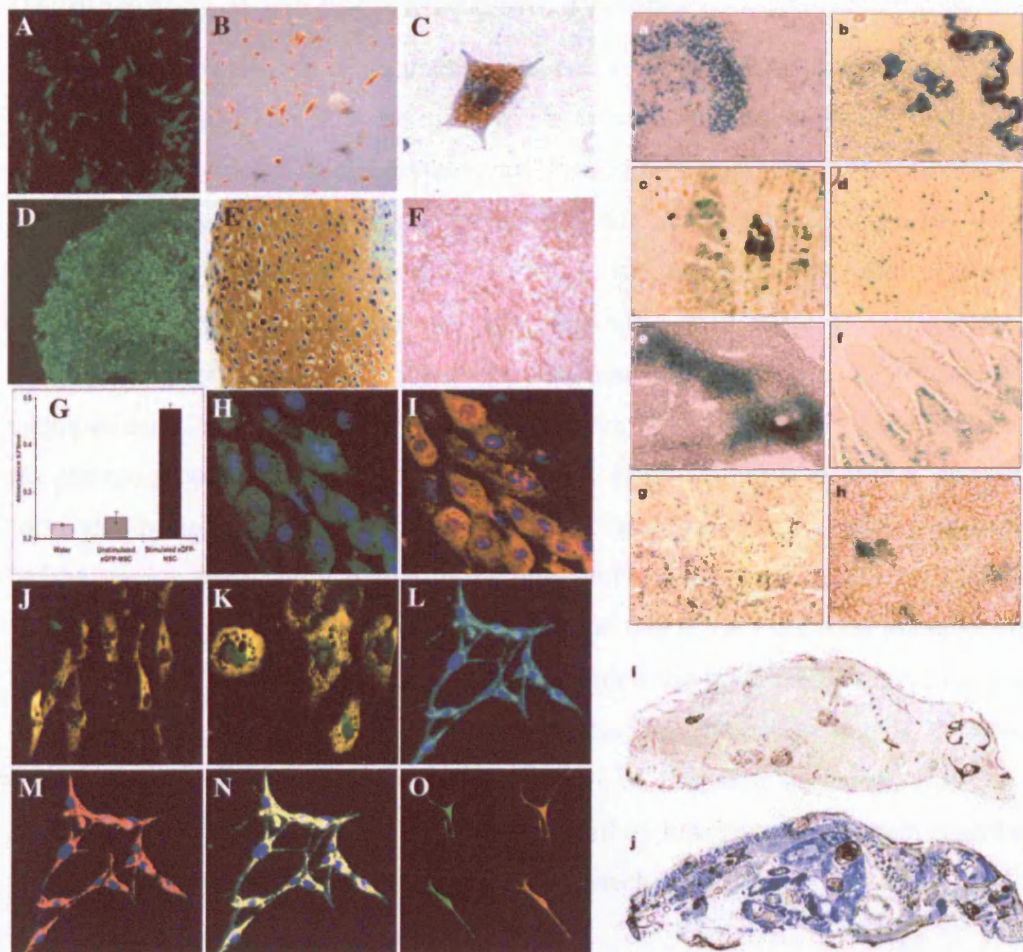
Figure 2 Differentiation potential of mesenchymal stem cells

Left Panel: *In vitro* differentiation. Unstimulated eGFP-MSCs under UV light (A). After 14 days of induction, cells were fixed and stained with Oil Red O (B, C). Chondrogenic differentiation was revealed with Safranin O staining which reveals proteoglycans and glycosaminoglycans (E) with a representative section of the micropellet viewed under the fluorescent microscope before staining (D). The osteogenic potential of MSCs was determined by staining for alkaline-phosphatase (F) and calcium production (G): stimulated eGFP-MSCs (black bar), non-stimulated eGFP-MSCs (grey bar), control-water (light grey bar). eGFP expression alone on myocyte-like cells (H). Myogenic differentiation was confirmed by staining with dystrophin-Cy3 (I, J) and FTM-Cy3 (K). eGFP expression alone on astrocyte- (L) and neuronal-like (O) cells. Neuronal differentiation was confirmed by staining with GFAP-Cy3 (M, N) and Tau-TRITC (O). Overlay of eGFP and dystrophin (J), eGFP and FTM (K) and eGFP with GFAP (N). Cells were counterstained with haematoxylin (B, C, F), DAPI (H-J, L-N) or methyl green (E). Magnifications: x100 (A, B, F); x200 (D, L-N); x400 (C, E, H-K, O) (Anjos-Afonso *et al.* 2004). Right Panel: *In vivo* differentiation. X-Gal staining of tissue sections after injection of ROSA26 beta-galactosidase positive MSC into blastocysts of wildtype hosts. Brain (a), skin (b), muscle (c), heart (d), liver (e), intestine (f), kidney (g), spleen (h). Uninjected mouse (i) and blastocysts chimera (j). Taken from (Jiang *et al.* 2002).

Development of the haematopoietic system

In humans, the first signs of haematopoiesis occur in the yolk sac during the 3rd week of embryogenesis. This first haematopoiesis is called primitive haematopoiesis and produces embryonic nucleated erythrocytes. Progenitors from primitive haematopoiesis colonise the liver and also the bone marrow for accelerated procurement of vital myeloerythroid blood cells (Moore *et al.* 1970). True haematopoietic stem cells are not part of primitive haematopoiesis and arise separately in a different environment. At about 3-4 weeks of gestation clusters of haematopoietic cells emerge in the ventral endothelium of the human embryonic arteries prior to the onset of circulation between the embryo proper and the yolk sac (Tavian *et al.* 1996; Tavian *et al.* 1999). These cells form the basis of definitive haematopoiesis. From the aorta-gonads-mesonephros (AGM) region these cells migrate to the liver and replace primitive macrocytes (large definitive enucleated erythrocytes) already hosted there. This is called extramedullary haematopoiesis. At about the 4th month of gestation the bone marrow spaces begin to fill with haematopoietic cells and become important haematopoietic organs, later taking over to become the final site of haematopoiesis of the adult organism. However, if sufficient stress is placed on the adult, extramedullary haematopoiesis again contributes to haematopoiesis and becomes a compensatory mechanism.

Assays

Various methodologies exist to measure the frequency of haematopoietic stem cells or progenitors within a given population of cells. They include *in vitro* clonogenic assays, *in vitro* phenotyping and *in vivo* transplantation assays. However, the main standard by which every haematopoietic stem cell is measured is its ability to continuously and long-term repopulate all blood lineages, myeloid and lymphoid, of an irradiated recipient after bone marrow transplantation. This fundamental activity can only be adequately shown in chimeric models where a distinction between cells of the host and the transplanted cells is possible. Upon injection of haematopoietic stem cells into lethally irradiated recipients two features of the stem cells are crucial for survival of the host. The stem cells have to be able to rescue the recipient animal from the effects of the total body irradiation in the short term, and they have to be able to provide long

term engraftment for sustained survival. The repopulation assay is the gold standard to demonstrate the long-term repopulating ability of haematopoietic stem cells.

In vitro assays

Long-term bone marrow cultures showed that HSC could be cultured on pre-established stromal cell layers mimicking the natural environment of HSC in close vicinity of supporting stroma (Dexter *et al.* 1977). From this observation assays which analyse the formation of colonies were derived. In these assays the frequency and nature of colony forming cells (CFC's) is tested (Eaves *et al.* 1992). The CFC is a cell that is already committed to a specific myeloid lineage and has limited proliferative potential. An assay which demonstrates more primitive cells is the assay for long term culture initiating cells or LTC-IC. Using a different endpoint the long-term culture initiating cell (LTC-IC) assay tests for the presence of cells capable to initiate haematopoiesis on a stromal cell layer for up to 60 days (Sutherland *et al.* 1989). In a modified protocol some cells grew underneath the supporting stromal layer forming the so called cobblestone areas (Ploemacher *et al.* 1991). It could be demonstrated that the frequency of cobblestone area forming cells (CAFCs) showed good correlation with different assays, like colony forming unit in culture, colony forming units in the spleen and marrow repopulating ability. To assay even more primitive cells than the LTC-IC the protocol was further modified and used to identify a small subpopulation of LTC-IC termed the extended–LTC-IC which is able to support haematopoiesis on stroma for up to 100 days (Hao *et al.* 1995). However, since growth conditions of human LTCs do not support the development of all blood lineages and these assays are unable to assess repopulating capacity, little is known about the relationship of LTC-ICs and pluripotent stem cells. Ultimately, the only conclusive assay for stem cells is their ability to reconstitute the entire haematopoietic system after transplantation.
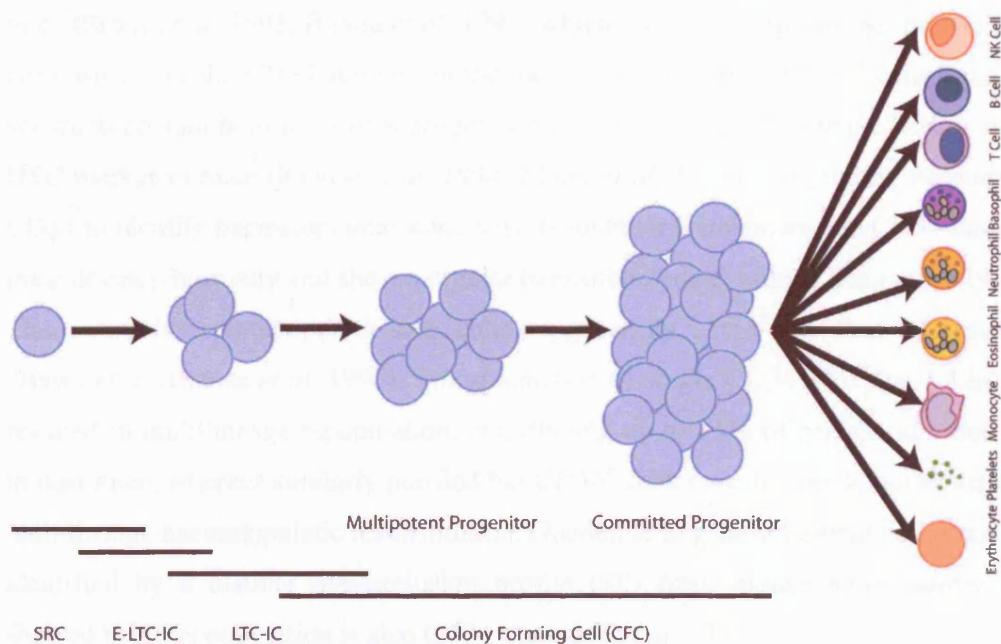
Figure 3 *In vitro* assays for stem and progenitor cells

While no *in vitro* assay exists to measure true stem cells, very early progenitor cells can be measured with the E-LTC-IC (extended long-term-culture initiating cell) assay, which highlights a very primitive subpopulation of the LTC-IC (long-term-culture initiating cell) population. Progenitors of various stages of differentiation can be measured in the CFC (colony forming cell) assays.

Phenotypic Assays

Recent advances in flow cytometry have helped immensely in defining the phenotype of primitive haematopoietic stem cells. While many different sorting strategies have been tested over time, a general consensus has emerged that stem cells lack lineage specific markers, i.e. markers identifying mature granulocytes, macrophages B and T cells and reticulocytes. Another very important marker for stem cells is CD34. It was first identified as a haematopoietic cell-surface antigen using the early human myeloblastic cell line KG1a which highly expresses CD34 and displays a strong potential for myeloid colony-forming cells (Civin *et al.* 1984). CD34$^+$ cells have been shown to engraft in baboons (Berenson *et al.* 1988) and have since been used both for autologous and allogeneic transplantations in human medicine, resulting in a rapid reconstitution of all blood lineages (Civin *et al.* 1996; Link *et al.* 1996). Human CD34$^+$ and Lin$^-$CD34$^+$ cells have also been found to engraft in foetal sheep and NOD/Scid

mice (Srour *et al.* 1993; Bhatia *et al.* 1997) which led to the concept that human HSCs are positive for the CD34 antigen. In the mouse model, murine CD34$^+$ cells have been shown to contain both functional progenitors and HSCs, indicating that CD34 is also an HSC marker in mice (Krause *et al.* 1994; Morel *et al.* 1996). Despite the versatility of CD34 to identify haematopoietic stem cells its function is unknown and CD34 knockout mice develop normally and show a regular haematopoietic profile (Cheng *et al.* 1996). The notion that haematopoietic stem cells are generally CD34$^+$ was first challenged by Osawa *et al* (Osawa *et al.* 1996). Transplantation of single CD34$^-$c-kit$^+$Sca-1$^+$Lin$^-$ cells resulted in multilineage repopulation, contributing up to 85% of peripheral blood cells in host mice, whereas similarly purified but CD34$^+$ cells revealed early, but unsustained multilineage haematopoietic reconstitution. Goodell *et al* purified a stem cell population identified by a distinct dye-exclusion profile (SP) from mouse bone marrow, and showed that this population is also CD34$^-$ (Goodell *et al.* 1997).

To explain the different findings with regard to CD34 expression of stem cells Sato *et al.* exposed CD34$^-$ HSCs to early acting cytokines like interleukin-11 and stem cell factor in culture, resulting in a population of CD34$^+$ cells. When these cells were injected into lethally irradiated mice they generated long-term multilineage engraftment, suggesting that CD34$^-$ cells can develop into CD34$^+$ cells and retain their HSC capacity (Sato *et al.* 1999). In the NOD/Scid mouse model Bhatia *et al.* could show engraftment of Lin$^-$CD34$^-$CD38$^-$ stem cells purified from human cord blood (Bhatia *et al.* 1998). While these cells had low clonogenic activity *in vitro*, they regenerated multilineage haematopoiesis in mice. It could also be shown that CD34$^-$ cells give rise to CD34$^+$ cells resulting in a greater repopulating activity in cytokine-supported short-term cultures, whereas CD34$^+$ cells lost their stem cell potential in culture. Using in utero transplantation into pre-immune sheep, Zanjani *et al.* observed engraftment of human haematopoietic cells with Lin$^-$CD34$^-$ bone marrow cells (Zanjani *et al.* 1998). Human CD34$^+$ cells could also be observed in sheep transplanted with CD34$^-$ cells, again suggesting that CD34$^-$ HSC can give rise to CD34$^+$ cells *in vivo*. Human Lin$^-$CD34$^-$CD38$^-$ cells from normal BM and G-CSF-mobilised peripheral blood do not grow well in methylcellulose, but proliferate and differentiate rapidly into erythrocytes, granulocytes and megakaryocytes in serum-free culture. They also turn into CD34$^+$ cells after 10 days of culture and significantly increase their colony forming potential (Fujisaki *et al.* 1999). Nakamura *et al.* show that CD34$^-$ cord blood cells with initial low colony forming potential gain the ability to form colonies during 7 days of

culture, coinciding with the formation of $CD34^+$ cells (Nakamura *et al.* 1999). While the original population of $CD34^-$ cells had only low repopulation activity this activity was increased after culture and the cells could repopulate the bone marrow of NOD/Scid mice and also give rise to $CD34^+$ cells. This supports the theory that $CD34^-$ cells are more primitive than $CD34^+$ cells. In the sheep model Zanjani *et al.* reported that $CD34^-$ cells showed significantly higher levels of engraftment than $CD34^+$ cells 15 months post transplantation (Zanjani *et al.* 2003). The phenotype of CD34 and CD38 expression on human cord blood cells is shown in Figure 4d.

The apparent lack of markers on true stem cells made it necessary to find other ways of identification. One functional property of stem cells seems to be the ability to efficiently extrude dyes from the cytoplasm. This property may be beneficial for stem cells to protect them from toxins like chemotherapy and can be exploited for purification. The dye Hoechst 33342 gets efficiently extruded from a stem cell population leading to a characteristic picture in the FACS plot when the emission of the dye is plotted in two dimensions. This population has been termed the side population (SP) (Goodell *et al.* 1996). SP cells have been shown to reside in bone marrow (Goodell *et al.* 1996), liver (Uchida *et al.* 2001), skin (Yano *et al.* 2005), lung (Majka *et al.* 2005) and even in the corneal stroma (Du *et al.* 2005). SP populations have also been found in cells from patients with acute myeloid leukaemia (Wulf *et al.* 2001) and in cell suspensions from solid tumours (Hirschmann-Jax *et al.* 2004; Patrawala *et al.* 2005). Figure 4a depicts a typical SP cell population from murine bone marrow taken from (Pearce *et al.* 2004). Another possible physiological property of stem cells seems to be a high activity of aldehyde dehydrogenase (Hess *et al.* 2004). Using a fluorescent substrate these cells can be purified by FACS sorting. Figure 4c depicts the stem cell population highlighted by aldefluor staining (Pearce *et al.* 2005).
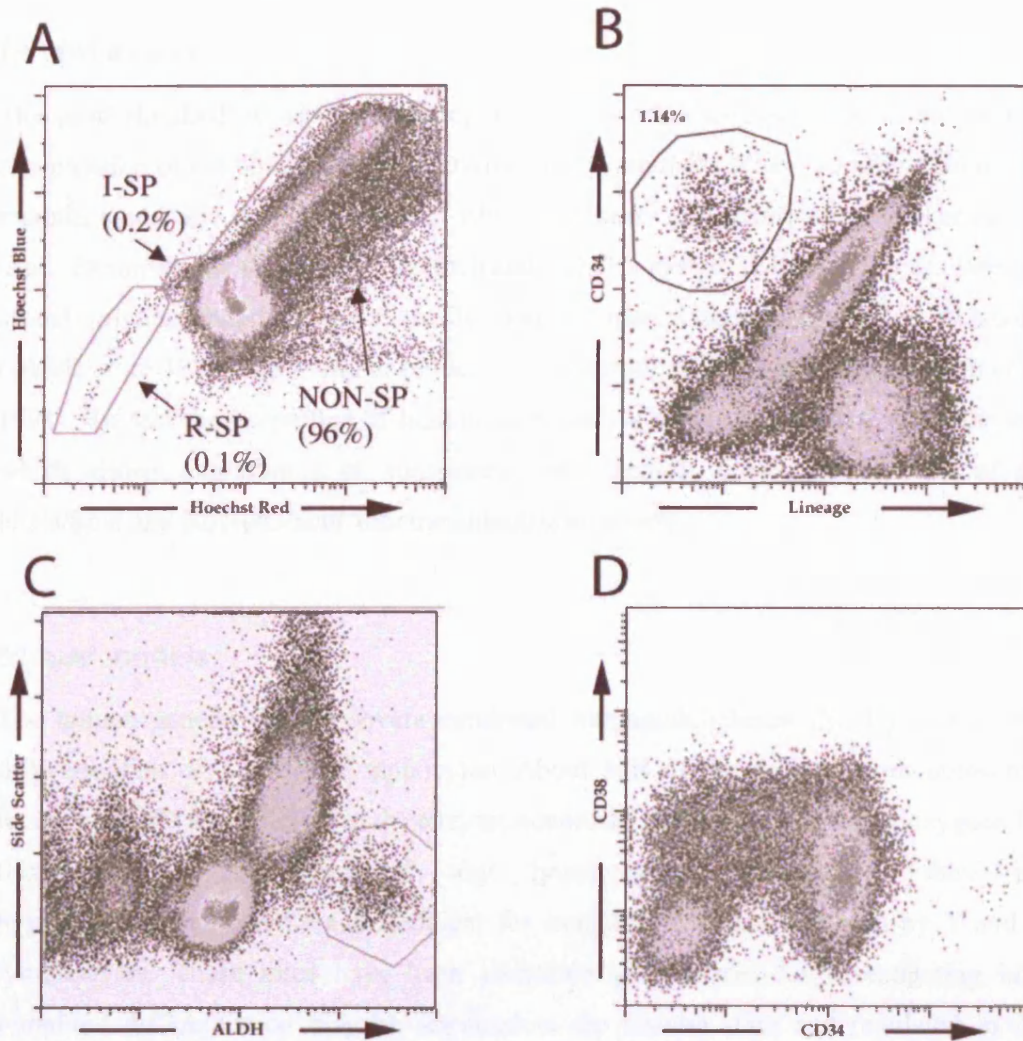
Figure 4 Phenotypic stem cell assays

Hoechst dye exclusion (A). Stem cells efficiently extrude Hoechst dye leading to a tail of stem cells in the blue vs. red Hoechst emission FACS plot (R-SP). From Pearce *et al* (Pearce *et al.* 2004). Staining for lineage antigens and CD34 reveals CD34$^+$/Lin$^-$ stem cells (B). Stem cells identified by high aldehyde dehydrogenase activity (C). From Pearce *et al* (Pearce *et al.* 2005). CD34$^{+/-}$/CD38$^{+/-}$ stem cell populations (D). Pearce D, pers.comm.

In vivo assays

The gold standard at which haematopoietic stem cells are measured is the *in vivo* repopulation of the bone marrow of irradiated host animals. When working with mouse models, syngeneic strains of mice of which one bears an identification marker can be used. Examples for this are the CD45.1 and CD45.2 system (Mardiney *et al.* 1996), a model utilizing cells from a genetically modified mouse expressing GFP in all tissues (Okabe *et al.* 1997) and a similar model using a mouse expressing lacZ (Friedrich *et al.* 1991). To test the properties of human stem cells a mouse model had to be devised which allows engraftment of xenogeneic cells leading to the development of the NOD/Scid and β2/NOD/Scid xenotransplantation models.

Mouse models

The human genetic disease severe combined immunodeficiency (SCID) impairs the differentiation of T and B lymphocytes. About half of the patients with autosomal recessive SCID are deficient in the enzyme adenosine deaminase. Mice homozygous for this mutation have few if any lymphocytes; consequently they are hypogammaglobulinaemic and deficient for immune functions mediated by T and B lymphocytes. These mice have been identified as a model for investigating how lymphoid differentiation may be impaired in the disease state and regulated in the normal state (Bosma *et al.* 1983). It was soon after discovered that these mice can be engrafted with human peripheral blood leukocytes (PBL) allowing studies of the human immune system in a murine model (Mosier *et al.* 1988). Suboptimal engraftment of human cells in the scid/scid mouse hampered the use of this model for many years, but nevertheless first haematopoietic stem cell populations were found to engraft when human foetal bone marrow was grafted into scid/scid mice (Baum *et al.* 1992). The investigation of the influence of mouse strain background on the ability to support xenotransplanted cells led to the discovery of the non obese diabetic/Scid (NOD/Scid) mouse model (Shultz *et al.* 1995). Improved engraftment of human cells was shown with human spleen cells (Greiner *et al.* 1995) and with human cord blood cells (Lowry *et al.* 1996). NOD/Scid mice were then further crossed with mice harbouring a defect in beta-2-microglobulin, leading to a lack of cell surface MHC class 1 expression and absence of detectable levels of class 1 dependent cells, including $CD8^+$ T cells, NK

cells and NK1$^+$ T cells. These β2/NOD/Scid mice are even further immunocompromised and provide excellent hosts for human haematopoietic stem cells (Kollet *et al.* 2000) and also human leukaemic stem cells (Feuring-Buske *et al.* 2003).

Foetal sheep model

Another model for testing human haematopoietic stem cells is in-utero transplantation into pre-immune sheep (Flake *et al.* 1986). This method has been successfully used to show engraftment of purified human haematopoietic cells (Srour *et al.* 1992) and has helped define novel stem cell populations (Zanjani *et al.* 1998).

The stem cell niche

The environment in which stem cells reside is called the stem cell niche. In the adult mammal the bone marrow (BM) is the main specialised microenvironmental niche for both self-renewal and differentiation of HSC. The concept of a stem cell niche was first proposed for the human haematopoietic system in the 1970's (Schofield 1978). A similar concept was later postulated for stem cells of the epidermis, intestinal epithelium, nervous system and gonads (Fuchs *et al.* 2004). The niche of the HSC is not yet as well defined as the Drosophila germ stem cell niche(Spradling *et al.* 2001), or the niche of the skin stem cell in the bulge region of the hair follicle (Fuchs *et al.* 2004).

The purpose of the niche is to provide stem cells with an environment in which the maintenance of the quiescent stem cell pool and the asymmetric division giving rise to differentiating cells can be regulated and take place.

Two different niche environments for HSC have been studied, the vascular haematopoietic niche which is predominantly utilised in embryonic development, and the osteoblastic niche which is the main environment of HSC in the adult organism.

The vascular niche

The vascular niche is the main source of haematopoietic cells in the developing organism. Endothelial cells give rise to HSCs in the aorta-gonad-mesonephros (AGM)

region and the placenta labyrinth (de Bruijn *et al.* 2002; Ottersbach *et al.* 2005). This highlights the existence of a common progenitor of haematopoietic and endothelial cells, the hemangioblast (Choi *et al.* 1998). Endothelial cells and HSCs co-express CD34, CD133, Glk1, VEGFR and Tie2 (Rafii *et al.* 2002) suggesting a ligand-receptor signalling relationship between HSC and endothelial cells. Vascular endothelial progenitor cells are also essential for organogenesis of the liver and pancreas underlining the role of endothelial cells to provide inductive signals for organ development (de Bruijn *et al.* 2002; Ottersbach *et al.* 2005).

The osteoblastic niche

The osteoblastic niche provides the environment for the main haematopoietic organ of the adult organism. Osteoblasts play a crucial role in the bone marrow by providing the niche environment for HSC (Calvi *et al.* 2003; Zhang *et al.* 2003). Osteoblasts are a heterogeneous population including mature cells contributing to bone formation as well as immature cells. Osteoblasts are derived from mesenchymal stem cells. Mesenchymal cells also induce the formation of bone resorbing cells, the osteoclasts, from haematopoietic stem cells (Yasuda *et al.* 1998).

HSC can be divided into two populations according to their cell cycle state. Most HSCs divide frequently, (Zhang *et al.* 2003) but some label-retaining cells remain over several months representing a population of quiescent stem cells. These quiescent cells are maintained in the resting state by their close proximity to osteoblasts. Zhang *et al* showed that a small subset of osteoblastic lining cells expressing N-cadherin are the niche cells for HSCs in the bone marrow. An increase in the number of osteoblasts after administration of parathyroid hormone-related protein (PTHrP) also leads to a increase of haematopoiesis (Calvi *et al.* 2003). Chemokines and chemoattactive proteins are responsible for homing and mobilisation of HSC and also for the interaction of HSC with the stromal cells. The protein stromal cell-derived factor-1 (SDF-1) is involved in homing to the haematopoietic organs. Deletion of the genes for SDF-1 or its receptor, CXCR4 severely affects homing of stem cells to the bone marrow so that in mutant animals foetal liver haematopoiesis is normal, but marrow engraftment of HSC is not observed (Nagasawa *et al.* 1996; Tokoyoda *et al.* 2004). As CXCR4 is not expressed in quiescent HSC the factors for homing of HSC are probably different to adhesion molecules in the osteoblastic niche.

Tie2-Ang-1 signalling is one molecular mechanism which is implicated in suppressing cell division and thus maintaining stem-ness of HSC in the bone marrow. Slow cycling HSCs express the receptor tyrosine kinase Tie2 and are a SP fraction of HSCs(Arai *et al.* 2004). Ang-1, which is a ligand for Tie2 is expressed primarily by osteoblasts in the adult bone marrow. The signalling from Tie2 to Ang-1 promotes tight adhesion of HSCs to osteoblasts and maintains an immature HSC phenotype with upregulated N-cadherin expressions and no cell cycle progression. In mice lacking the family of Tie proteins (Tie1 and Tie2) postnatal haematopoiesis is impaired, whereas foetal haematopoiesis is unaffected (Puri *et al.* 2003). Other adhesion molecules such as activated leukocyte cell adhesion molecule (ALCAM) (Arai *et al.* 2002) and osteopontin (Chen *et al.* 1993) are expressed by osteoblasts, and N-cadherin (Arai *et al.* 2004) is expressed in both quiescent HSCs and osteoblasts.

The Liver

In Greek mythology, Prometheus was punished by the gods for revealing fire to humans by being chained to a rock where a vulture would peck out his liver, which would grow back again overnight. It thus may already have been known to the Greeks that the liver is the only human internal organ that actually can regenerate itself to a certain extent, a characteristic which is even better preserved in rodents.

Introduction

The liver is an organ in vertebrates which plays a major role in metabolism and has a number of functions in the body including detoxification, glycogen storage and plasma protein synthesis. It also produces bile, which is important for digestion.

The adult human liver normally weighs between 1.0 - 2.5 kilograms, the liver of a 20 week old mouse approximately 2.4 grams.

The liver is supplied by two major blood vessels: the hepatic artery and the portal vein. The hepatic artery supports the liver with oxygen. The arteric blood is pumped into the capillaries of the liver stroma and from there joins the interlobular hepatic veins. The portal vein brings venous blood from the digestive tract, so that the liver can process the

nutrients and toxic by-products of food digestion. The hepatic veins drain directly into the inferior vena cava.

The bile produced in the liver is collected in bile capillaries, which merge to form bile ducts. These eventually drain into the right and left hepatic ducts, which in turn merge to form the common hepatic duct. The cystic duct (from the gallbladder) joins with the common hepatic duct to form the common bile duct. Bile can either drain directly into the duodenum via the common bile duct or be temporarily stored in the gallbladder via the cystic duct.

The major functions of the liver are:

- Production and excretion of bile required for food digestion. Some of the bile drains directly into the duodenum, and some is stored in the gallbladder.

- The liver performs several roles in carbohydrate metabolism:
    - Gluconeogenesis (the formation of glucose from certain amino acids, lactate or glycerol)
    - Glycogenolysis (the formation of glucose from glycogen)
    - Glycogenesis (the formation of glycogen from glucose)
    - LDL uptake
    - Ketogenesis

- The breakdown of insulin and other hormones

- The liver also performs several roles in lipid metabolism:
    - Cholesterol synthesis
    - The production of triglycerides (fats).

- Production of coagulation factors I (fibrinogen), II (prothrombin), V, VII, IX, and XI, as well as protein C, protein S and antithrombin.

- Breakdown of haemoglobin (bile pigments are its metabolites), toxic substances and most medicinal products. This sometimes results in toxication, when the metabolite is more toxic than its precursor.

- Conversion of ammonia to urea.

- Storage of a multitude of substances, including glucose in the form of glycogen, vitamin B12, iron, and copper.

- In the first trimester foetus, the liver is the main site of red blood cell production. By the 42nd week of gestation, the bone marrow has almost completely taken over that task.

These tasks are accomplished by specialised cells, the hepatocytes. During embryonic development hepatoblasts generate both hepatic epithelial cell lineages, hepatocytes and biliary cells. The liver is made up of lobules, each of which is a functional unit. (Figure 5) On the outside the lobe is surrounded by the limiting plate and portal tracts. The portal tract consists of an artery which supplies oxygen, a bile duct which collects bile produced by hepatocytes and a branch of the portal vein which brings nutrient rich blood from the intestine for processing by the liver. The portal vein blood then flows in sinusoids between hepatocytes towards the central vein. The bile, produced by hepatocytes, flows in the opposite direction collecting in the bile ducts for drainage.
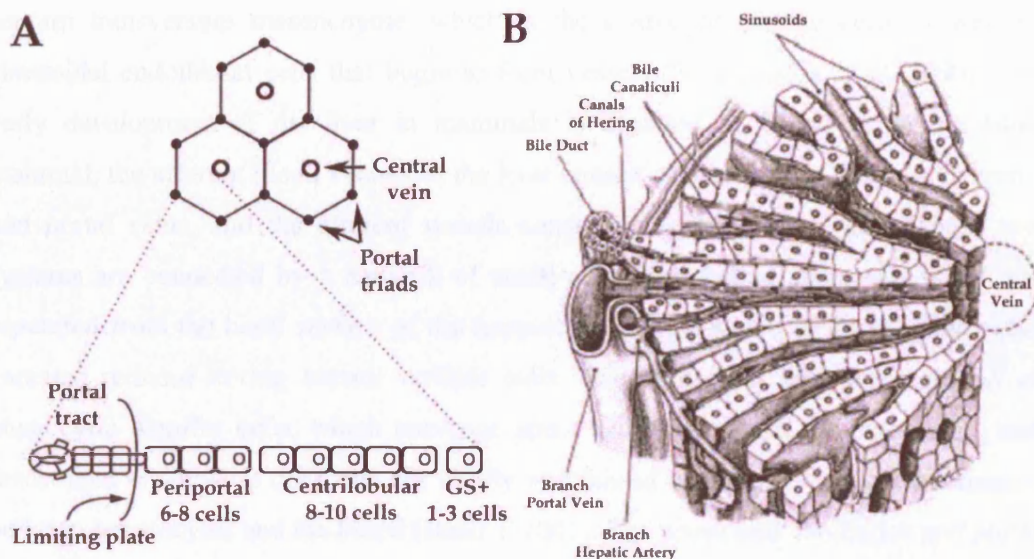
Figure 5 Organization of the liver

Hexagonal liver lobes have portal triads on the outside and the central vein in the middle. Hepatocytes have different characteristics from the outside to the inside. Schematic drawing (A, redrawn) and artistic impression (B) taken from Fausto *et al* (Fausto *et al.* 2003).

Origin of the liver

Several decades of work in numerous vertebrate model systems have firmly established that hepatocytes and bile duct cells originate from a common precursor, the hepatoblast, which derives from the definitive endoderm (Chalmers *et al.* 2000; Deutsch *et al.* 2001; Field *et al.* 2003). In the mouse, at around embryonic day (E)7.0 the definitive endoderm emerges from the primitive streak to displace the extraembryonic endoderm of the yolk sack. By approximately E8.0, in mouse embryos containing seven somite pairs, the ventral wall of the foregut endoderm is positioned adjacent to the developing heart, and signals from the heart induce the underlying endoderm to initiate its development towards a hepatic fate by releasing bone morphogenetic proteins (BMP) and fibroblast growth factors (FGF) (Jung *et al.* 1999). The endoderm responds to this induction by generating the primary liver bud that can be identified as an anatomical outgrowth from the ventral wall of the foregut by E8.5 to E9.0. By E9.5 the nascent hepatoblasts delaminate from the endoderm and cords of hepatoblasts invade the septum transversum mesenchyme, which is the source of stellate cells as well as sinusoidal endothelial cells that begin to form vessels (Sosa-Pineda *et al.* 2000). The early development of the liver in mammals is depicted in Figure 6. In the adult mammal, the afferent blood vessels of the liver consist of branches of the hepatic artery and portal veins, and the efferent vessels consist of centrolobular veins. These two systems are connected by a network of small capillaries called sinusoids, which are separated from the basal surface of the hepatocytes by the space of Disse, which also contains retinoid-storing hepatic stellate cells. The sinusoidal capillaries consist of phagocytic Kupffer cells, which scavenge spent cell debris from the circulation, and fenestrated endothelial cells that are highly specialised to facilitate selective transport between hepatocytes and the blood (Braer F 2001). The sinusoidal capillaries and portal veins are among the first hepatic vessels to develop, with centrolobular veins and portal arteries forming later (Gouysse *et al.* 2002).

E8.0   E8.5   E9.5

FGF, BMP

He

S

VE

E

Lb

E

S

H
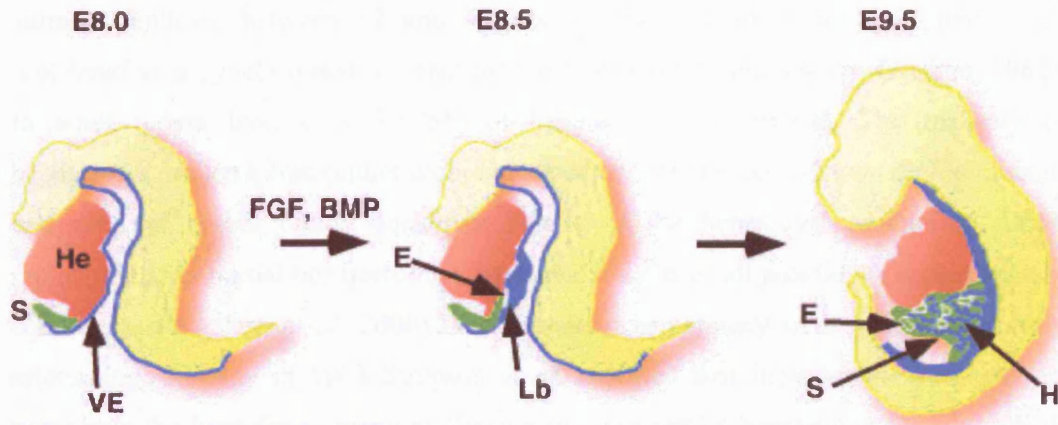
Figure 6 Overview of early stages of liver development in mouse embryos.

Definitive ventral endoderm (VE, blue), developing heart (He), mesenchymal septum transversum (S, green). Induction by FGFs and BMP's leads to formation of the liver bud (Lb) from specialised endoderm (E). Hepatoblasts (H) then delaminate from the endoderm (E) and invade the septum transversum mesenchyme (S). Taken from Zhao *et al* (Zhao *et al.* 2005).

The hepatocyte

Hepatocytes make up 60-80% of the cytoplasmic mass of the liver. They are involved in protein synthesis, protein storage and transformation of carbohydrates, synthesis of cholesterol, bile salts and phospholipids, and detoxification, modification and excretion of exogenous and endogenous substances. The hepatocytes also initiate the formation and secretion of bile.

The hepatocytes are the only cells in the body that manufacture albumin, fibrinogen, and the prothrombin group of clotting factors. It is the main site for the synthesis of lipoproteins, ceruloplasmin, transferrin, and glycoproteins.

Hepatocytes have the ability to metabolise, detoxify, and inactivate exogenous compounds such as drugs and insecticides, and endogenous compounds such as steroids. The drainage of the intestinal venous blood into the liver requires efficient detoxification of miscellaneous absorbed substances to maintain homeostasis and protect the body against ingested toxins. One of the detoxifying functions of hepatocytes is to modify ammonia to urea for excretion.

After severe damage to the liver the hepatocytes can rapidly divide and replace lost liver mass. The usually quiescent hepatocytes divide rapidly only a few hours after the mitogenic stimulus, which is usually partial hepatectomy (the removal of large parts of the liver) or CCl_4 intoxication. After partial hepatectomy 95% of hepatocytes of young

animals replicate between 12 and 48 hrs in rats and 30 to 60 h in mice. Cell proliferation is synchronised, at least for the first wave of replication (Grisham 1962). In adult rodent liver only 20-25% of hepatocytes are diploid. The majority of hepatocytes are tetraploid (either mononucleated or binucleated with two diploid nuclei) and cells of higher ploidy constitute 5-10% of the hepatocyte population. DNA replication after partial hepatectomy takes place in cells of all ploidies at approximately equal rates (Weglarz et al. 2000). The regenerative capacity of hepatocytes is truly astounding. Already in 1963 Simpson et al. reported that hepatocytes were able to regenerate the liver for as many as five consecutive partial hepatectomies, after which less than 5% of the original liver mass remained and more than 95% of the liver was generated by replication of hepatocytes (Simpson et al. 1963). The model of hepatectomy is not suitable to assess the proliferative capacity of hepatocytes in more detail, as the regeneration of the hepatectomised liver requires only few divisions of resident hepatocytes. A different model, the regeneration of the liver of newborn urokinase-type plasminogen activator (uPA) transgenic mice allows for the almost complete liver repopulation from a starting population of only few transplanted human hepatocytes. In these animals the hepatocytes need 10-15 rounds of replication to generate the normal liver mass (Grompe 2001). This transplantation can even be done serially leading to an expansion of the original transplanted hepatocytes of 7.3×10^{20} corresponding to 60-80 population doublings (Overturf et al. 1997).

The oval cell

Despite the hepatocytes being able to repopulate the liver mass even after substantial loss, there also seem to be stem cells in the liver. These cells do not participate in the aforementioned regeneration and only become apparent in special circumstances. While in proliferative tissues such as the skin and intestinal epithelia stem cells continually generate progenies which differentiate thereby losing the replicative capacity, the liver is mostly quiescent and hepatocytes divide very rarely in steady state conditions. The liver is unique in that intrahepatic stem and progenitor cells constitute a secondary proliferative compartment in addition to differentiated cells which can also replicate readily. The facultative stem cells of the liver have their niche in the canals of Hering, the most distal part of the bile canaliculi in the liver lobe. These cells are components of a functional segment of the biliary system and are not part of a separate compartment of

proliferative cells such as the basal cells in the skin (Theise *et al.* 1999). Oval cells, the presumed progeny of these cells are not detectable in normal liver and only become abundant as an amplifying transit compartment after suitable induction. Oval cell proliferation is prominent in many models of liver injury including carcinogenesis induced by azo-dyes and choline deficient/ethionine-containing diets (CDE diet), injury caused by D-galactosamine and injury produced by acetyl aminofluorene in conjunction with partial hepatectomy (AAF/PH) (Sell *et al.* 1981; Shafritz *et al.* 2002). In the AAF/PH and galactosamine models as well as in rodents fed the CDE diet, oval cells can constitute more than 50% of cells in the liver. Although there was speculation that these cells are derived from the bone marrow (Petersen *et al.* 1999), more recent research does not support that hypothesis (Menthena *et al.* 2004).
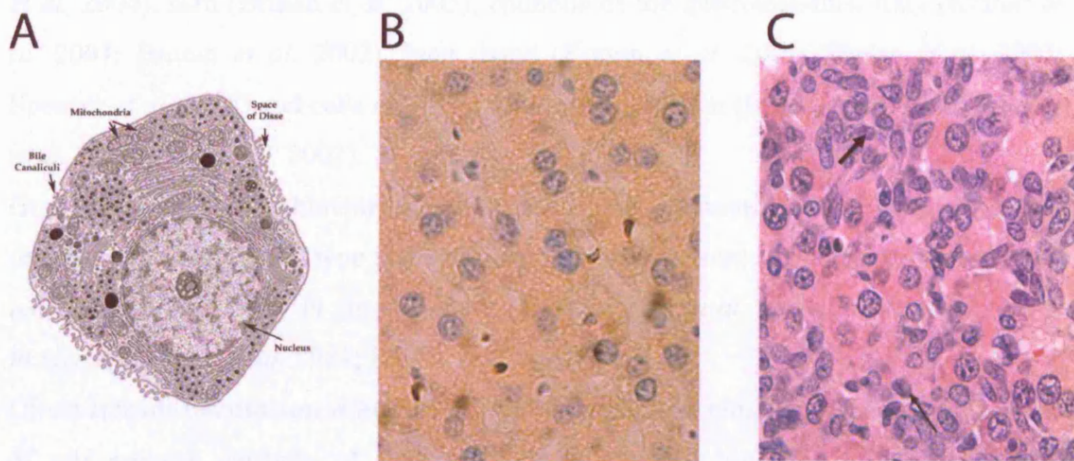
Figure 7 Hepatocyte and oval cell morphology

(A) Drawing of hepatocyte morphology displaying the space of Disse, mitochondria, bile canaliculi and the nucleus. Murine hepatocytes in healthy liver (B), and oval cells after 2-acetylaminofluorene treatment and CCl_4 injury (arrows) (Yang *et al.* 2002).

Plasticity and Transdifferentiation

Introduction

Until recently it was thought that tissue specific stem cells could only differentiate into cells of the tissue of origin or at least would be restricted to a specific lineage of cells. However, recent developments have suggested that stem cells from various origins are capable of transgressing the limits of their lineage and give rise to cells of unrelated tissues. Bone marrow derived cells (BMDCs) have been shown to contribute to skeletal muscle and this contribution was enhanced upon damage with a toxin or genetic muscle disease (Ferrari *et al.* 1998; Gussoni *et al.* 1999; LaBarge *et al.* 2002). BMDCs also incorporate into the cardiac muscle(Jackson *et al.* 2001), liver (Krause *et al.* 2001; Jang *et al.* 2004), skin (Brittan *et al.* 2005), epithelia of the gastrointestinal tract (Krause *et al.* 2001; Brittan *et al.* 2002), lung tissue (Kotton *et al.* 2001; Theise *et al.* 2002; Spencer *et al.* 2005) and cells of the central nervous system (Kopen *et al.* 1999; Bonilla *et al.* 2002; Corti *et al.* 2002).

One possibility for achieving plasticity is transdifferentiation of a committed cell directly into another cell type as a response to environmental cues. Transdifferentiation has been shown mainly *in vitro* (Tosh *et al.* 2002; Jang *et al.* 2004), but can also occur *in vivo* (Scarpelli *et al.* 1981; Eguchi *et al.* 1993).

Direct transdifferentiation would be difficult to exploit in clinical situations, as the lack of self renewal capacity of differentiated cells would limit the efficiency of any treatment based on direct transdifferentiation. If bone marrow cells could on the other hand give rise to stem cells of another tissue then they could in theory repopulate whole organs from a few starting cells.

Genetic analysis of cells of donor origin *in vivo* and *in vitro* has brought to light another possible mechanism. The fusion of host and donor cells can give rise to mature tissue cells without trans- or dedifferentiation. The resulting heterokaryons are able to cure a lethal genetic defect and do not seem to be prone to give rise to cancer. All these models will clinically face the problem of accessibility of healthy primary cells for transplantation. This underlines the importance of the recent identification of a population of mesenchymal stromal cells with stem cell properties similar to ES cells. These cells can be cultured and expanded *in vitro* without losing their stem cell

potential making them an attractive target for cell therapy (see introduction) (Pittenger *et al.* 1999; Pittenger *et al.* 2000; Anjos-Afonso *et al.* 2004).

Finally, stem cells of various tissues could be circulating in the peripheral blood, or be present in the bone marrow and could be directly purified from these sources. Identification of putative tissue stem cells would be necessary before purification strategies can be devised(Ratajczak *et al.* 2004; Kucia *et al.* 2005).
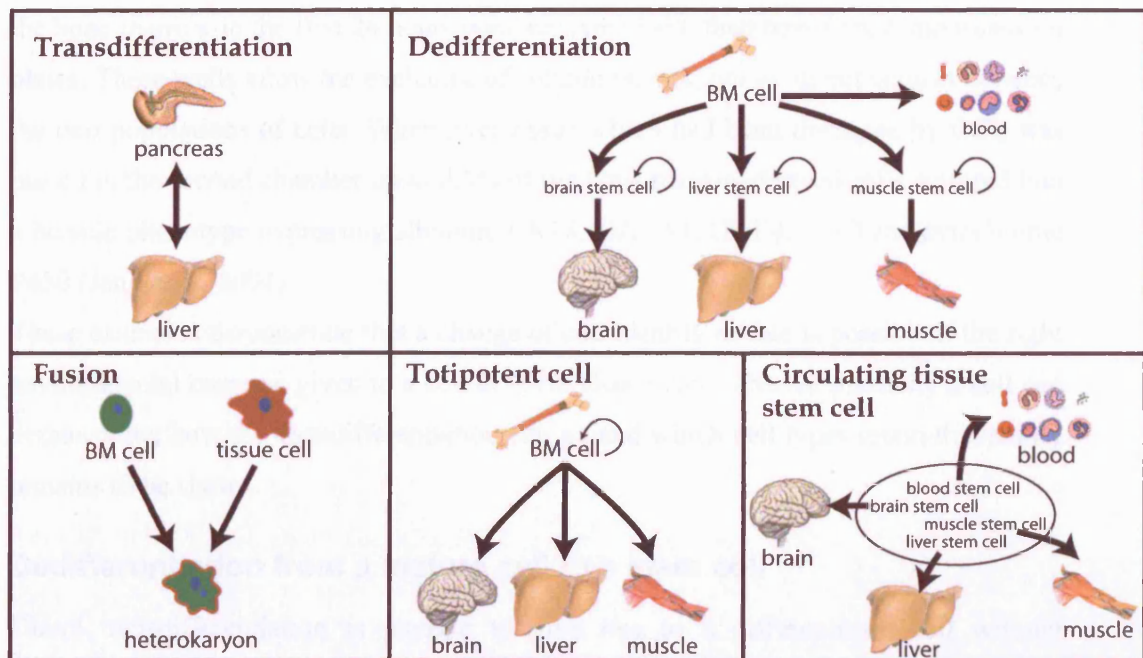
Figure 8 Different proposed mechanisms of cell fate change

Transdifferentiation: change of cell type of a fully differentiated cell, Dedifferentiation: reacquisition of stem cell phaenotype, Fusion: merging of two different cells, Totipotent cell: no lineage restriction, Circulating tissue stem cell

Transdifferentiation *in vitro* across different germ layers

Differentiation *in vitro* provides an effective way of exploring the intrinsic capabilities of cells. Hepatic foci in the pancreas have been known to arise in rodents from copper depletion in the diet or in transgenic mice overexpressing keratinocyte growth factor in the pancreas. In an *in vitro* assay using a pancreatic cell line, AR42J-B13, foci of hepatic cells could be induced by exposure to the synthetic glucocorticoid dexamethasone. Dexamethasone can induce hepatic differentiation in the pancreatic bud

of a normal mouse embryo and its effect is mediated by C/EBP-α. Transdifferentiated cells expressed albumin, glucose-6-phosphatase and amylase. Residual GFP protein which had been expressed from the elastase promoter, specific for mature exocrine cells, demonstrates that these albumin producing cells have been derived from fully differentiated exocrine cells (Tosh et al. 2002).

In a different study by Jang et al a cell population with hepatic potential was purified from mouse bone marrow. Bone marrow cells were elutriated, depleted of mature haematopoietic cells and injected into primary host animals. The cells which homed to the bone marrow in the first 24 hours were recovered and then transferred into transwell plates. These wells allow the exchange of soluble factors, but no direct contact between the two populations of cells. When liver tissue which had been damaged by CCl4 was placed in the second chamber up to 2.5% of the bone marrow derived cells matured into a hepatic phenotype expressing albumin, CK18, GATA4, HNF4, TDO and cytochrome P450 (Jang et al. 2004).

These examples demonstrate that a change of cell identity or fate is possible if the right environmental cues are given to a cell in vitro. How much inherent plasticity a cell can demonstrate, how far transdifferentiation can go and which cell types retain this ability remains to be shown.

Dedifferentiation from a mature cell to a stem cell

Direct transdifferentiation is thought to give rise to a differentiated cell without generating an intermediate tissue stem cell. In the lung some experiments suggest a different mechanism. The high level of engraftment observed in this organ could be linked to damage induced by whole body irradiation used as part of the bone marrow transplantation protocol. Histological signs of tissue damage in the lung are first present on day 3 and are countered by proliferation and repair first apparent on day 5. From this timepoint on donor derived type II pneumocytes could be shown by Y-fish and RNA in-situ. The percentage of marrow derived type II pneumocytes increased over time from 0.9% to 13% at month 6. As type I pneumocytes are progeny of type II pneumocytes the latter are regarded as the tissue stem cell in the lung. The authors argue that dedifferentiation of a bone marrow cell to an epithelial stem cell must have occurred to explain these results (Theise et al. 2002).

LaBarge et al studied the dedifferentiation of a bone marrow cell into a muscle stem cell and from there to mature muscle fibers. The authors show that cells from the bone

marrow integrate into muscle tissue in two distinct stages. First the irradiation used for the bone marrow transplant clears the tissue stem cell niche from the native satellite cells followed by repopulation from bone marrow derived cells. The engrafted cells expressed markers of satellite cells (cMet-R and Myf-5) and where phenotypically indistinguishable from native satellite cells in situ. (Figure 9c) After this stage cells contribute to the muscle mass by creating muscle fibers, albeit at a low level which could be increased by a training regimen for the mice (from 0.17% to 3.52% donor nuclei). Exercise induces damage to intracellular and membrane components of the muscle and satellite cells respond to this environment by becoming mitotic and fusing with the muscle tissue. When bone marrow derived satellite cells were isolated in high purity from the muscle these cells were able to self renew and produce muscle fibers *in vitro*. Furthermore when injected into the TA muscle of experimental mice they again contributed to the muscle tissue in the secondary recipient. No gross abnormalities were found in the karyotype of these cells indicating that a bone marrow cell has successfully adopted an unrelated stem cell phenotype (LaBarge *et al.* 2002).

In the second study by Camargo *et al* single sorted side population (SP) cells from mouse bone marrow where introduced into hosts. Upon successful bone marrow engraftment muscle damage was induced. Repeated injections of cardiotoxin into the TA muscle on one side of the animal induce damage which is subsequently repaired. Analysis of the injured and the non-injured muscle revealed donor derived nuclei only in muscle fibers of the injured side. However, even with extensive analysis of the muscle fibers the authors where unable to find donor derived satellite cells in sections of the muscle, by flow cytometry or after isolation of all satellite cells in an *in vitro* assay of myotube formation. Instead the authors demonstrate that a cell of the macrophage lineage is the main contributor to donor myotubes in this model, likely attracted by the inflammation caused by the toxin used to induce tissue damage (Camargo *et al.* 2003).

Spontaneous cell fusion *in vitro* and *in vivo*

In an attempt to generate pluripotent stem cells *in vitro* from adult bone marrow Terada *et al* established co-cultures of murine puromycin resistant GFP[+] bone marrow cells with wild type puromycin sensitive embryonic stem cells. After 7 days of co-culture puromycin was added to the culture medium to eradicate the embryonic stem cells. A surviving cell fraction was obtained which expressed markers of the donor animal

(GFP$^+$ and puromycin resistant) but exhibited the proliferation rate of embryonic stem cells and also the expression of ES-cell markers (Oct3/4 and UTF1). These cells could successfully be differentiated into various lineages similar to the potential found in embryonic stem cells. However subsequent DNA analysis showed that all 13 cell lines derived with this protocol had more than diploid DNA content and microsatellite analysis revealed genomic content from both mouse strains used in the co-culture (Terada et al. 2002).

Yiang et al initiated neurosphere cultures from dissociated forebrains of ROSA26 foetuses and cultured them with ES cells. After selection they could demonstrate frequent generation of hybrids showing genomic markers of both mouse strains used. Interestingly, upon introduction into a blastocyst these cells contributed to intestine, kidney, heart and most prominently liver (Ying et al. 2002). Cell fusion was also shown in a model of co-culture of small airway epithelial cells with human MSC (Spees et al. 2003). In vitro fusion is not a property equally shared by all cell types. Mesenchymal stem cells and long term marrow culture cells are more susceptible to fusion than CD34$^+$ cells (Shi et al. 2004).

An example of in vivo fusion was found in the brain. When GFP$^+$ bone marrow was transplanted into normal hosts green purkinje neurons could be found in the brain. Purkinje neurons are mononucleate diploid cells that constitute the only efferent from the cerebellum to other brain regions. Each purkinje neuron can receive over one million inputs from other neurons, and lack of purkinje neurons results in ataxias. Close inspection of the GFP$^+$ purkinje neurons revealed that these where not generated de-novo, but had acquired the GFP gene by fusion of a bone marrow derived cell with a resident purkinje neuron. The fusion of the two cells gives rise to stable heterokaryons, and the morphology of the bone marrow derived nucleus changes to a typical purkinje neuron nucleus over time. (Figure 9d) GFP expression could only be found in these specialised neurons, indicating a predisposition to fusion in the purkinje neurons (Weimann et al. 2003).

In the FAH$^{-/-}$ mouse model of hereditary tyrosinaemia functional rescue from a lethal genetic disease could be achieved by bone marrow transplantation.(Figure 9a) Hepatocytes derived from the donor bone marrow contributed about 65% of the final recipient liver after serial hepatocyte transplantation, but the percentage of original karyotype was only 30% by southern blot inconsistent with simple transdifferentiation. Analysis of metaphase spreads of these cells revealed that more than 30% of cells had a

karyotype consistent with fusion of a diploid donor cell with a diploid or tetraploid host cell. (Figure 9b) Additionally many cells displayed aberrant numbers of chromosomes, and 94% had a Y chromosome which was not present in the original donor (Wang *et al.* 2003). Analysis of viral integration sites established that these hepatocytes where derived from a clonal cell population also present in the bone marrow of the recipient mice (Vassilopoulos *et al.* 2003). Camargo *et al* demonstrate that the bone marrow derived fusion partner has once in its development activated the lysozyme-M promoter which is thought to only be active in the monomyelocytic lineage (Camargo *et al.* 2004).

Common myeloid progenitor cells which lack self-renewal capacity, but give rise to a burst of differentiated myelomonocytic cells were also able to create hepatocytes by fusion as where mature macrophages derived *in vitro* from bone marrow (Willenbring *et al.* 2004).

It can be concluded that in the FAH$^{-/-}$ model of damage and repair fusion of macrophages with resident hepatocytes is the cause of the recovery from metabolic disease. The absence of fusion in early stages of development when macrophages are not yet present in the foetal liver further strengthens this observation (Stadtfeld *et al.* 2005).

Not all conversion of bone marrow to other cell types is the result of fusion

As already discussed earlier a highly purified haematopoietic stem cell could be induced to a hepatocyte phenotype by factors released from damaged liver tissue (Jang *et al.* 2004). These cells where introduced into animals and as early as two days later the authors found donor cells which produce albumin and where fully integrated into the hepatic plate. This integration of bone marrow derived cells into the liver could be enhanced with damage of the liver tissue by irradiation or with the liver toxin CCl_4. Analysis of the allosomes of many donor derived cells did not reveal any other genetic compositions as the ones expected from multinucleated liver cells. The speed of integration (few days), the extent (up to 4.5%) and the genomic stability of the cells in this experimental setup makes this study very promising (Jang *et al.* 2004).

Almeida-Porada *et al* use a different animal model for their experiments. The transplantation into a pre-immune sheep foetus has several advantages: The cells are introduced into an environment where all the organs have differentiated but still need to

grow exponentially and when the lack of a native immune system allows engraftment without the usual conditioning regimens necessary in other models. Haematopoietic and mesenchymal stem cells from various sources have been shown to populate the bone marrow and other organs of the sheep in this model (Almeida-Porada et al. 2004). Human lineage negative cells from either adult bone marrow or cord blood where transplanted into foetal sheep and contributed 2-4% of the haematopoietic cells in the bone marrow. Analysis of the livers of these animals revealed many hepatocytes of human origin staining positive for human hepatocyte antigen (HEPAR-1) and human albumin but negative for CD45. Analysis of serum revealed secreted human albumin, and genomic probes for human and sheep DNA failed to detect any events of fusion (Almeida-Porada et al. 2004).

Bone marrow transplantation in the mouse also leads to engraftment in the stem cell compartment of the skin. Bone marrow derived cells identified by GFP staining could be detected in the CD34-positive bulge region of hair follicles, in the interfollicular epidermis and the sebaceous glands. When the skin was injured by full thickness cutaneous wounds an increase of contribution from 7% to 11% could be achieved. In a male into male transplant all GFP positive cells had only one Y chromosome indicating that transdifferentiation and not fusion had taken place (Brittan et al. 2005).

Another possibility to probe for fusion events in vivo utilises the Cre-Lox system. When bone marrow cells of a reporter strain harbouring a stop-floxed GFP gene are introduced into a host expressing intracellular Cre recombinase in all cells any cells arising from fusion would excise the stop codon before the GFP coding region and become GFP positive. Tissues of recipients were analyzed 8 and 12 weeks after transplantation for BM-derived (Y-chromosome positive) epithelial cells and GFP expression. FACS analysis of single cell suspensions of lung tissue revealed that donor cells contribute up to 0.6% of cytokeratin positive cells. None of these cells were positive for GFP and all had normal autosome content, thus they could not have been created by fusion. Y-chromosome containing cytokeratin positive hepatocytes were identified in all experimental animals at levels close to 0.05%. None of these cells where GFP positive. Analysis of the skin revealed up to 0.1% of donor-origin keratinocytes again without any fusion events. RT-PCR failed to detect any GFP transcript from the muscles of transplanted animals. However, when the muscle tissue was damaged by notexin injection GFP transcript was detected in the damaged tissue but not in the contralateral uninjured muscle. The toxin also leads to necrosis of the

liver and consequentially two GFP positive hepatocytes could be found. In the experimental settings presented here the profound damage by a strong toxin seems to promote fusion events while a non-damaged environment is permissive for transdifferentiation (Harris et al. 2004).

BM cells harbouring a stop-floxed GFP-gene and Cre under the INS2 promoter which leads to GFP expression in cells activating the insulin promoter were transplanted into wild type mice by Ianus et al. Analysis of the pancreatic islets revealed multiple green cells containing a Y-chromosome which further demonstrated donor origin. These cells where expressing insulin, glucose transporter2 and transcription factors typically found in pancreatic β cells. In a second set of experiments cells which express Cre under the INS2 promoter where introduced into hosts harbouring the stop-floxed GFP gene. A fusion event would lead to excision of the stop-codons in front of the GFP gene and thus to green cells with a Y-chromosome. Although multiple Y-chromosome positive cells could again be detected in the pancreas of the experimental animals, none of them where GFP positive excluding any possibility of fusion (Ianus et al. 2003).

Cells with properties similar to ES cells reside in adult tissues

Jiang et al purified a cell population from mouse bone marrow which is viable for more than 120 population doublings in vitro. These cells termed multipotent adult progenitor cells (MAPC) express markers of embryonic stem cells like RexI and Oct4. Consistent with the ES marker expression these cells could also contribute to many adult tissues after injection into a blastocyst (Jiang et al. 2002). (Figure 2 right panel) Clonal populations of these cells where established and could be differentiated into mesodermal endothelium by VEGF-B and into neuronal lineages by bFGF. Endodermal cell types induced by FGF-4 and HGF showed functional characteristics of hepatocytes (Jiang et al. 2002). These differentiated cells express early hepatocytic markers HNF-1α, HNF-3β and GATA4 after 4 days and late hepatic markers CK18 and albumin after 14 days. A convincing demonstration of the functionality of the cells was provided by six different assays measuring urea production and secretion, albumin production, cytochrome activity, LDL uptake and gluconeogenesis. Remarkably, MAPCs differentiated to the hepatic lineage produce levels of albumin similar to those seen in monolayer cultures of primary rat hepatocytes (Schwartz et al. 2002).

When murine MAPCs where cultured with a series of growth factors specific for the neuronal lineage a mature neuronal phenotype emerged. Thorough analysis revealed

that 25% of the cells expressed markers of dopaminergic neurons, 18% expressed markers of serotonergic neurons and 52% expressed markers of GABA-nergic neurons. Co-culture of these cells with primary mouse astrocytes further matured the cell and led to a more elaborate array of axons. In a series of patch-clamp recordings the authors show occurrence of spiking behaviour that can be attributed to voltage-gated sodium channels and also suggested the occurrence of synaptic events (Jiang et al. 2003).

The fact that MAPCs can be efficiently transduced with retroviral vectors underlines their potential applicability for clinical purposes. However, the current isolation procedure involves extensive culture and replating to enrich for MAPCs which could be prohibitively slow for clinical application underlining the importance of devising new methods for direct isolation of MAPCs.

Stem cells similar to ES cells seem to be retained in multiple tissues, as evidenced by the fact that MAPCs can be isolated from bone marrow, muscle or brain. A cell population with similar potential has been isolated by Fernandes et al from skin. These cells termed skin derived precursors can be differentiated into multiple tissues in vitro, and are derived from neural crest cells (Fernandes et al. 2004). Kogler et al describe isolation of a stem cell population with hepatic potential from placental cord blood (Kogler et al. 2004), and Gianluca et al use culture conditions mimicking the microenvironment of the marrow niche to isolate multipotent cells from bone marrow (D'Ippolito et al. 2004).

Tissue stem cells may circulate in the adult organism

Work done by Ratajczak et al suggests a different model to explain the plasticity phenomena seen in many experiments. Cells which express CXCR4 and can be isolated from bone marrow according to their migration towards the CXCR4 ligand SDF-1 seem to display properties consistent with a tissue committed stem cell (TSC) phenotype (Ratajczak et al. 2003; Ratajczak et al. 2004). Markers usually associated with tissue stem cells from muscle, neuronal tissue, liver, cardiac tissue and pancreas are expressed in TCSC. Interestingly also markers usually found in more primitive cells, like Oct4, Nanog and REX-1 are present. These cells are similar to haematopoietic stem cells in the presence and absence of surface markers which could mean that they co-purify in the extraction protocols for HSC used by other researchers. As upregulation of SDF-1 is a common feature of the damage done in transdifferentiation experiments it could play a role in recruiting these stem cells to the site of damage (Kollet et al. 2003). Ratajczak

et al propose that the bone marrow is not only the niche for haematopoietic stem cells, but also a hideout for already differentiated non-haematopoietic CXCR4$^+$ tissue committed stem cells. Specific tissue stem cells isolated from the bone marrow or from peripheral blood would be the ideal candidate for cell replacement therapies.
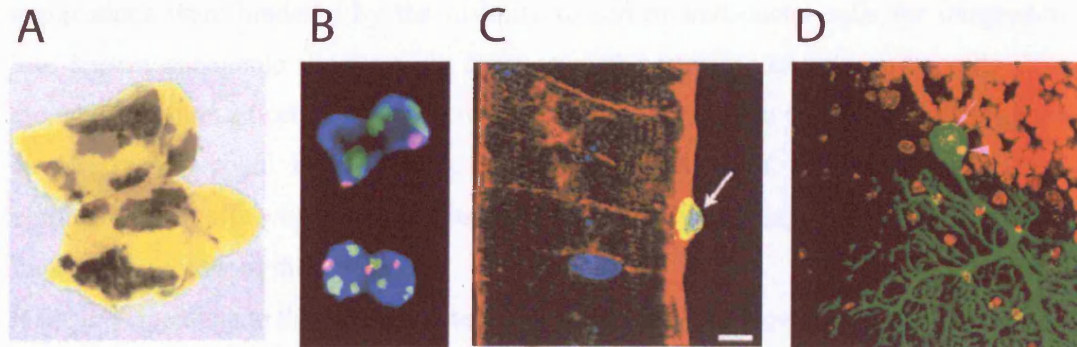
Figure 9 Bone marrow cells can have stem cell properties or fuse with resident cells

(a)HSC fuse with liver cells to rescue a fatal liver disease (blue X-Gal staining) (Lagasse *et al.* 2000). (b)Aberrant karyotype of hepatocytes generated by fusion (FISH: Y red, X green) (Wang *et al.* 2003). (c) Muscle satellite cell generated from donor bone marrow (LaBarge *et al.* 2002). (d) Binucleate purkinje cell with one host and one donor nucleus (Weimann *et al.* 2003).

Summary

Several different mechanisms which could explain stem cell plasticity have been discussed so far. Any clinical application of stem cells will have to be preceded with research into the mechanism by which cellular plasticity is achieved, to allow a realistic estimate of the impact and risks of any future treatments arising from this research.

If stem cells are to be used directly to regenerate damaged tissues the issue of fusion is of serious concern. As shown in the FAH$^{-/-}$ model fusion can create therapeutically active cells without overt negative reactions. The heterokaryons shown in the liver and brain of experimental mice do not seem have any detrimental effect and have so far not given rise to tumours. However, as the observation period of all the experiments done to date is only a small fraction of the total lifetime of the animals no final conclusion can be drawn yet. If a clinical application accepts fusion as a way of delivering therapeutic

genetic material into cells then the consequences of fusion need to be studied in more detail.

Culture of primary cells is complicated and successful culture and expansion is not possible for most stem cell populations. The possibility of generating multipotent cell lines would allow for genetic manipulation of these cells. Earlier gene-therapy applications were hindered by the inability to screen transduced cells for integration into known oncogenic sites, mainly because of the inability to culture the cells. If a clonal population of cells can be derived after transduction the problems of untargeted virus insertion could be overcome. Thorough screening of the insertion site and elimination of cells with multiple hits, or without transgene expression would greatly improve the safety of this approach.

If the damage done to the organ of interest in the patient is not genetic in nature then the generation of tissue stem cells *in vitro* would be another promising approach. Autologous transplantation would not only remove the need to find suitable donors, but would also eliminate the problem of immunological incompatibility. To achieve this, a better understanding of the mechanisms of transdifferentiation and of the molecules involved needs to be achieved.

Aims of this study
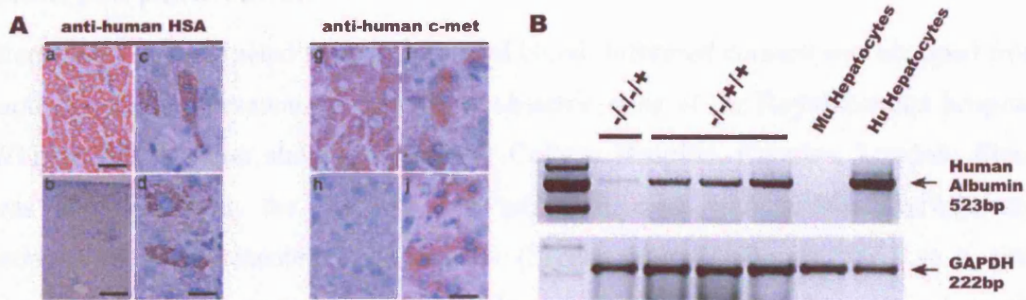
Figure 10 Human hepatocyte like cells after bone marrow transplantation

A) Immunohistochemical staining for human hepatocyte specific antigen and human c-met, B) mRNA analysis for human albumin and GAPDH

We described in 2002 that human stem cells purified from cord blood give rise to hepatocyte like cells when transplanted into NOD/Scid mice (Danet *et al.* 2002).

In these experiments stem cells were isolated by FACS sorting for a population of cells that were $CD38^-C1qRp^+CD34^{+/-}$. C1qRp (CD93) is a phagocytic receptor for C1q and the homologue to AA4 in the mouse. These cells were injected into NOD/Scid mice and after 8 weeks bone marrow engraftment could be observed. At the same time analysis of purified liver mRNA by RT-PCR revealed the expression of human albumin. Immunohistochemical staining of liver sections revealed a population of cells with clear hepatocyte morphology staining for human hepatocyte specific antigen and human c-met. (Figure 10)

The aim of this study is to further analyse the functionality and identity of these hepatocyte like cells. At the same time we attempt to devise an animal model system for enhancement of human hepatocyte like cell engraftment in the murine liver.

Materials and Methods

Stem cell purification

Stem cells were extracted from human cord blood. Informed consent was obtained from mothers awaiting cesarean section at the obstetric units of the Royal London hospital, Whitechapel, London and the University College Hospital, Camden, London. Blood was extracted from the placenta and umbilical cord with a 50ml syringe and immediately supplemented with heparin (Sigma Aldrich, Dorset, UK) to a final concentration of 1 mg/ml in 50 ml falcon tubes. Tubes were transferred to the laboratory, and stored over night on a rocker at room temperature for extraction of stem cells on the next day.

The cord blood was diluted 1:4 with sterile phosphate buffered saline (PUBS). 15 ml of ficoll-paque plus, a solution of Ficoll 400 and Diatrizoate Sodium with a density of 1.077 g/ml (Stem Cell Technologies, Meylan, France), was put in the bottom of a 50 ml tube, and 35 ml of diluted cord blood was carefully applied on top of the ficoll. Tubes were then spun at 400g for 25 minutes with no brake applied. Mononuclear cells which form a layer at the interphase of serum and ficoll were collected with a Pasteur pipette into new tubes. Cells were resuspended in a suitable volume of PBS, and three times that volume of Ammonium Chloride solution (Stem Cell Technologies, Meylan, France) was applied for red cell lysis. Cells were stored on ice for 4 min, after which 5 ml of foetal calf serum were added to stop the cell lysis. Cells were resuspended in PBS supplemented with 2% FCS and counted on a haemocytometer.

Lineage depletion

Mononuclear cells were depleted of cells expressing lineage antigens using the StemSep column system from Stem Cell Technologies. Cells were diluted to 5×10^7 cells/ml in dilution medium and 100μl of StemSep enrichment cocktail was added per ml of cells. The enrichment cocktail contains monoclonal antibodies for CD2, CD3, CD14, CD16, CD19, CD24, CD56, CD66b and Glycophorin A. An additional aliquot of 10μl of CD41 antibody was added to enhance depletion of platelets. After incubation on ice for 30 minutes 60μl/ml of thoroughly vortexed magnetic colloid was added. After another incubation of 30 minutes on ice cells were processed through a metal mesh column suspended in a strong magnetic field according to the manufacturer's

recommendations. The flowthrough of the column, containing unmarked lineage negative cells was collected. Cells were spun, counted and either frozen in FCS supplemented with 10% dimethyl-sulfoxide (DMSO) (Sigma Aldrich, Dorset, UK) or used immediately for transduction or transplantation. The column, containing the lineage positive cells was washed with 2% PBS and the cells were either discarded, or frozen down and used as accessory cells in transplantation experiments.

CD34 enrichment

Enrichment for $CD34^+$ stem cells was performed with the CD34 MiniMax enrichment kit from Miltenyi Biotec, Germany. Mononuclear cells from human cord blood were diluted in 300µl buffer per 10^8 cells. Per 10^8 cells 100 µl of FcR blocking reagent and 100 µl of Hapten-labelled Anti-CD34 antibody were added. After incubation on ice for 15 min cells were washed with 20x the volume in buffer, and resuspended in 400 µl per 10^8 cells. 100µl anti-Hapten microbeads were added, mixed and incubated again 15 min on ice. After this the cells were washed and resuspended in 500 µl Buffer. The cells were filtered through a 30µm nylon mesh and applied on an appropriate column in the provided separating magnet. After three washes the column was removed from the magnet and cells were eluted with the provided plunger. The column separation step was repeated to raise purity. Finally CD34+ cells were either frozen in FCS with 10% DMSO or used directly for transduction with lentivirus.

Lentiviral vector

The lentiviral vector used in the GFP experiments was a kind gift from Prof. A. Thrasher, Institute of Child Health, London, UK. Its backbone comprises several specialised sequences which have been shown to give high efficiency transduction of haematopoietic stem cells. (Demaison, Parsley et al. 2002; Siapati, Bigger et al. 2005)

The central polypurine tract (cPPT) sequence facilitates reverse transcription, nuclear entry and transduction. (Follenzi, Ailles et al. 2000) The Woodchuck hepatitis virus posttranscriptional regulatory element increases the level of transgene expression in non-haematopoietic cell lines (Zufferey, Donello et al. 1999) and in haematopoietic

cells. (Demaison, Parsley et al. 2002) The promoter that drives the expression of the GFP gene is from the spleen focus forming virus (SFFV) as the activity of the cytomegalovirus (CMV) promoter is suboptimal in haematopoietic cells. (Figure 11)

HIV2G (pHRSINcPPTSEW)
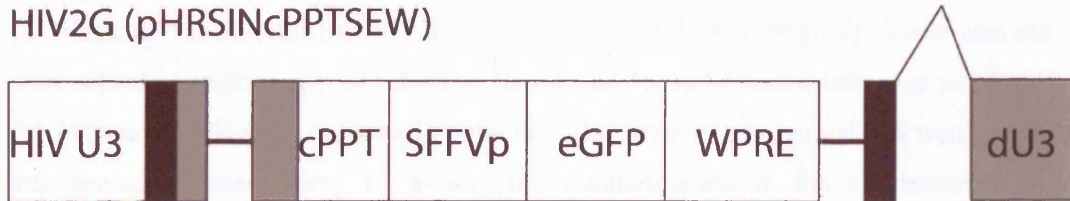
Figure 11 Schematic of GFP lentivirus used for transduction

HIV-U3: 3' LTR region, cPPT: central polypurine tract, SFFV: promoter from spleen focus forming virus, GFP: green fluorescence protein, WPRE: woodchuck hepatitis virus postranscriptional regulatory element, dU3: 5' LTR

Vector production

The viral vector used to transduce HSC was produced by transient transfection of three plasmids into 293T cells, namely the self-inactivating transfer vector plasmid, a multideleted packaging plasmid and pMD.G which provides the viral envelope. (Zufferey, Donello et al. 1999)

A total of 10^7 293T cells were seeded in a 150 cm^2 flask overnight prior to transfection. Cells were cultured in Dulbecco's modified Eagle medium (DMEM) with 10% FCS, penicillin (100 iU/ml), and streptomycin (100 µg/ml) in a 5% CO2 incubator. 17.5µg of the envelope plasmid, 32.5µg of packaging plasmid and 50µg of transfer vector plasmid were precomplexed with 0.25 mM polyethylenimine (PEI) (Sigma Aldrich, Dorset, UK) (22 kDa) in 10 ml of Optimem at room temperature for 15 min. The DNA plus PEI complexes were added to the cells, and after 4 hr incubation at 27° C the medium was replaced with fresh DMEM supplemented with 10% FCS. At 36 hrs and 60 hrs post-transfection the medium was harvested cleared by low-speed centrifugation (12000 rpm, 5 min) and filtered through 0.45µm filters. Vector particles were concentrated 20 to 100 fold by ultracentrifugation at 50.000g for 90 min at 4°. The pellet was resuspended in serum-free X-VIVO10 medium (BioWhittaker Europe, Belgium) and kept at -80°C until use. Vector titer was determined by titration on HeLa cells with serial dilutions of virus and analyzing for GFP expression at 3 to 5 days postinfection.

Lentiviral gene transfer

HSC were plated in plastic dishes with serum free X-VIVO10 medium. After adherence of the cells on Fibronectin coated petridishes the medium was supplemented with 1% human serum albumin (HSA), polybrene (4µg/ml), stem cell factor (SCF) (100 ng/ml), flt-3 ligand (FL-3) (100 ng/ml), IL-3 (20ng/ml) and IL-6 (20ng/ml). Virus particles were added at multiplicity of infection (m.o.i.) of 35 and transduction was performed for 24 hours. Cells were harvested on the next day after virus removal and transplanted into pre-conditioned mice. To avoid viral contamination in the administered cell suspensions the transduced HSCs were washed several times with culture medium before cell infusion into mice. A small aliquot of cells was analyzed for eGFP expression by flow cytometry.

Mice

NOD/Scid mice were originally obtained from The Jackson Laboratories (Bar Harbor, ME). Mice were bred in house or at Charles Rivers, UK. Animals were kept in sterile microisolators, fed rodent chow and provided with sterile water. Animals used for transplantation were 8-12 weeks old. All procedures were conducted in accordance with the Home Office Animals (Scientific Procedures) Act of 1986. In few experiments β2/NOD/Scid mice were used. To obtain methallothionein null mice suitable for xenotransplantation the 129S7/SvEvBrd-Mt1tm1BriMt2tm1Bri mouse strain stock number 002211 was obtained from Jackson lab and backcrossed with NOD/Scid mice. Maintenance of MT-/- and SCID mutations was supervised by genomic PCR and 8 rounds of backcrossing were performed before the first experimental animals were used. uPA$^{+/-}$rag2$^{-/-}$ mice were a kind gift from Dr. Jörg Petersen.

Liver toxin administration

Administered toxins were carbon-tetra-chloride (CCl$_4$) (BD Biosciences, Oxford, UK), Paracetamol and Retrorsine (Sigma, Dorset, UK). The average weight of the experimental animals at time of injection was 25 grams. CCL$_4$ was diluted in autoclaved corn oil (Sainsburys) on the day of injection. To apply 40µl CCl$_4$ per animal a mixture of 40µl CCl$_4$ and 260µl oil was injected. Paracetamol was diluted in PBS and filtered through a .22µm filter. 20mg/ml Retrorsine was dissolved in pure sterile

Ethanol at 55°C with shaking over night to obtain a stock solution which was divided into aliquots and frozen. To administer a 70mg/kg dose to a 25g mouse 87µl of stock solution was diluted with 213µl sterile PBS and immediately injected.

Cadmium treatment of NOD/Scid/met mice

To induce liver damage in the metallothionein knockout mouse model NOD/Scid/Mt$^{-/-}$ animals were treated with 5 to 10µmol/kg $CdSO_4$ dissolved in PBS by i.p. injection. Treatment was given in two week intervals. The dose which was well tolerated was determined to be 5 µmol/kg for both males and females.

Bone marrow transplantation

To facilitate bone marrow transplantation animals were treated with 375 RAD gamma radiation. Mice aged 8-12 weeks were irradiated inside the sterile microisolator for 264 seconds at 1.42 RAD/second delivering a total of 375 RAD using a ^{137}Caesium source up to 24 hours before intravenous injection of cells. Cells for injection were diluted in PBS supplemented with 2% FCS to obtain a final injection volume of 200µl. The mice were placed in a hotbox at 42°C for several minutes to dilate superficial blood vessels. After that mice were restrained and the cells were injected into the tail vain with a 0.5ml syringe. After a period of observation mice were returned to the storage racks in their cages.

Assessment of BM engraftment

Engraftment into the bone marrow was determined by flow cytometry. Animals were sacrificed by cervical dislocation, and femurs, tibias and the iliac crest were collected. Using a 1 ml syringe containing sterile PBS the bone marrow was flushed from the bone cavity into 4 ml polypropylene tubes. After dissociation of clumps 3 ml of Ammonium Chloride solution were added and tubes were stored on ice for 7 min to lyse red cells. Cells were spun down, washed once and then resuspended in 500µl PBS 2% FCS and filtered through a sterile 40µm mesh. 50µl of this solution which contained an average of 2 million cells was used for staining. 5µl of monoclonal, fluorochrome conjugated antibodies against human CD45, CD19 and CD33 were added

to the aliquot of cells and incubated for 30 min on ice. After two washing steps cells were resuspended in 300μl PBS 2%FCS supplemented with DAPI (4,6 diamidino-2-phenylindole). Analysis was performed using an LSR (Becton-Dickinson).

Assessment of liver engraftment

Liver perfusion

Animals were anaesthetised in a chamber flooded with Halothane (2-Bromo-2-Chloro-1,1,1-Trifluoro-ethane). During the operation constant anaesthesia was provided by a face mask supplying an air/halothane mixture. After successful anaesthesia the animal was immobilised with tape on a sterile workbench on top of several paper towels. The abdomen was cleaned with 70% ethanol and opened with scissors from the sternum to the genitals. The intestines were relocated to one side with a cotton swab, and the liver lifted to expose the inferior vena cava and the portal vein. Eagles basic salt solution (EBSS) without Ca and Mg (GIBCO, Paisley, UK) supplemented with 0.5mM EGTA (solution 1), EBSS with Ca and Mg plus 10mM Hepes, ph7.4 (solution 2) and collagenase solution (solution 2 with 0.15 Wünsch units /ml Liberase 3 (Roche UK, Welwyn Garden City, UK)) were prewarmed in a 39° water bath. A standard infusion drip and a children vein catheter were used for perfusion. The tubing of the infusion drip was placed in the buffer, and then through a Pharmacia peristaltic pump operating at 5ml/min. The vena cava was cleared of surrounding tissue. A standard surgical thread was looped around the vena cava before the vein was catheterised and the thread was tied around the vein and the catheter to prevent slipping. Then the peristaltic pump was switched on and the portal vein on the liver was cut open. Now the chest cavity was opened and the superior vena cava was clamped. The liver was perfused with solution 1 for 3 minutes, then solution 2 for 2 minutes and then with collagenase solution. After 8-15 minutes the liver was completely digested and the catheter removed. The gall bladder was dissected out and the liver removed from the animal. In a petridish the liver was now carefully dissociated in warm collagenase solution. The cells were collected and filtered through a nylon mesh into a sterile 50ml tube containing warm DMEM with 10% FCS. The cells were pelleted by a 60-90sec spin at 1000g. The supernatant was removed and the pellet resuspended in 50ml medium for another wash. Viability was assessed by trypan blue staining (0.04%) and was typically between 70 and 80%.

Histology

Animals were sacrificed and tissues were removed. One part of the tissues was fixed in 4% NBF over night and embedded in paraffin blocks. Other parts were frozen in liquid nitrogen. For histology paraffin sections and frozen sections were cut and stained with haematoxylin and eosin.

Immunohistochemistry

Liver tissue was collected from animals and either immediately frozen in liquid nitrogen or fixed overnight in 4% neutral buffered formalin (NBF). Cryosections were thawed, fixed for 5 minutes in NBF at room temperature, washed, incubated in acetone at -20°C for 10 minutes and blocked with 1:25 swine serum with 0.1 % Triton-X for 30 minutes. After washing, antibodies against human nuclei or human mitochondria (Chemicon, Temecula, CA) were applied at 1:20 dilution in PBS for 1 hr. Secondary anti-mouse antibodies bearing fluorochromes Alexa 488 or Alexa 594 were used at 1:100 dilution for visualization. Paraffin sections were cut, de-waxed in Histoclear (RaLamb, East Sussex, UK) and blocked in 3% hydrogen peroxide for 10 minutes. Antigen unmasking was performed by microwaving at 700 watts for 10 minutes in citrate buffer pH 6. After blocking, anti-eGFP polyclonal rabbit serum (Invitrogen, Paisley, UK) was applied 1:500 in PBS while anti-human-albumin antibody (Cedarlane, Ontario, Canada) was used 1:25. Secondary antibodies conjugated to a fluorochrome (anti-mouse or anti-rabbit Alexa Fluor 594 or Alexa Fluor 488, Invitrogen) were used at 1:100 dilution, while horseradish peroxidase conjugated secondary antibody (Dakocytomation, Cambridgeshire, UK) was used at 1:400 for visualisation with DAB (Sigma-Aldrich, Dorset UK). Detection of incorporated BrDU into mitotic cells was performed on paraffin sections. After de-waxing and blocking, rat anti-BrDU antibody (Seralab, Leicestershire, UK) was applied in a 1:500 dilution for 1 hr. Anti-rat HRP-conjugated secondary antibody (Sigma, Dorset, UK) was used at 1:100.

RT-PCR

Approximately 25 mg of liver tissue were cut from frozen tissue samples. Tissue was homogenised in Trizol reagent (Invitrogen) with a pistil, and RNA was extracted according to the manufacturer's protocol. 3 µg of RNA were subjected to DNase digestion (Quiagen Ltd. Sussex UK) and subsequent generation of cDNA was

performed with the Sensiscript kit (Quiagen) in 20 μl volume. 2 μl of cDNA was added to PCR reactions with primers for

GAPDH (5'-catcaagaaggtggtgaagcag/ 3'-tgtgggccatgaggtccaccac),

human β-Actin (5'-caggctgcttccagctcc/ 3'-gggtataacgcaactaagtcatag),

eGFP (5'-accccgaccacatgaagcagc/ 3'-cgttggggtctttgctcaggg),

human alpha-anti-Trypsin (5'-gctgaagaccttagtgatgc/ 3'-ctttgaagtcaaggacaccg) and

human Albumin (5'-cattagctgctgattttgttgaaag/ 3'-tgtgcagcattttgtgactctg).

PCR was performed with the High fidelity PCR kit (Roche) using buffer 3. PCR conditions were 94°C 30 seconds, annealing temperature for 30 seconds and extension at 72°C for 1 minute. Annealing temperature was 60°C for β-Actin, albumin and GAPDH, 62°C for α-anti-Trypsin and 67°C for eGFP. PCR products were separated by agarose gel electrophoresis and stained with ethidium bromide.

Micro-dissection and single cell PCR

Frozen tissue sections were stained for eGFP, but after dehydration no cover-slip was applied. Sections were placed on the stage of a PALM micro-dissection microscope (PALM microlaser technologies AG, Bernried, Germany). A standard PCR tube cap containing 15μl of PCR buffer supplemented with 0.5% Triton was placed above the section, and eGFP stained cells were positioned in the centre of the field of view. The laser was used to excise the single eGFP positive cell from the surrounding tissue, and then to catapult it into the tube cap. The tube was closed, supplemented with 2 μl proteinase K (20 μg/ml) and incubated at 48° C overnight. This was followed by 60 rounds of i-PEP PCR as described. (Dietmaier, Hartmann et al. 1999) 3 μl of the reaction were used as template for nested PCR specific to the human and mouse TNFα locus and for eGFP.

Primers:

human TNFα

outer: 5'-aggaacagcacaggccttagtg/ 3'-aggaacagcacaggccttagtg,

inner: 5'-ggatactcagaacgtcatggcc/ 3'-ctcataccagggcttggcct,

mouse TNFα

outer: 5'-ccaccatcaaggactcaaatg/3'-cactgggtcctccaggaca,

inner: 5'-ggctttccgaattcactggag/ 3'-ccccggccttccaaataaa.

eGFP outer as mentioned before,

inner: 5'-gcatcgacttcaaggaggac/ 3'-tgctcaggtagtggttgtcg.

PCR was performed as mentioned before with an annealing time of 65°C for the first round and 55°C for the second round. Efficiency of PCR was determined by cutting hepatocytes from normal human and mouse liver tissue.

Fluorescence In Situ Hybridisation

Frozen sections were fixed in 4% PFA for 10 minutes and pictures of natural eGFP fluorescence were immediately taken on a Zeiss LSM 510 confocal microscope. The position of individual eGFP positive hepatocytes was saved with custom made software, and subsequent FISH analysis was performed on the slide. The slides were digested with 0.005% pepsin in 0,9% saline at pH 1.5 for 2-5 minutes. Following dehydration, probes for either mouse Chromosome Y, human Chromosome 1 or human centromeres (Cambio Cambridge, UK) were applied according to the manufacturer's recommendations. The tissue section was then covered with a cover-slip and sealed with rubber glue. Sections were then incubated at 80° C for 10 minutes for co-denaturation of nuclei and probes. After overnight incubation at 37° C the sections were washed in 0.4% SSC at 72° C for 30 seconds and mounted in fluorescence mounting medium (Dakocytomation, Cambridgeshire, UK) supplemented with DAPI. The slides were again inserted into the confocal microscope, the exact position saved earlier was reloaded, and pictures of the nuclei of the same cells photographed before were taken. Overlay images of eGFP and FISH signals were produced using Adobe Photoshop.

To obtain FISH signals on paraffin embedded tissues, sections were dewaxed, rehydrated and incubated in 1M sodium thiocyanate at 80° C for 10 min. Then sections were washed in distilled water and incubated in 5mg/ml pepsin in 0.9% Saline ph 2 for 5-15 min at 37°C. After this sections were washed and probes were applied similar to the protocol for frozen sections. If HSA staining was performed before the FISH

protocol the digestion time was reduced as the tissue was already more accessible to the protease due to the microwaving step in the HSA immunohistochemistry protocol.

Results

Chapter 1 Generation of an environment conducive to cell engraftment

Introduction

The engraftment of cells within an organ can be conceived as a two stage process. The first stage is the homing following the transplantation of cells. This stage could be facilitated by damage to the organ. If liver tissue is in an active process of regeneration, accompanied by the production of growth factors and signalling molecules the homing of cells injected into the tail vein could be enhanced. Increasing the homing would lead to a higher amount of cells in the tissue from the beginning of the experiment. The second stage of cellular contribution to an organ would be expansion following later stage damage. If damage to a tissue would occur when there is already a nascent population of engrafted cells in the organ, these could be induced to proliferate and expand, thus producing higher levels of donor derived cells in the tissue.

To establish an animal model in which we can selectively induce damage to liver tissue we tested several chemical compounds for their effect. The toxins used in this study where selected according to several criteria.

Specificity
When applying a toxin to induce damage to a specific organ, all non-specific impairment of other organs is detrimental to the aims of the study. Toxins selected for this study had to have an established phenotype in liver tissues without causing destruction of other cell types. Absolute specificity is very difficult to achieve, so a compromise had to be made between dosage and damage to retain the tissue specificity of the toxin.

Reversibility
The damage done to the tissue needed to be reversible. The rodent liver has an amazing ability to regenerate itself even after severe damage. Regeneration from damage caused

by the toxins used here usually commenced after 7 to 14 days. Liver morphology returned to a normal phenotype, and animals looked healthy again.

Repeatability

As we hoped to expand a putative stem cell population engrafted into the liver to generate therapeutically promising levels of liver repopulation our treatments had to be repeatable. This would allow to induce damage not only at the timepoint of actual cell transplantation, but also at a later stage, where successful bone marrow engraftment has been established, and secondary colonization by bone marrow derived cells via the circulation was possible.

Legal considerations

As all our animal experiments had to be approved by the Home Office in a lengthy process, we were restricted in the possibilities of not only choice of toxins, but also in experimental design.

Acetaminophen (Paracetamol)

Acetaminophen is a commonly used analgesic and antipyretic compound. Acetaminophen hepatotoxicity due to overdose is the most frequent cause of fulminant liver failure, with a mortality rate up to 90% (Makin et al. 1994). The mechanism of this liver injury is not fully understood, however, the generation of reactive oxygen species, the transcription factor NF-κB, nitric oxide and lipid peroxides have been postulated to be the major factors involved in this mechanism. Oral administration of antioxidants significantly attenuates the acetaminophen induced liver damage (Oz et al. 2004). As the toxicity of acetaminophen in NOD/Scid mice was not known in advance, a pilot experiment using three doses of acetaminophen (100, 200, 300 mg/kg) was performed. Liver sections where analyzed for overt signs of necrosis 24 hrs after i.p. injection. 300 mg/kg acetaminophen induced only mild morphologic changes when analyzed with hematoxylin & eosin (H&E) staining. As the maximal dose included in our animal experimentation license was 350 mg/kg we subsequently performed a timecourse analysis of 350 mg /kg acetaminophen in 16 mice. Animals were injected intra-peritoneal with 200μl PBS containing 8.75 mg acetaminophen which is equivalent to 350 mg/kg for NOD/Scid mice of an average body weight of 25 grams. To assess the

mitotic activity in the liver tissue mice where additionally injected with BrDU i.p. at a dose of 50 mg/kg body weight 24 hours before sacrifice. Mice were analyzed at 2, 3 and 4 days after i.p. injection of acetaminophen.

The top panel of Figure 12 depicts hematoxylin & eosin staining of the livers of experimental animals. The leftmost image is from a control animal, which had not received any acetaminophen. The other three panels follow the timecourse from left to right. Morphological changes are barely visible in any of the three timepoints. (Figure 12a) The BrDU incorporation into newly formed nuclei is shown in Figure 12b. Nuclei that have been subject to mitosis in the last 24 hours are stained by the anti-BrDU antibody. However, no increase in the number of stained nuclei is visible when comparing the untreated control (leftmost panel) with sections from experimental animals.

As evidenced by Figure 12, liver damage with the maximal dose of acetaminophen permitted by our animal licence was limited, and no increase in mitotic activity of the liver parenchyme could be observed. Acetaminophen is well tolerated in NOD/Scid mice at a dose of 350 mg/kg body weight and does not induce gross changes in liver morphology or increased mitosis. This observation prevented use of acetaminophen as a hepatotoxin in this study.

A H&E

B BRDU
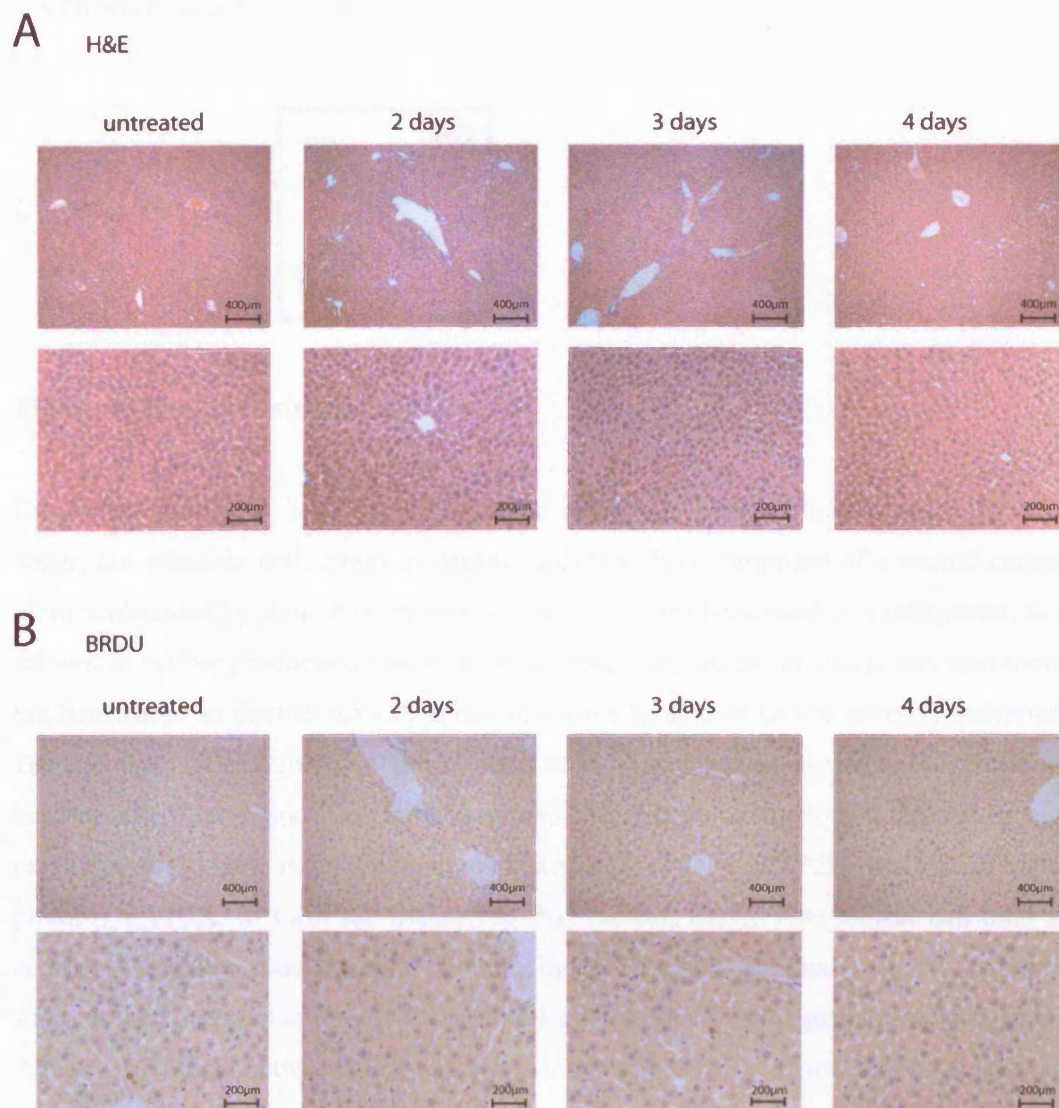
Figure 12 Acetaminophen toxicity of NOD/Scid mice

A) Timecourse of acetaminophen intoxication in H&E staining. Mice were injected with 350mg acetaminophen per kilogram body weight. 24 hours before sacrifice mice were treated with BrDU to allow staining of cells that have performed mitosis in the last 24 hours. At the indicated timepoints animals were sacrificed, livers were harvested and processed for histology. B) Tissue sections from the same animals stained for BrDU incorporated by cell division.

Carbon-Tetra-Chloride
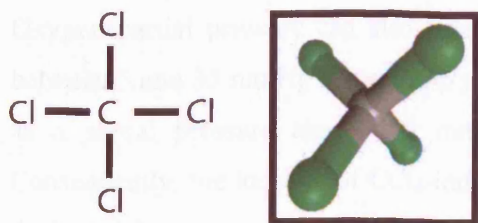
Figure 13 Chemical structure of CCl₄

Carbon-tetra-chloride is a heavy (1.6g/ml), colourless liquid which is not soluble in water, but miscible with common organic solvents. It is composed of a central carbon atom surrounded by four chlorine atoms. (Fig. 13) It has been used as a refrigerant, as a solvent in rubber production and as a grease removing agent for machinery and tools, but because of its distinct toxicity it has now been banned or its use severely restricted. Despite this, CCl_4 remains a potent tool to elucidate the mechanisms of action of hepatotoxic effects such as fatty degeneration, fibrosis, hepatocellular death, and carcinogenicity. CCl_4 is activated by cytochrome (CYP)2E1, CYP2B1 or CYP2B2, and possibly CYP3A, to form the trichloromethyl radical, CCl_3. This radical can bind to cellular molecules (nucleic acid, protein, lipid), impairing crucial cellular processes such as lipid metabolism with the potential outcome of fatty degeneration (steatosis). Adduct formation between CCl_3 and DNA is thought to function as an initiator of hepatic cancer. This radical can also react with oxygen to form the trichloromethylperoxy radical CCl_3OO, a highly reactive species. CCl_3OO initiates the chain reaction of lipid peroxidation, which attacks and destroys polyunsaturated fatty acids, in particular those associated with phospholipids. This affects the permeability of mitochondrial, endoplasmic reticulum, and plasma membranes, resulting in the loss of cellular calcium sequestration and homeostasis, which contributes heavily to subsequent cell damage.

None of these processes per se is considered the ultimate cause of CCl_4-induced cell death, but by cooperation they achieve a fatal outcome, provided the toxin acts in a high single dose, or over longer periods of time at low doses. At the molecular level CCl_4 activates tumour necrosis factor (TNF)alpha, nitric oxide (NO), and transforming

growth factors (TGF)-alpha and -beta in the cell, processes that appear to direct the cell primarily towards (self-)destruction or fibrosis. TNF alpha pushes toward apoptosis, whereas the TGFs appear to direct towards fibrosis.

Oxygen partial pressure can also direct the course of CCl_4 hepatotoxicity. Pressures between 5 and 35 mmHg favour lipid peroxidation, whereas absence of oxygen, as well as a partial pressure above 100 mmHg, both prevent lipid peroxidation entirely. Consequently, the location of CCl_4-induced damage mirrors the oxygen gradient across the liver lobule.

DNA of dividing cells. In the normal liver only very few hepatocytes are mitotically active (Figure 12b). After damage however this number rises rapidly leading to up to 50% BrDU positive hepatocytes (Figure 15). As BrDU will stain the parent cell as well as the daughter cell after cell division, this allows to estimate that about 25% of hepatocytes have been generated de novo in the course of one day of damage repair. The highest percentage of mitotic nuclei is present at day 4. (Figure 15b)
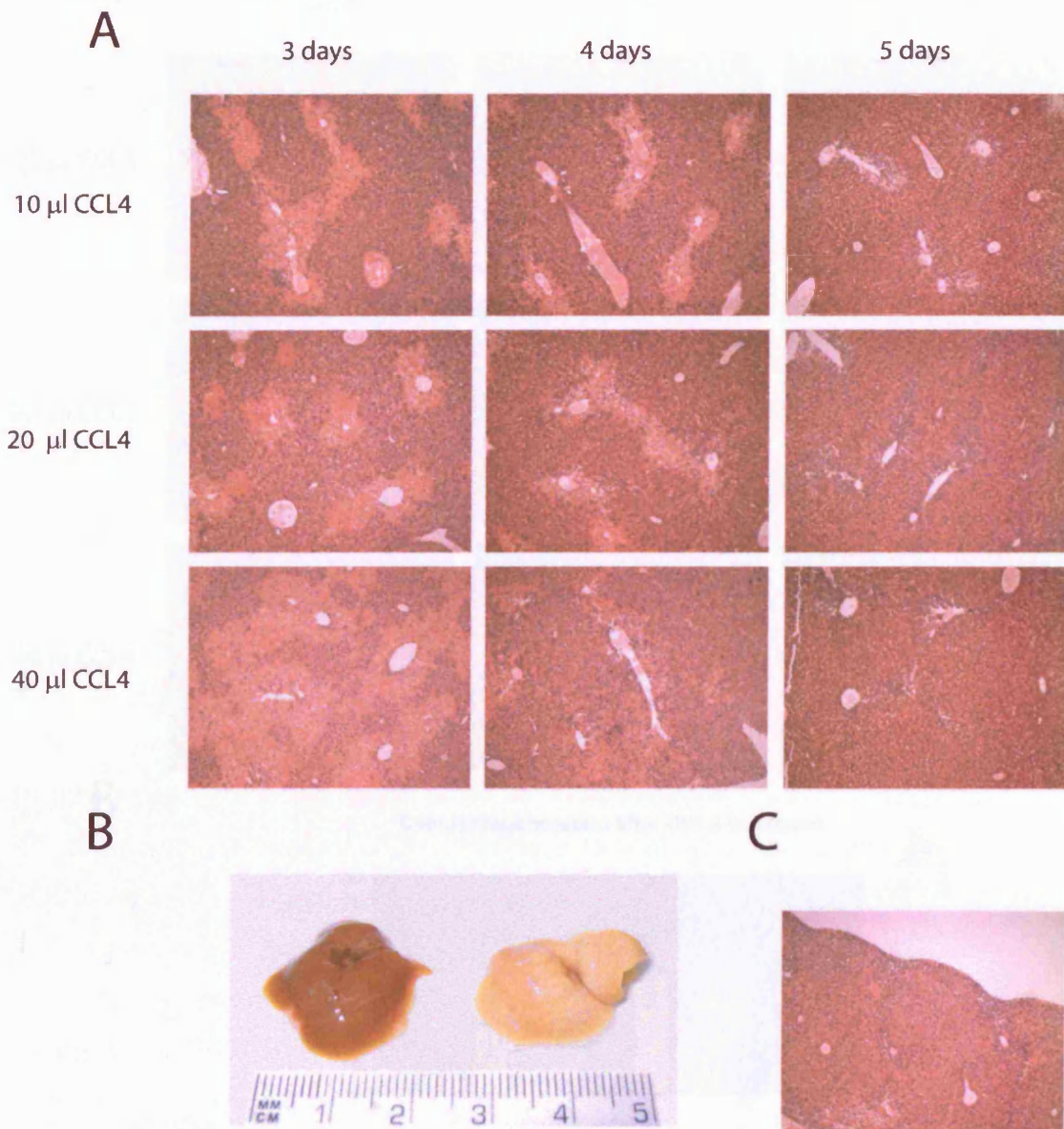
Figure 14 Liver damage by different doses of CCl$_4$

A) H&E staining of liver sections from experimental animals. Clearly visible is extensive damage around the central veins in all treatment groups on the 3rd day of the timecourse experiment. B) Macroscopic view of whole liver after 7 days. Although cellular regeneration will have taken place by now the liver still displays discolouring and liver tissue is hard and rigid. C) Because of necrosis inside the liver lobe the surface of the liver sinks in above sites of damage leading to an uneven surface and rugged look of the organ on day three of regeneration.
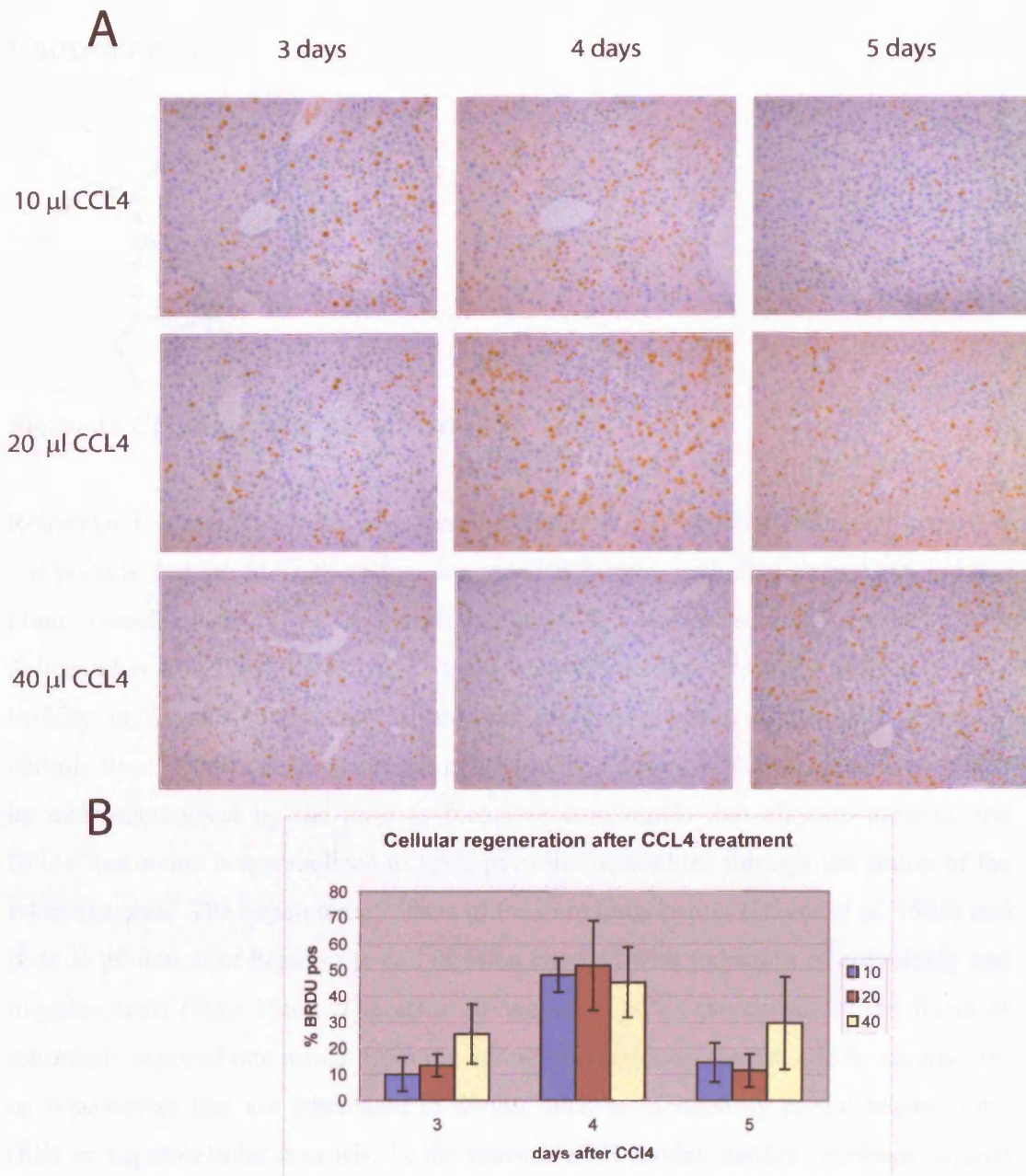
Figure 15 BrDU staining of liver sections after CCl₄ damage

A) The same tissue samples shown in Figure 14 stained for BrDU B) BrDU positive and negative cells were counted and the percentage of BrDU positive nuclei was calculated from three different fields of view.

Retrorsine
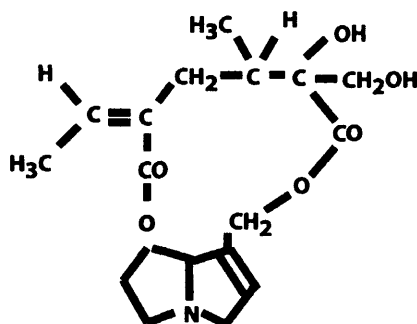
Figure 16 Chemical structure of retrorsine

Retrorsine is a member of the pyrrolizidine alkaloid (PA) family of naturally occurring compounds that are toxic to various mammalian tissues, including liver, lung, kidney, brain, muscle, heart, thymus, lymph nodes, and blood vessels (Bull *et al.* 1959; Schoental *et al.* 1959). Pyrrolizidine alkaloids were studied originally because of their toxicity in animals, particularly sheep and cattle where they cause both acute and chronic liver injury. These agents are natural plant substances that are selectively taken up and metabolised by the liver to bioactive compounds that alkylate proteins and DNA. Retrorsine is metabolised to toxic pyrrolic metabolites through the action of the P450 enzymes. The hepatotoxic effects of PAs are long-lasting (Hayes *et al.* 1985) and include inhibition of hepatocyte cell division coupled with induction of polyploidy and megalocytosis (Jago 1969). The acute development of megalocytosis in the livers of retrorsine–exposed rats results from the antimitotic action of the PA and its metabolites on hepatocytes that are stimulated to divide, such as induced by partial hepatectomy (PH) or hepatocellular necrosis. In the retrorsine/PH model, neither retrorsine injured fully differentiated hepatocytes nor do oval cells proliferate abundantly to contribute significantly to the restoration of liver mass after PH. Instead the entire liver mass is reconstituted after PH through a cellular response that is mediated by the emergence and rapid expansion of a population of small hepatocyte-like progenitor cells, which share some phenotypic traits with foetal hepatoblasts, oval cells and fully differentiated hepatocytes (Gordon *et al.* 2000). Small hepatocytes appear as isolated clusters of 3 to 6 cells at 3 days post-PH and do not co-localise with oval cells. These small cells are found in all lobular zones unlike oval cells which typically locate in the periportal areas. Small hepatocyte-like cells proliferate readily and by 30 days post-PH normal liver

structure is restored and the tissue is nearly indistinguishable from that of control animals. Although the proliferation of small hepatocyte like cells ultimately leads to complete repair of damaged liver tissue it nevertheless takes significantly more time (30 days retrorsine/PH vs. 10 days control PH) to achieve complete regeneration. The origin of the small hepatocyte like cells is still being debated; however, more recent research indicates that mature hepatocytes escaping the mitotic block mediated by retrorsine might be the source (Avril *et al.* 2004).

The effect of retrorsine can be used to prevent regrowth of host liver tissue in transplantation experiments. Rats treated with retrorsine were subjected to PH and simultaneous infusion of isolated hepatocytes from a donor animal (Laconi *et al.* 1998). In this animal model donor hepatocytes are taken from a rat strain expressing an enzyme (DPPIV) missing in the host animal. Immunohistochemical staining for this enzyme allows for reliable detection of donor hepatocytes in the host liver. After 2 weeks donor hepatocytes contributed 3-5% of liver mass, rising to 15-25% at one month and peaking at 40-60% after 2 months. This level of engraftment is stable from there on. In a follow-up study the same group could show that the growth stimulus provided by PH is not necessary to achieve liver repopulation by transplanted hepatocytes. In rats treated only with retrorsine (30mg/kg 2x two weeks apart) transplanted hepatocytes occupied 80% of liver parenchyme after 9 months (Laconi *et al.* 2001). Another interesting issue raised in this study is the impact of different susceptibility of female and male rats to retrorsine treatment. Female rats are reported to be relatively resistant to the acute toxicity of retrorsine, with an LD50 almost five times as high as that for male rats of the same age, however female rats also undergo massive liver replacement by transplanted cells with percentages of repopulation similar to these observed in males. This finding underscores that the immediate toxic effects of retrorsine, i.e. dilation and congestion of hepatic sinusoids, mild inflammation and biliary epithelial cell proliferation are not a major factor in determining the efficiency of cell engraftment.

As the retrorsine model would be a powerful tool to investigate liver regeneration by hematopoietic progenitor cells we tested several aspects of retrorsine with regards to the NOD/Scid xenotransplantation model.

Administration of retrorsine

In the original publications retrorsine was administered by dissolution in low pH. Retrorsine (12,18-dihydroxysenecionan-11,16-dione;β-longilobine; Sigma, St. Louis, MO) was added to distilled water at 10mg/ml and titrated to pH 2.5 with 1N HCl to completely dissolve the solid. Subsequently the solution was neutralised using 1N NaOH and NaCl was added for a final concentration of 6mg/ml retrorsine and 0.15mol/L NaCl (pH 7.0). However, the neutralisation of small amounts of unbuffered solution was difficult, and the retrorsine precipitated immediately after neutralization rendering the solution unusable after approximately 20 minutes. In addition, the retrorsine solution was badly tolerated by animals, leading to visible stress and discomfort to the animals.

In subsequent experiments retrorsine was dissolved in EtOH. A stock solution of 20mg/ml was prepared and diluted with distilled water before administration. The alcoholic solution was well tolerated, leading to no visible stress other than deep sleep for several hours as an effect of the solvent.

Dose response:

All previous work with retrorsine was done in rat. To establish a dose of retrorsine that is tolerated in NOD/Scid mice we performed initial experiments with several different doses. Mice were injected intra-peritoneal with control saline, 30mg, 90mg and 300mg/kg body weight retrorsine in groups of 6 mice. All animals in the 90mg and 300mg groups died within few hours from the immediate effects of the toxin. In a subsequent similar experiment using retrorsine dissolved in alcohol we established 70mg as a dose well tolerated in NOD/Scid mice.

Long term tolerance

In the rat model retrorsine administration leads to visibly growth arrested hepatocytes even in the absence of a growth stimulus like PH or CCl_4 treatment. To exclude any long term toxicity in our model we performed long term observation of mice treated with retrorsine.

4 NOD/Scid animals were treated with retrorsine 30mg/kg four times in weekly intervals. After 8 weeks animals were sacrificed and liver morphology was analyzed in H&E stained liver sections. As is shown in Figure 17a no changes in liver morphology

could be observed. In rats the treatment with retrorsine induces formation of megalocytosis. In our model no obvious megalocytic hepatocytes could be observed.

Effectiveness of retrorsine in the mouse

In rats, retrorsine delays the recovery from PH about threefold from 10 days to more than 30 days. To assess the efficiency of retrorsine in the mouse model we induced massive tissue necrosis by CCl_4 intoxication after pre-treatment of animals with retrorsine. Animals received either alcohol alone or one or two injections of retrorsine (30mg/kg body weight, dissolved in ethanol) one week apart. Two weeks after the last retrorsine treatment an injection of 20μl CCl_4 in oil was given which has been shown to induce severe necrosis of liver parenchyme extending to up to 20% of the surface area in liver sections. Two animals of all three groups were sacrificed on days 3, 4, 5, 6 after CCl_4 treatment receiving a BrDU injection 24 hrs before sacrifice. Liver sections from all animals were stained with H&E. In contrast to the strong mitotic arrest induced in rat hepatocytes retrorsine does not impair liver regeneration in NOD/Scid mice as efficiently as in rats. As shown in Figure 17b regeneration of liver tissue is similar in retrorsine treated animals (upper panels) to animals without retrorsine pre-treatment (lower panels). The necrotic areas are quickly filled with hepatocytes and on day 5 post CCl_4 treatment liver morphology is nearly normal again. To assess regrowth efficiency we stained the liver sections with antibodies against BrDU and determined the percentage of BrDU positive nuclei by counting. As can be seen in Figure 17c animals treated with retrorsine show a higher percentage of BrDU positive hepatocytes on day 4 after CCl_4 treatment, but no other significant delay in tissue repair. Due to a shortage of retrorsine no more preparatory experiments were performed.

Figure 17 Effect of retrorsine on liver tissue in NOD/Scid animals

A) Long term retrorsine exposure has no negative effect on liver tissue morphology Animals were treated with 4x 30 mg/kg retrorsine and analysed after 8 weeks. B) Liver regeneration after hepatocyte damage with 20µl CCl_4 is not significantly inhibited by two doses of 30mg/kg retrorsine. C) Retrorsine treatment marginally delays repair after CCL_4 induced liver damage. 30mg/kg retrorsine were administered once or twice two weeks before CCl_4 damage. Animals were given injections of BrDU 24hrs before sacrifice, and the percentage of BrDU positive hepatocytes was counted.

Cadmium

Inducing damage to tissue with toxic substances allows preparing the tissue for engraftment and creating a regenerative environment. Unfortunately no mechanism exists to prevent administered toxins to damage freshly engrafted donor tissue making it impossible to apply repeated rounds of toxin after initial engraftment has taken place. The success of the FAH$^{-/-}$ mouse model in live regeneration research is based largely on its ability to discriminate between host and donor cells. This allows for selective removal of cells of the host while preserving the newly engrafted donor cells.

To generate a similar system, albeit able to be used in xenotransplantation of human cells we devised a backcrossing strategy to backcross a mouse strain in which the genes for both metallothionein I and II had been knocked out onto the NOD/Scid background.

Metallothioneins (MTs) are characterised by their low molecular weight, high cysteine content, lack of aromatic residues, and the presence of 7-12 metal atoms per molecule (Kagi et al. 1987). In mammals, the cysteine residues are absolutely conserved in number and serve to coordinate heavy metal atoms such as zinc, copper and cadmium via mercaptide linkages. Two major isoforms of MT have been described in mammals, and in mouse the genes encoding these two isoforms are 6 kb apart on chromosome 8. MTs have been postulated to detoxify metals, play a role in zinc and copper homeostasis during development and protect against reactive oxygen species. The MT$^{-/-}$ mouse strain was originally described by Masters et al in 1994 (Masters et al. 1994). In it both genes for metallothionein I and II were inactivated by insertion of a stop codon in the first exon. The mutant animals do not have an abnormal phenotype under standard conditions. However, the ability of MT-null mice to detoxify cadmium is severely impaired. A daily dose of 10μmol cadmium/kg body weight, which is well tolerated by wild type animals, killed all male animals within 48 hrs and 50% of females in four days. Livers from cadmium-injected MT-null mice exhibited consistent histopathological changes including focal areas of cellular degeneration and necrosis, congestion, and haemorrhaging. In addition, all control and MT-null males showed signs of extensive testicular necrosis. Repeated exposure of these animals to cadmium exacerbates the effect (Habeebu et al. 2000). In a different experimental setup Liu et al showed that this strain also is more sensitive to chronic oral cadmium-induced nephrotoxicity (Liu et al. 2000).

The MT$^{-/-}$ strain has been maintained at Jackson laboratories under the strain name 129S7/SvEvBrd-Mt1^{tm1Bri}Mt2^{tm1Bri}. We obtained the strain from Jackson laboratories, and used standard backcrossing to introduce the MT$^{-/-}$ mutation onto the NOD/Scid background. Backcrossing was performed by Charles Rivers UK for 10 generations.

Male NOD/Scid mice tolerate 5μmol/kg CdSO$_4$

To be able to selectively damage the host tissue in xenotransplantation experiments we needed to define a concentration of Cadmium that is well tolerated in normal NOD/Scid mice. This is necessary to prevent damage to engrafted hepatocyte cells. Because male MT$^{-/-}$ mice have been reported to be very sensitive to cadmium treatment only half the dose used for females was tested in this experiment. Due to a lack of animals we could not investigate the dose-response of female animals.

Normal NOD/Scid animals were intoxicated with a solution of CdSO$_4$ via i.p. injection. After 1, 3 and 7 days animals were sacrificed and H&E sections of liver and testis were prepared. As can be seen in the upper panel of Figure 18a this dose of cadmium did not have any influence on liver morphology in normal NOD/Scid animals. The sections from testis however present widespread necrosis as early as 24 hrs after cadmium treatment. Immediately after treatment complete tissue destruction is evident, and can not be repaired within the timeframe of this experiment

MT$^{-/-}$/NOD/Scid mice are more sensitive to hepatotoxic effect of cadmium

In male MT$^{-/-}$/NOD/Scid mice exposed to the same regimen of intoxication a clear hepatotoxic effect of cadmium is visible. 24 hrs after intoxication foci of necrosis appear in the liver tissue. In contrast to the centrilobular damage induced by CCl$_4$ these foci are not located around the central vein of the liver lobe but appear dispersed in the tissue well away from both central veins and portal triads. After initial necrosis at around day three small hematopoietic cells infiltrate the sites of necrosis. After one week the necrotic foci have been repaired, and liver morphology appears normal again. However, small aggregates of hematopoietic cells are still visible at this time.
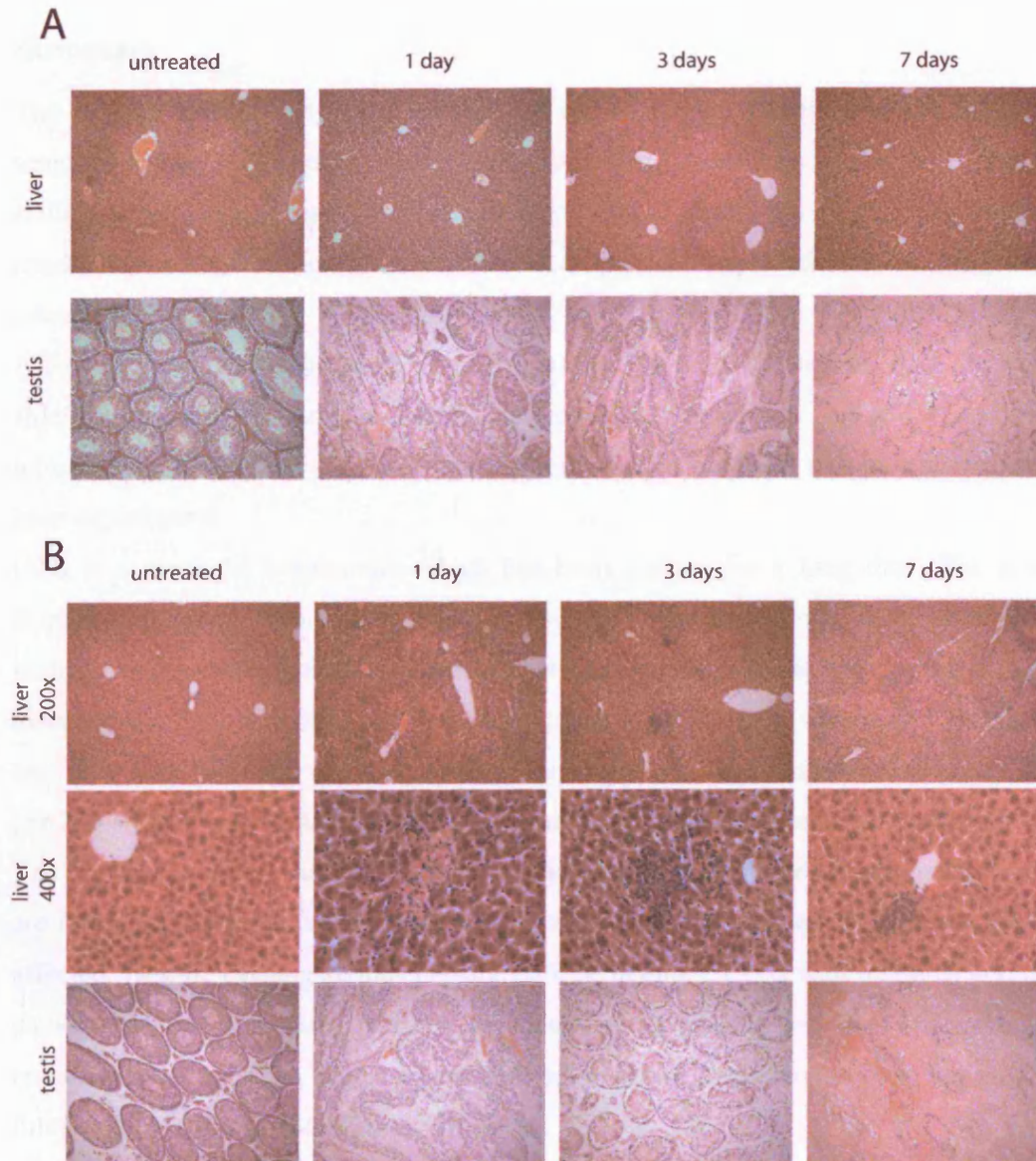
Figure 18 Tissue damage by cadmium toxicity in male MT$^{-/-}$/NOD/Scid mice.

Animals were treated with 5 µmol/kg CdSO$_4$ via i.p. injection. A) Male NOD/Scid mice show no tissue damage in the liver with this amount of CdSO$_4$. On all timepoints liver morphology is normal. Testicular damage however is widespread, and complete destruction of testis cords is present throughout the whole experimental timecourse. B) Tissue damage induced in male MT$^{-/-}$/NOD/Scid mice. In liver tissue clearly visible liver damage is present 24 hrs after CdSO$_4$ treatment. The necrotic patches are dispersed in the liver parenchyme. At day 3 post treatment hematopoietic cells can be seen infiltrating the foci of dead cells and removing debris. At day 7 visible recovery of liver tissue has taken place, and no more necrosis is present. The testicular damage in MT$^{-/-}$/NOD/Scid mice is similar to the damage in NOD/Scid mice.

Summary

The aim of this project was to study the environmental parameters that influence transdifferentiation of hematopoietic stem cells into hepatocytes. To achieve this we studied several animal models in which we can either generate a general environment conductive to regeneration or in which we can provide engrafted cells with a growth advantage.

Although acetaminophen can induce serious liver damage, the limited dose we were able to use in our experiments made it ineffective for our purpose. As NOD/Scid mice tolerate even the highest dose of 350mg/kg body weight very well we could not use it in later experiments.

CCl_4 is a powerful hepatotoxin which has been studied for a long time. The acute damage done by CCl_4 to liver tissue is very similar to the strong mitotic activation after partial hepatectomy. However, partial hepatectomy is a complicated procedure, and associated with a high risk of infection or other complications which lead to animal loss. The administration of CCl_4 is simple, and in healthy animals a dose of $40\mu l$ CCl_4 per 25g animal does induce severe liver damage without other detrimental side effects. The damage done is specific to hepatocytes, so even if transplanted hematopoietic cells are introduced into the organism quite early after CCl_4 intoxication they should not be affected. Despite causing serious hepatocyte destruction, CCl_4 is well tolerated and the damage induced is repaired within a very short period usually less than 10 days until complete recovery. CCl_4 thus is a powerful tool in preparing an environment engaged in fulminant repair and restoration in the animal.

The pyrrolizidine alkaloid retrorsine effectively inhibits mitosis of hepatocytes in the rat model. In the mouse however, its effectivity has not been tested before. In our experiments it did not significantly delay repair after CCl_4 damage. We could not observe megalocytic cells as described in the rat. However, the repair of damage after CCl_4 intoxication is providing a very strong mitotic stimulus, probably overcoming a weak mitotic block induced by retrorsine, and the effect of retrorsine has been described to be long lasting, so we could not rule out a long-term growth impairment of resident hepatocytes. Retrorsine is a naturally occurring compound and is extracted from plants. At the time of the start of this project retrorsine was readily available from Sigma Biochemicals. However, during the course of this project the supply of retrorsine had been used up, and retrorsine has since been unavailable. The residual amount of

retrorsine in our stocks was not sufficient to perform a full investigation into its effects; we could however perform one set of engraftment experiments described in chapter 2. The successful backcrossing of the MT$^{-/-}$ strain onto the NOD/Scid background presents us with a new mouse model for studying regeneration of liver tissue while providing a selective growth advantage for transplanted cells. The complete absence of functional MT I or II in these animals confers a genetic distinction which can not be overcome by gene rearrangement like is the case in the alb-uPA model (Sandgren *et al.* 1991). Another problem in other established genetic defect models, namely the FAH$^{-/-}$ model and the alb-uPA model is neonatal death and very difficult upbringing of pups. The MT$^{-/-}$/NOD/Scid mouse strain is very similar to the NOD/Scid strain in fertility and upbringing, so no special treatment of pups is necessary for survival. At last, no other mouse strain with an inducible liver specific genetic defect allows the engraftment of xenogeneic cells. The procedures established in the NOD/Scid model for engrafting various populations of cells in a host animal can now be applied to a mouse model with an inducible genetic disadvantage in its hepatocytes.

Chapter 2 Engraftment of human cells in the mouse

Introduction

Bone marrow transplantation is an established methodology in the treatment of diseases in human medicine. It can be used to cure haematopoietic disorders by replacing or supplementing the diseased bone marrow of a patient with healthy cells. To allow scientists to mimic these conditions in the clinic and to be able to conduct research on the potential of haematopoietic stem cells the Scid mouse model (Shultz *et al.* 1995; Lowry *et al.* 1996), and later the NOD/Scid model (Larochelle *et al.* 1996) were introduced. These animal models allow studying two aspects of bone marrow transplantation. The first aspect encompasses the intrinsic capabilities of cells of the haematopoietic lineage, and the second aspect is the influence of the environment into which these cells are transplanted.

In our model we use progenitor and stem cells purified from human cord blood. This population is readily available and thus is at the centre of research in many laboratories. The haematopoietic stem cells obtained from cord blood have been shown to repopulate the bone marrow of NOD/Scid animals, giving rise to multiple cell lineages of haematopoietic origin (Larochelle *et al.* 1996; Bhatia *et al.* 1997; Bhatia *et al.* 1998).

More recently several publications suggested a broader spectrum of developmental possibilities for haematopoietic stem cells, with reports of hepatocyte generation from bone marrow being at the forefront of this research.

We aimed to investigate the engraftment capabilities of human stem cells in an environment in which extensive damage of a non-haematopoietic organ is present, to elucidate if we can direct the development of non-haematopoietic cell types from bone marrow cells. The first step in this was to establish sufficient levels of bone marrow engraftment which is readily detectable and can be enumerated by FACS analysis. In the second phase we concentrated on other organs of the murine organism to find out if progeny of the haematopoietic cells can be detected there.

CCL₄ treatment enhances bone marrow homing of human progenitor cells

Damage to liver tissue by CCl₄ induces severe necrosis and cell death. The immediate reaction of the surviving hepatocytes is to enter mitosis and divide. In this environment of necrosis, inflammation and regeneration multiple homing molecules are upregulated and aide circulating cells in finding the site of damage.

To investigate if CCl₄ damage increases homing to the liver or the bone marrow we labelled cells with the lipophilic dye PKH26 and traced their movement in the murine organism. Mice were injected with one 40µl injection of CCl₄ i.p. and given 350 RAD irradiation on the following day. 48 hrs after CCl₄ treatment $2x10^6$ human cord blood mononuclear cells stained with the dye PKH26 were administered via i.v. transfusion. PKH staining of mononuclear cells is very strong and complete as can be seen Figure 19B. After 16 to 24 hours homing is finished and the animals were sacrificed. Bone marrow was harvested by flushing femurs and tibias, and livers were perfused by collagenase treatment. The experimental procedure is outlined in Figure 19A.

While the frequency of PKH positive cells could be conveniently derived as percentage of total cells in the bone marrow, in the liver the large amount of debris after liver perfusion made this impossible. As an alternative strategy the whole liver was perfused and dispersed in 5 ml of buffer and a fixed amount of fluorescent beads (Sigma Aldrich) was added to an aliquot of cells. The fluorescent beads are clearly visible in the FACS plot (Figure 19C). The PKH positive cells were counted in a large FACS gate depicted in Figure 19C and put in relation to the number of beads counted in a second gate.
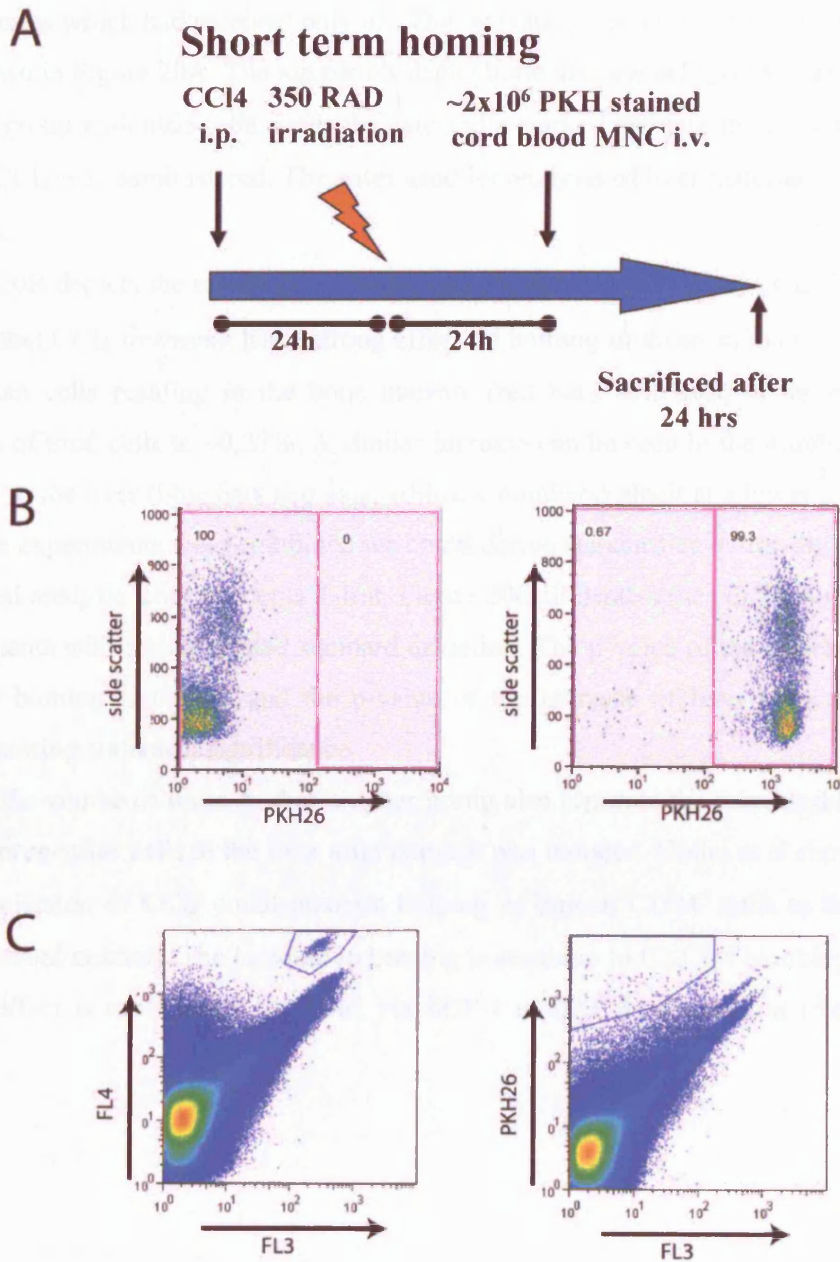
Figure 19 Tracking of cells to measure short term homing

a) Experimental setup b) PKH26 stained cells give a bright signal in FL2 (left unstained, right stained) c) Fluorescent beads form a distinct population in the FACS plot (left) and do not overlap with the gate used to count PKH positive cells (right). Empty channels (FL3 and FL4) were used to separate populations by autofluorescence.

The effect of CCl$_4$ on stem cell homing can be derived by comparing the amount of cells resident in the respective organ after transplantation in mice treated with CCl$_4$ to that of mice which had received only oil. The relevant gates used in the FACS analysis are shown in Figure 20A. The top panels depict bone marrow cells, on the left the control group with little cells inside the gate and a marked increase in the right panel where CCl$_4$ was administered. The gates used for analysis of liver material are shown beneath.

Figure 20B depicts the results of a homing experiment using 25 µl of CCl$_4$. It is clearly visible that CCl$_4$ treatment has a strong effect on homing in these animals. The amount of human cells residing in the bone marrow (red bars, left axis) is increased from ~0.05% of total cells to ~0.27%. A similar increase can be seen in the numbers of cells lodging in the liver (blue bars and axis, arbitrary numbers) albeit at a lower level. When multiple experiments were combined we could derive standard deviation and perform a statistical analysis using students T-test. Figure 20C illustrates the combination of three experiments with the calculated standard deviation. The p-value of the increase of bone marrow homing is 0.0011 and the p-value of the increase of liver homing is 0.018 demonstrating statistical significance.

During the course of these studies another group also reported the increased homing of human progenitor cells to the liver after damage was induced. Kollet et al showed that a single injection of CCl$_4$ could increase homing of human CD34$^+$ cells to the liver of experimental animals. The increase in homing is sensitive to CXCR4 blocking antibody so the effect is most likely mediated via SDF-1 to CXCR4 interaction (Kollet *et al.* 2003).
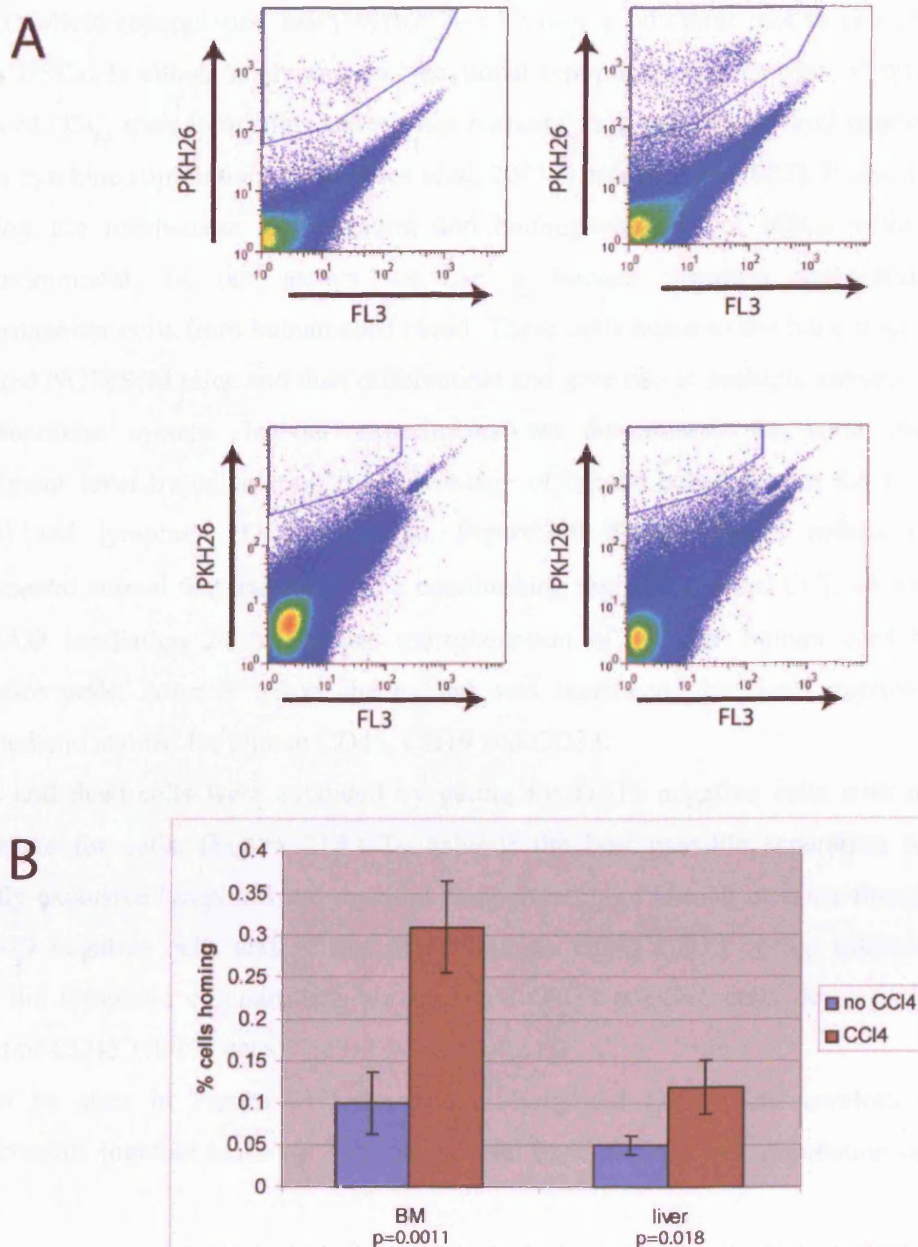
Figure 20 Enhanced homing of human progenitors after CCl4 injury

a) Human progenitors home to bone marrow in greater numbers when CCl4 damage is present (top right) than without damage (top left). The same effect is visible in liver tissue (bottom panels). b) 25µl of CCl4 induce a clear increase in the homing to bone marrow (left) and liver (right) Statistical analysis of homing data shows a threefold increase in homing to bone marrow and a twofold increase in homing to the liver. Students T-test demonstrates statistical significance with a p-value < 0,02.

Phenotype of cell engraftment in NOD/Scid bone marrow

The NOD/Scid repopulation assay system has become a powerful tool to characterise human HSCs. It allows analyzing the functional repopulation properties of different classes of HSC, their frequency, cell surface markers, cell cycle status, and response to *in vitro* cytokine stimulation (Guenechea *et al.* 2001; Lapidot *et al.* 2002). It also allows deducing the mechanism of migration and homing/adhesion of HSCs within the xenoenvironment. In our assays we use a lineage negative preparation of stem/progenitor cells from human cord blood. These cells home to the bone marrow of irradiated NOD/Scid mice and then differentiate and give rise to multiple subsets of the haematopoietic system. In our experiments we determined the bone marrow engraftment level by calculating the percentage of human cells of both the myeloid (CD33) and lymphoid (CD19) lineage. Figure 20 depicts FACS results of an experimental animal that had received a conditioning regimen of 40μl CCl_4 48 hrs and 375 RAD irradiation 24 hrs before transplantation of 10^5 lin⁻ human cord blood progenitor cells. After 8 weeks the animal was sacrificed, the bone marrow was harvested and stained for human CD45, CD19 and CD33.

Debris and dead cells were excluded by gating for DAPI negative cells with a size appropriate for cells. (Figure 21A) To achieve the best possible separation of the mutually exclusive lymphoid and myeloid compartments of human cells we then gated on CD19 negative cells and in this population on $CD45^+CD33^+$ cells. Likewise to obtain the lymphoid compartment we excluded CD33 positive cells determined the amount of $CD45^+CD19^+$ cells.

As can be seen in Figure 21D the human lymphoid (27%) and myeloid (9%) compartments together make up 36% of the total bone marrow cell population of this mouse.
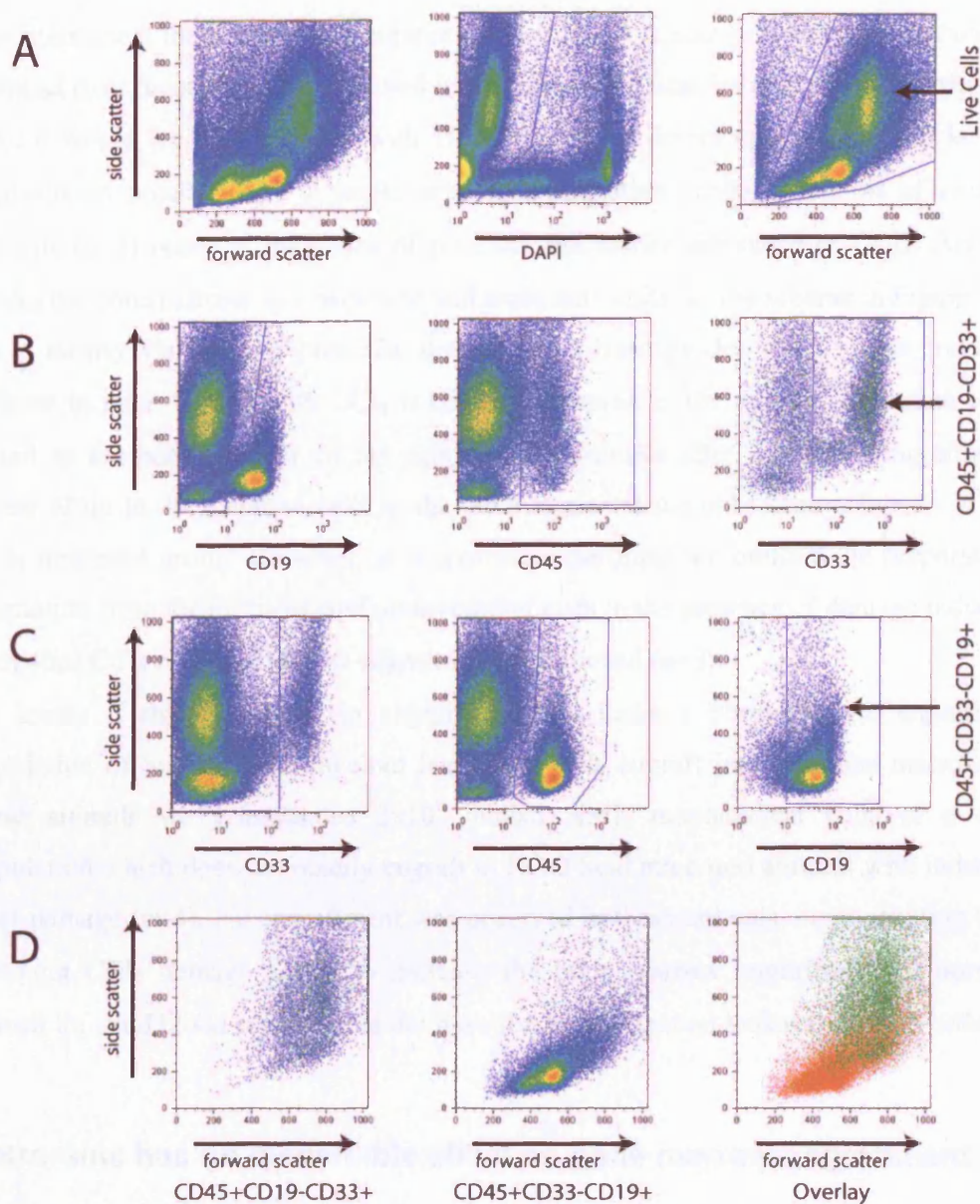
Figure 21 FACS analysis of human cell engraftment in the NOD/Scid mouse bone marrow

Bone marrow of a highly engrafted NOD/Scid mouse conditioned with CCl_4 and irradiation before cell transplantation, sacrificed 8 weeks post transplantation. A) Removal of debris and dead cells by size and DAPI staining B) myeloid CD33 positive engraftment, C) lymphoid CD19 positive engraftment, D) myeloid and lymphoid engraftment in side/forward scatter plot and overlay of both populations

Efficiency of bone marrow engraftment reflects homing

To determine if the increase in bone marrow homing of human progenitors in mice with induced liver damage is also reflected in the amount of final bone marrow engraftment after 8 weeks we injected mice with 10 or 40μl CCl₄ before engraftment and let the engraftment proceed until 8 weeks after transplantation (n=6). A cohort of control animals (n=3) received injections of pure oil, the carrier substance of CCl₄. After 8 weeks the bone marrow was harvested and analyzed similar to the scheme in Figure 21.

As is clearly visible in Figure 22a, the homing advantage described in the previous chapter in mice treated with CCl₄ is directly reflected in the amount of human cells found in the bone marrow of the experimental animals after 8 weeks. Engraftment levels of up to 49% human cells in the bone marrow have only been achieved in the CCl₄ treatment group. However, in a separate experiment we omitted the preparatory irradiation from the protocol, and observed that even in the presence of damage induced with 40μl CCl₄ no bone marrow engraftment is achieved (n=9).

To assess if this advantage in engraftment can make a normally non engrafting population of human acute myeloid leukaemia cells engraft into the bone marrow of these animals we transplanted 2×10^6 human AML mononuclear cells of a cell population which does not readily engraft in NOD/Scid mice into animals with induced liver damage (n=4). No engraftment was observed in these animals, demonstrating that although CCl₄ damage seems to increase the bone marrow engraftment of normal human lin⁻ cord blood cells, it does not have the same effect on leukaemic AML cells.

Retrorsine has no discernible effect on bone marrow engraftment

As we used retrorsine to inhibit hepatocyte regrowth we also determined the possible influence of retrorsine on the regenerative potential of host bone marrow cells, and on the homing and engraftment success of transplanted human cord blood cells.

In this experiment animals were treated with two injections of retrorsine 4 and 2 weeks before transplantation of human lin⁻ cells. 3 different amounts of retrorsine were tested, namely 0, 30 and 70mg/kg body weight. One half of the experimental animals received 40μl CCl₄ 3 days before the transplantation. All animals were given 375 RAD irradiation 24 hrs before transplantation.

The amount of bone marrow engraftment in all the experimental animals is shown in Figure 22b. Again it is clearly visible that the group of animals which has received CCl_4 has a much higher percentage of human cells in the bone marrow than the groups without CCl_4. There is however no statistically relevant difference in the two retrorsine treatment groups as the p-value of a students T-test is between 0.3 and 0.7 when comparing the group without retrorsine to the two groups having received retrorsine.

A

B
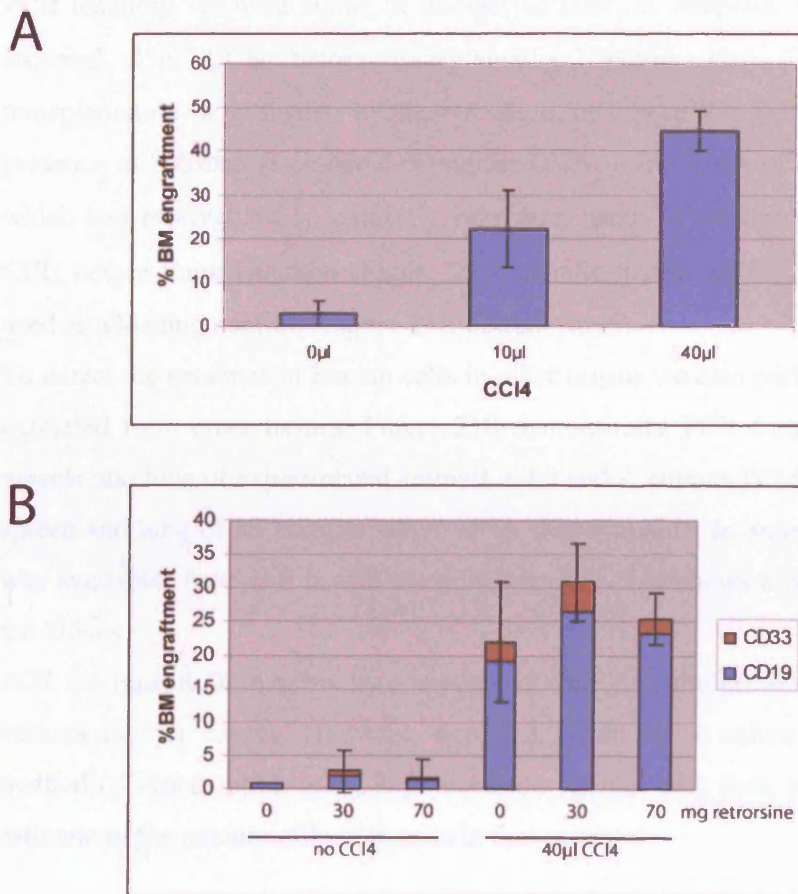
Figure 22 Effect of CCl_4 and retrorsine on bone marrow engraftment

A) Bone marrow engraftment of mice which had received 10 or 40μl CCl_4 before transplantation of human cord blood lin- cells is significantly higher than in control animals (n=3 in each group) (B) Additional treatment of animals with retrorsine does not have a significant influence on the engraftment levels. (p=0.3-0.7)

Human DNA can be detected in several organs of experimental animals

Detection of human cell engraftment in multiple tissues can be performed by PCR for human genes. After DNA extraction from liver, lung, gut, spleen, kidney, muscle and lung we performed PCR for the human and mouse TNFα locus. Murine TNFα primers yield a 264bp product while human TNFα primers produce a 495 bp product. Figure 23a shows an agarose gel of a BamH1 digest of 1µg of DNA in the top panel. In the PCR reactions we used 500ng of undigested DNA as template. Experimental animals received 25µl CCl₄ before transplantation, and/or 25µl CCl₄ 4 weeks after transplantation as indicated by the +/- signs in Figure 23. PCR reactions show the presence of substantial amounts of human DNA in the livers of experimental animals which had received CCl₄, and only very faint bands in mice which had not received CCl₄ before transplantation (Figure 23A, middle panel). PCR for murine TNFα was used as a loading control. (Figure 23A bottom panel)

To detect the presence of human cells in other organs we also performed PCR on DNA extracted from other tissues. Figure 23B demonstrates PCR from gut, spleen, kidney muscle and lung of experimental animals 2,4,5 and 8. Human DNA could be detected in spleen and lung of all animals where DNA was available. In animal 8 no spleen tissue was available. Animal 8 is also the only sample which shows a positive PCR result in the kidney.

PCR for human DNA provides a method of verifying the presence of human cells in various murine tissues. However, due to the non-linear nature of PCR the simple method of visualization of PCR products on agarose gels does not provide a reliable estimate of the amount of human cells in these tissues.
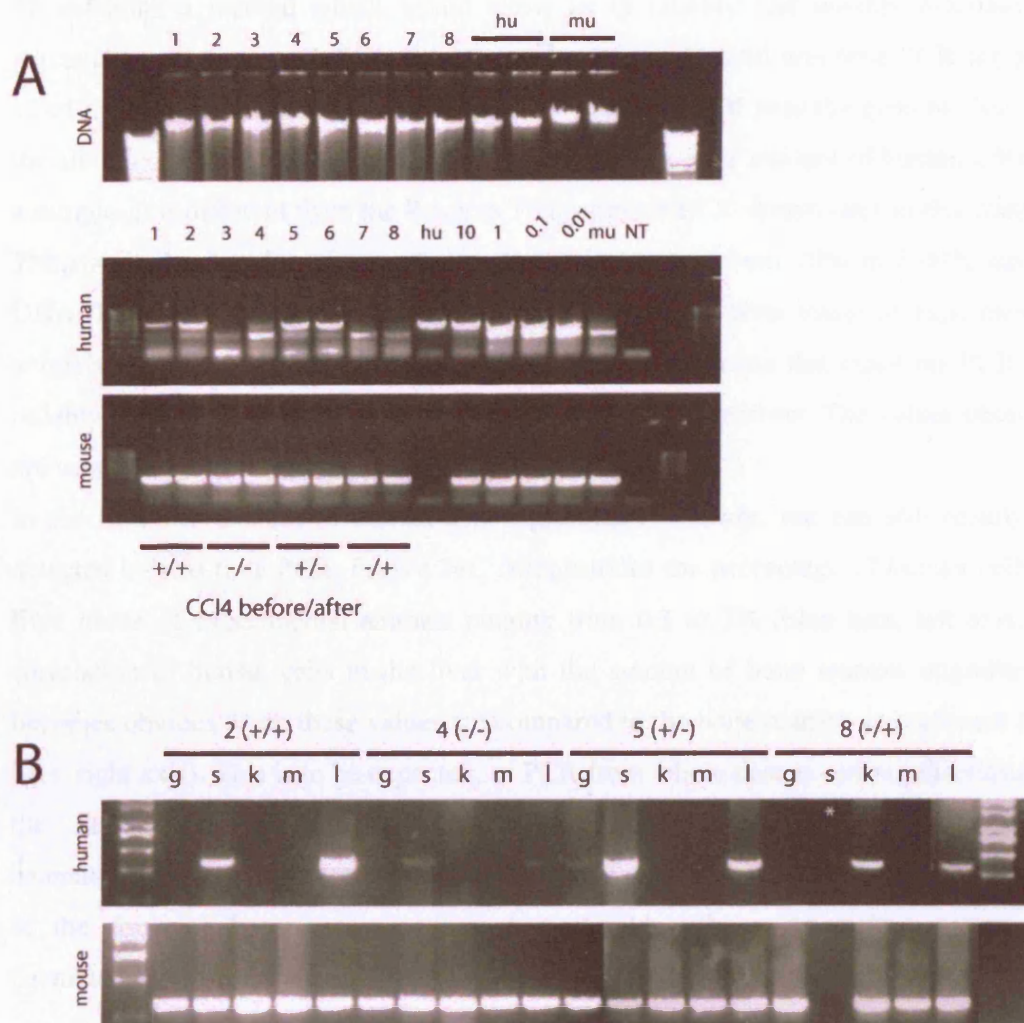
Figure 23 PCR reveals presence of human DNA in multiple tissues

DNA was extracted from several tissues of experimental animals. A) Quality of DNA preparation was confirmed by agarose gel electrophoresis of 1μg BamH1 digested DNA. PCR for human TNFα locus reveals presence of human DNA in livers of highly engrafted mice. Mouse TNFα PCR was used as a loading control. B) PCR on several other tissues (gut, spleen, kidney, muscle, lung) reveals presence of human DNA in spleen, lung and kidney. (No spleen tissue was available for mouse 8) of the same animals shown in A

Real time PCR of tissue DNA allows estimation of engraftment level

To establish a method which would allow us to reliably and quickly estimate the percentage of human cells in multiple samples we established real-time PCR for exon 12 of the human albumin genomic locus. This genomic PCR uses the genomic locus of the albumin gene on the human chromosome to estimate the amount of human DNA in a sample. It is different from the Reverse Transcription-PCR shown later in this chapter. The standard curve for this reaction is linear in a range from 20% to 0.04% human DNA (Figure 24A). Samples from bone marrow cells and liver tissue of experimental animals were measured in triplicates. Figure 24B demonstrates that real-time PCR can reliably determine the percentage of human cells in bone marrow. The values obtained are very similar to the values obtained by FACS analysis.

In the liver the amount of human cell engraftment is lower, but can still readily be detected by real-time PCR. Figure 24C demonstrates the percentage of human cells in liver tissue of experimental animals ranging from 0.3 to 7% (blue bars, left axis). A correlation of human cells in the liver with the amount of bone marrow engraftment becomes obvious when these values are compared to the bone marrow engraftment (red bars, right axis). This is to be expected, as PCR from whole tissues can not discriminate the identity of cells, and will inevitably also measure the amount of human haematopoietic cells in the tissue. Nevertheless, if substantial human liver engraftment in the form of hepatocytes is present it should still be detectable against the haematopoietic background.

A

B

C
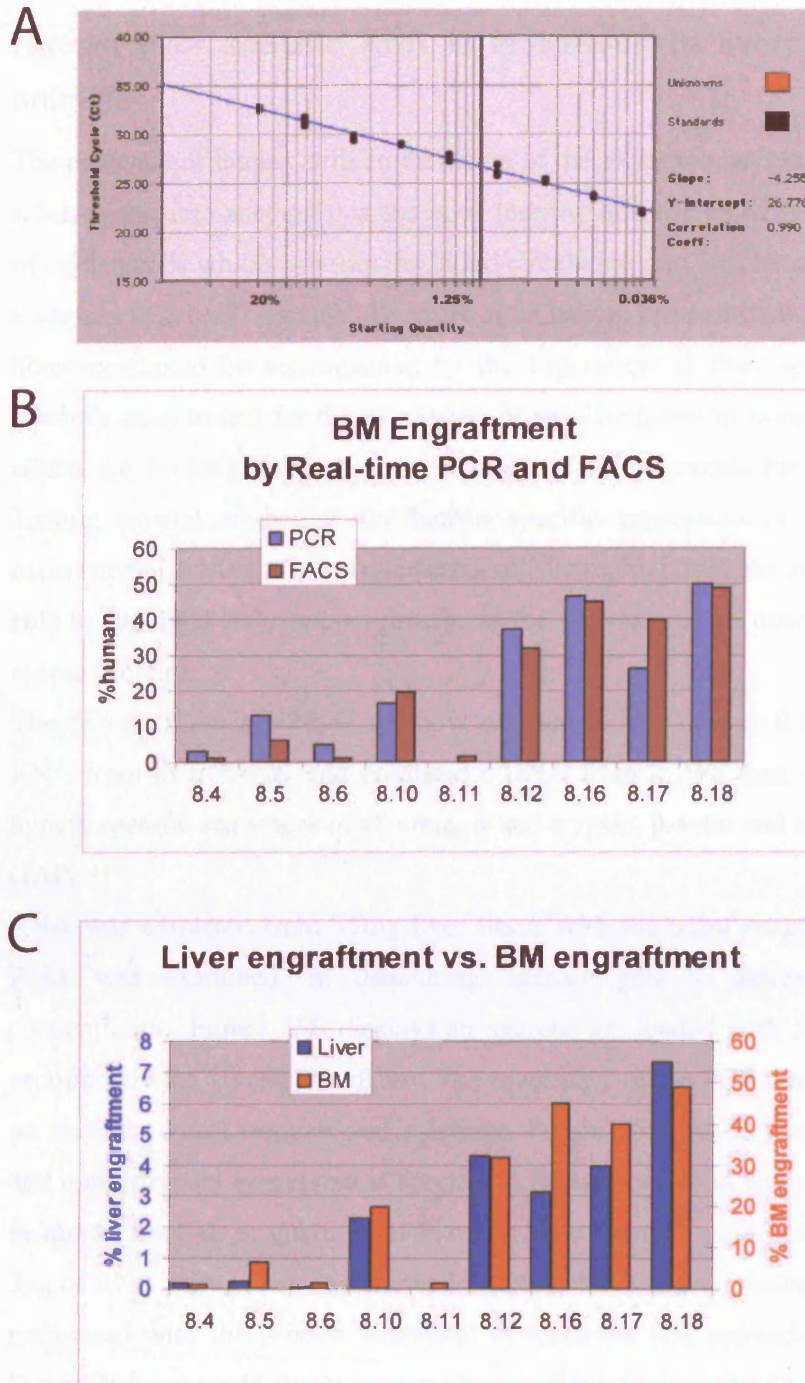
Figure 24 Real-time PCR can be used to estimate engraftment levels

A) Real-time PCR for exon 12 of the human albumin locus was performed on 2μg of DNA containing a mixture of human and mouse DNA ranging from 20% to 0.036% human DNA. The standard curve is linear over the whole range, and the slope of -4.3 indicates an efficient reaction. B) Real-Time PCR was performed on bone marrow samples of 8 experimental mice. Bone marrow engraftment estimated by real-time PCR and FACS is shown. C) Real-time PCR was performed on liver tissue from the same 8 mice. Percentage human DNA in the liver (blue bar, left axis) is shown in comparison to bone marrow engraftment (red bars, right axis).

Human liver specific RNA is expressed in livers of experimental animals

The presence of human cells in the livers of the experimental animals is not surprising when taking into account that the bone marrow of these animals contains a proportion of human cells which will join the blood circulation and thus be present in all organs to a varying degree. The transdifferentiation of human bone marrow cells into hepatocytes however should be accompanied by the expression of liver specific genes. Several methods exist to test for the expression of specific genes in samples. The first method which we investigated was western blotting which reveals the presence of protein. Testing several antibodies for human specific expression in control samples and experimental tissues we were unsuccessful in finding suitable antibodies which were able to highlight only human protein in the presence of an overwhelming amount of mouse protein.

The second reliable method to show expression of genes is RT-PCR. We extracted RNA from liver tissue, and produced c-DNA from it. We then used PCR to amplify human specific sequences of albumin, α-anti-trypsin, β-actin and sequences of GFP and GAPDH.

RNA was extracted from 25mg liver tissue with the trizol reagent (GibcoBRL). The RNA was examined on denaturing agarose gels to assess purity and verify concentration. Figure 25B displays an agarose gel loaded with 5μg of RNA showing prominently the 16 and 18s rRNA. The specificity of the PCR reactions was confirmed on several control samples and reactions. Figure 25D shows that the human albumin and α-anti-trypsin expression is specific to human liver, and no expression can be seen in mouse liver or in mixtures of human haematopoietic cells with mouse liver RNA. 3μg of RNA were reverse transcribed utilizing the Quiagen sensiscript kit and PCR was performed with the primers described in materials and methods. As can be seen in Figure 25A we could detect human albumin RNA in several of our experimental mice, transplanted with different populations of cells. Figure 25A displays PCR on liver tissue from animals which had received either $\sim 10^5$ lin⁻ or a similar amount of CD34⁺ GFP transduced cells. Pre-conditioning consisted of 40 or 10μl of CCl_4 and irradiation. In the top panel the bands show expression of human albumin mRNA in 5 animals, 4 in the CD34 group and one in the lin⁻ group. The second panel shows human α-anti-trypsin expression in the same animals, and also in two additional samples. Controls consist of

PCR for GAPDH which is not species specific so it will give an estimate of the total RNA content of the PCR sample, and also PCR for human β-actin which demonstrates the level of general human cell content. Cells in this panel have also been transduced with GFP via a lentiviral vector (except animal E8.3), so the expression of GFP is another indication of the presence of human cells.

Figure 25C demonstrates human albumin expression in several other experimental animals. The upper panel shows expression of human albumin in animals 8.4, 8.10 and 8.17. These animals have already been shown to have substantial bone marrow engraftment in the previous chapter. It is interesting to note that the expression of albumin is not only present in animals with the highest levels of bone marrow engraftment (8.17), but also in intermediate (8.10) and lowly engrafted animals (8.4). In this experiment, as well as in the experiment shown in Figure 25A all animals which demonstrate human albumin expression in the liver have received CCl_4 pre-treatment.

The lower panel in Figure 25C shows albumin expression in animals which had received highly purified populations of human stem cells, either $CD34^+CD38^-$ or $CD34^-$ $CD38^-$. These animals had not received any CCl_4 as conditioning. It is noteworthy that animals of the first group which had been transduced with only 2400 $CD34^+CD38^-$ cells show very little albumin expression 8 weeks after transplantation, while at 12 weeks after transplantation both the amount of expression, and the number of animals positive for albumin have increased. The other group of animals in this experiment has been transplanted with two doses of $CD34^-CD38^-$ human stem cells. While in the group with the lower dose only one sample shows a faint band for human albumin, in the group transplanted with 8×10^5 cells the albumin band is clearly present. In these two groups the level of bone marrow engraftment has only been determined approximately. Nevertheless it can be deduced that with a bone marrow engraftment level of lower than 0.5% first signs of albumin expression appear in the liver.
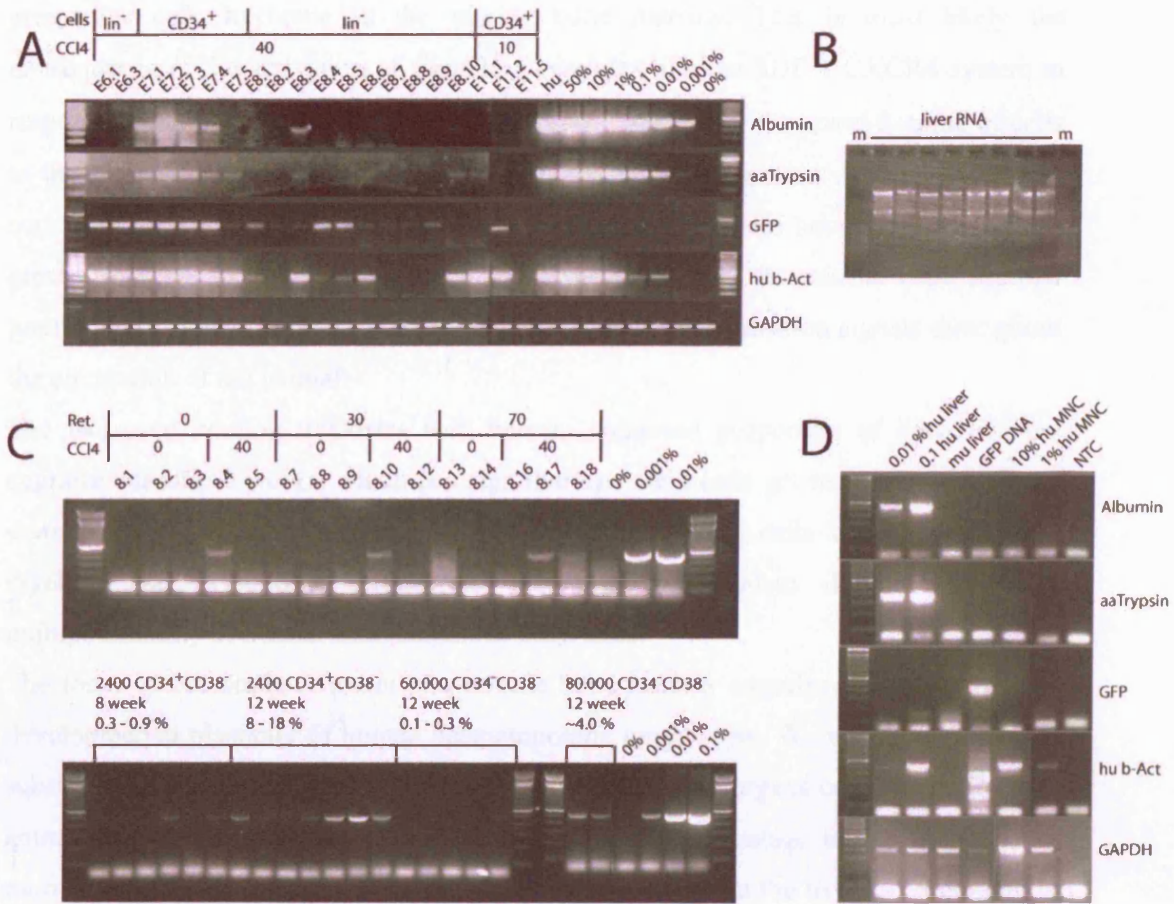
Figure 25 Expression of human liver specific RNA in experimental animals

RNA was prepared from frozen liver samples using the trizol reagent. 3μg RNA were then reverse transcribed and PCR was performed using 10% volume of the RT reaction. A) RT-PCR for albumin, α-anti-Trypsin, GFP, β-actin and GAPDH of samples from animals which have been treated with CCl_4, transplanted with GFP transduced stem cells and sacrificed 8 weeks after transplantation. B) RNA was prepared from 25mg of tissue. 5μg RNA was loaded on a denaturing agarose gel. C) Albumin RT-PCR in animals treated with CCl_4 and retrorsine (upper panel) or without any toxic pre-treatment (lower panel). Pre-treatment of animals is explained above the upper panel for retrorsine and CCl_4, whereas in the lower panel the amount and nature of transplanted cells, the analysis timepoint and the average bone marrow engraftment are given. D) Control reactions to test for specificity of PCR.

Summary

We have demonstrated that CCl4 has a profound influence on the ability of human progenitor cells to home to the murine bone marrow. This is most likely the consequence of the activation of signalling cascades like the SDF-1 CXCR4 system in response to damage induced by CCl4 (Kollet *et al.* 2003). The increased homing of cells to the liver after liver damage is well explained by the excessive damage and repair occurring in this organ at the time of cell transplant. We could however find an even greater increase in homing of bone marrow progenitors to the murine bone marrow possibly as a sign of overall distribution of homing and regeneration signals throughout the circulation of the animal.

The increased homing translates well into an increased proportion of bone marrow engraftment after 8 weeks, which is a sign that true stem cells get recruited to the bone marrow by the homing mechanism. The cord blood stem cells contribute to both myeloid and lymphoid lineages in the murine organism demonstrating the multipotentiality of human haematopoietic stem cells.

The focus of this study however was not the bone marrow engraftment per se, but the developmental plasticity of human haematopoietic progenitors. We were able to detect substantial amounts of human DNA in non-haematopoietic organs of the experimental animals, and established a method for measuring the percentage of human DNA in murine organs with specific focus on liver tissue. The fact that the liver DNA content is closely correlated to the bone marrow engraftment levels indicates that the circulating human blood cells will make it difficult to detect low level human engraftment in non-haematopoietic tissues over the background of haematopoietic cells. Nevertheless, the expression of hepatocyte specific genes like albumin and α-anti-Trypsin demonstrate that a proportion of the human cells detected in the liver are not of the haematopoietic lineage anymore.

Chapter 3 HSA positive hepatocytes

Introduction

Many of the recent results in human bone marrow to liver transdifferentiation have relied on a specific antibody against an unknown protein called HSA (hepatocyte specific antigen) or HepPar-1 (hepatocyte-paraffin). It was raised by immunization of a mouse with paraffin embedded human liver tissue. (Anti-hepatocyte, clone OCH1E5, DAKO M7158)

It has been previously used in the diagnosis of hepatocellular carcinomas in human medical diagnosis (Lamps *et al.* 2003). In recent publications it also has found widespread use to demonstrate the differentiation of mature human hepatocytes from transplanted cells in the murine liver. Danet et al. reported the occurrence of HSA positive hepatocytes after stem cell transplantation in the NOD/Scid model (Danet *et al.* 2002). Additionally to the HSA staining in liver sections these animals also express RNA for human albumin and display staining for human c-met.

In the sheep model Zanjani et al. reported the emergence of a similar population of cells of hepatocyte morphology strongly expressing the antigen recognised by this antibody (Almeida-Porada *et al.* 2004; Kogler *et al.* 2004). Again the authors succeed in demonstrating other markers of human hepatocyte differentiation, i.e. albumin expression and fluorescence-in-situ-hybridisation (FISH) for human ALU sequences. The authors also show dual FISH for human and sheep genomic DNA to exclude fusion of human and sheep cells.

HSA positive cells emerge in the murine liver after stem cell transplantation

In our experiments in mice transplanted with human lin⁻ stem cells we observed HSA positive cells in several experimental animals. Figure 26 demonstrates several sections of mouse livers from experimental animals. Figure 26A shows HSA staining of the liver of a mouse, which had 40% bone marrow engraftment, and had been treated with CCl_4 before transplantation. Very strong HSA staining was visible in cells surrounding the vessel. Dispersed cells in the parenchyme further away from the vessel also show HSA staining.

Figure 26B demonstrates more HSA positive cells in higher magnification. Cells have been stained with HSA and visualised with DAB, anti-mouse-FITC or anti-mouse-Alexa488. In all examples the staining is clearly inside cells of hepatocyte morphology. These cells are also very similar in appearance to cells shown in pictures in the aforementioned publications.

One of several disadvantages of this antibody is that it is only producing signal on paraffin embedded tissue. This makes dual staining strategies very difficult, as most of the antibodies tested in our lab only work on frozen sections. Additionally the FISH protocols optimised in the course of this study produce poor results on paraffin sections with only the mouse Y chromosome paint working reliably on paraffin sections. It is also true that while the HSA staining is strong and clear in liver sections of experimental mice we could only obtain weak positive staining on the human liver paraffin sections available to us. No staining is detected without primary or secondary antibody.
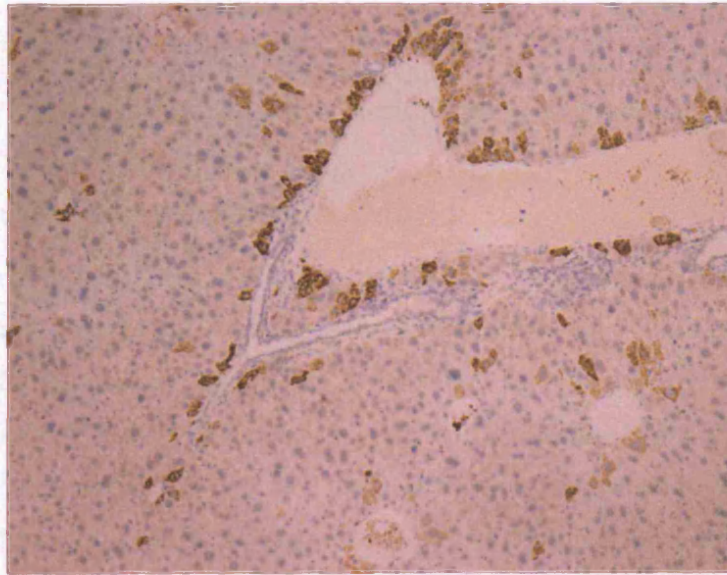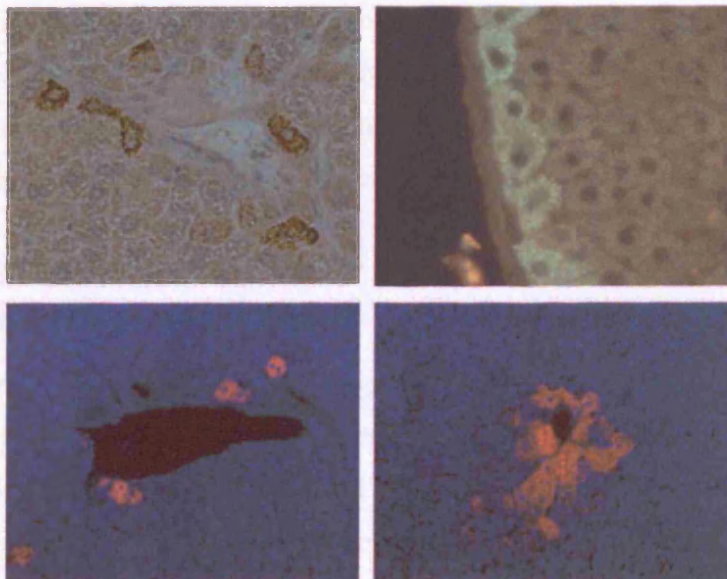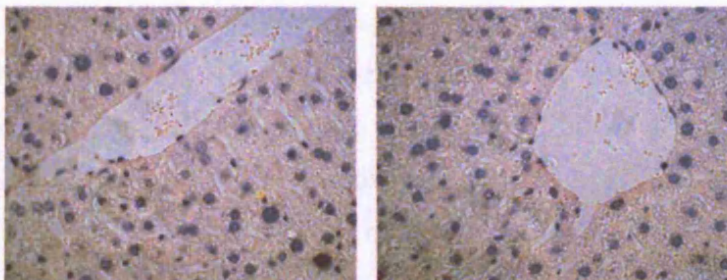
Figure 26 HSA positive cells present in experimental animals

Animals have received CCl$_4$ before transplantation of human cells. A) HSA positive cells visualised with anti-mouse-HRP and DAB. Clearly visible single cells are stained in dark brown. B) Different detection methods highlight similar cells. DAB staining (top left), anti-mouse-FITC (top right) and anti-mouse-Alexa488 (bottom panels) all highlight similar cell populations. C) Control sections showing absence of HSA staining in untreated animals

HSA positive cells do not express CD45

Although these cells exhibit clear hepatocyte morphology, their location so close to the vessels of the murine liver raised concerns that CD45 positive cells could be the source of the staining. Multiple human cells of haematopoietic origin, expressing the common leukocyte antigen CD45 can be found in these livers, due to the repopulation of the bone marrow with human cells. To exclude the possibility that these HSA positive cells are of the haematopoietic lineage we performed CD45 staining and HSA staining on consecutive liver sections. Figure 27A shows CD45 staining in the left panel and HSA staining in the right panel. Although the two populations of cells are both located around the vessels, they are clearly distinct in morphology and identity. The CD45 positive cells are small, round and have a big nucleus with little cytoplasm, whereas the HSA positive cells are of clear hepatocyte morphology.

The amount of HSA positive cells is not closely correlated with the degree of bone marrow engraftment

To assess the correlation of bone marrow engraftment and HSA positive cells in the liver we enumerated HSA positive cells on liver sections. On three different sections of liver tissue all HSA positive cells were counted under the microscope. Then the sections were scanned on a high resolution scanner to obtain an image of the section. The total number of hepatocytes on several fields of view was counted and the ratio of pixels/hepatocyte was determined. Then the number of pixels of the whole section was determined in Adobe Photoshop, allowing an estimation of the number of hepatocytes per section and the percentage of HSA positive hepatocytes . In Figure 27B the amount of bone marrow engraftment and HSA positive cells are shown. It is evident from samples 8.4, 8.5 and 8.10 that the amount of bone marrow engraftment does not correlate with the number of HSA positive cells present in the liver.
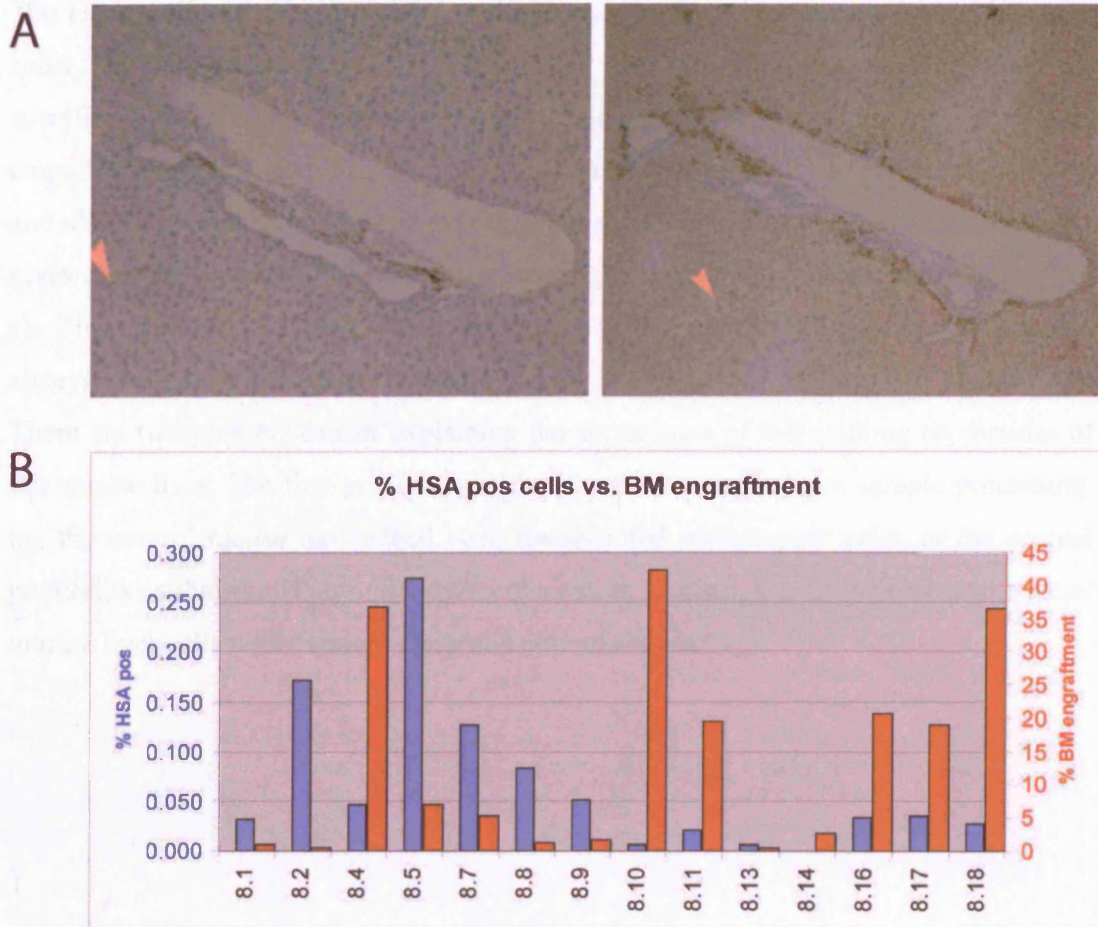
Figure 27 CD45 and HSA are mutually exclusive.

A) Serial sections of liver tissue were stained with anti-human-CD45 and anti-HSA both visualised with DAB. CD45 and HSA are expressed in cells of different morphology and different location. There is no overlap of CD45 positive cells with HSA positive cells. B) Percentage of HSA positive cells and percentage of bone marrow engraftment. Percentage of HSA positive engraftment is shown in blue bars and corresponds to the blue axis on the left, BM engraftment is shown in red bars and corresponds to the red axis on the right. No statistically valid correlation of bone marrow engraftment with the amount of HSA positive in the liver could be derived.

HSA positive cells appear in an untransplanted mouse

The HSA antibody clearly highlights single cells in the mice transplanted with human cells. We used several control mice which had not been transplanted to verify specificity and absence of staining. Figure 28d represents typical staining on a non-engrafted control mouse. This absence of staining is seen in all our control mice (n=4) and also in a large proportion of experimental mice. One control mouse liver however gives clear HSA staining similar to the staining seen in transplanted mice (Figure 26a-c). This staining was repeated several times with different detection methods and always yielded the same positive result.

There are two possible causes explaining the appearance of this staining on sections of this mouse liver. The first possibility is that there was a mistake in sample processing, i.e. the control mouse has indeed been transplanted with human cells, or the second possibility is that the HSA antibody recognises an antigen, which is present in normal murine liver cells under certain abnormal circumstances.
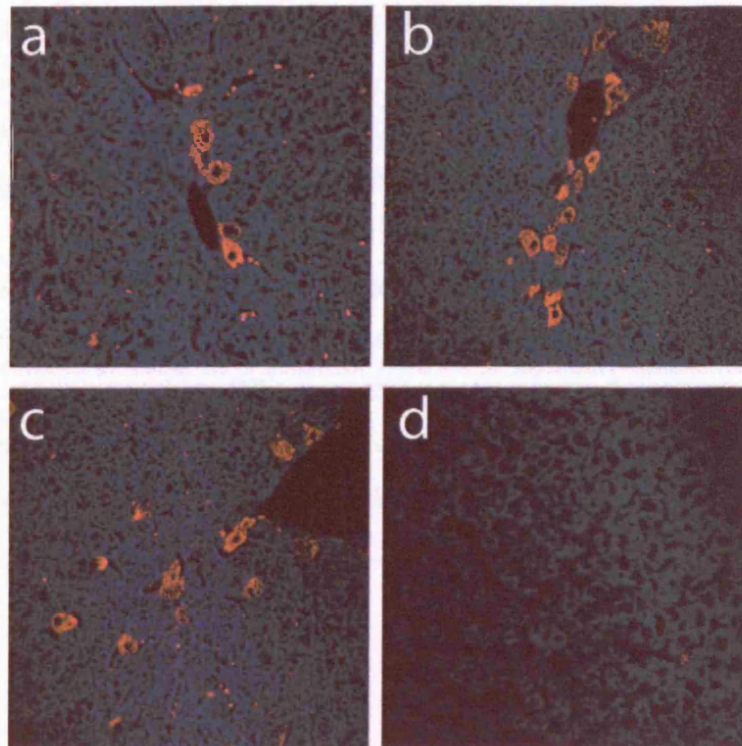
Figure 28 HSA positive cells on non-engrafted mouse

a-c) Positive staining for HSA similar to experimental animals on a control mouse which has not been transplanted with human cells. d) Representative photograph of negative staining obtained on all other control mice used in this study.

HSA positive cells harbour a mouse Y chromosome

As the HSA antibody seems to highlight cells in murine liver as well as in mice transplanted with human cells we attempted to gain further proof of the human origin of these cells. Fluorescence In Situ Hybridisation is a method which allows determining the origin of cells by defining their genetic content. The difficulty faced in this study was to optimise the FISH protocol so we could obtain staining on paraffin embedded sections after performing HSA staining. We succeeded by using a combination of iso-thiocyanate treatment and protease digestion, however the efficiency of detection was reduced and the morphology of the cells was compromised. The only probe which could be used on paraffin embedded tissue sections was the mouse chromosome Y probe.

Figure 29 demonstrates 4 different high magnification images of HSA positive cells obtained from a bright-field microscope (left) and from a fluorescence microscope (right).

In Figure 29a three cells contain murine Y chromosomes, two cells not stained by the HSA antibody on the top right of the image, and also the HSA positive cell. Figure 29 demonstrates three more HSA positive cells containing murine Y chromosome.

This result indicates that the information gained from HSA staining is not as clear as was previously thought. This result is inconsistent with the theory that human bone marrow cells give rise to these HSA positive hepatocytes by direct transdifferentiation. It is however still not clear if these cells could be the result of fusion of murine hepatocytes with human haematopoietic cells.
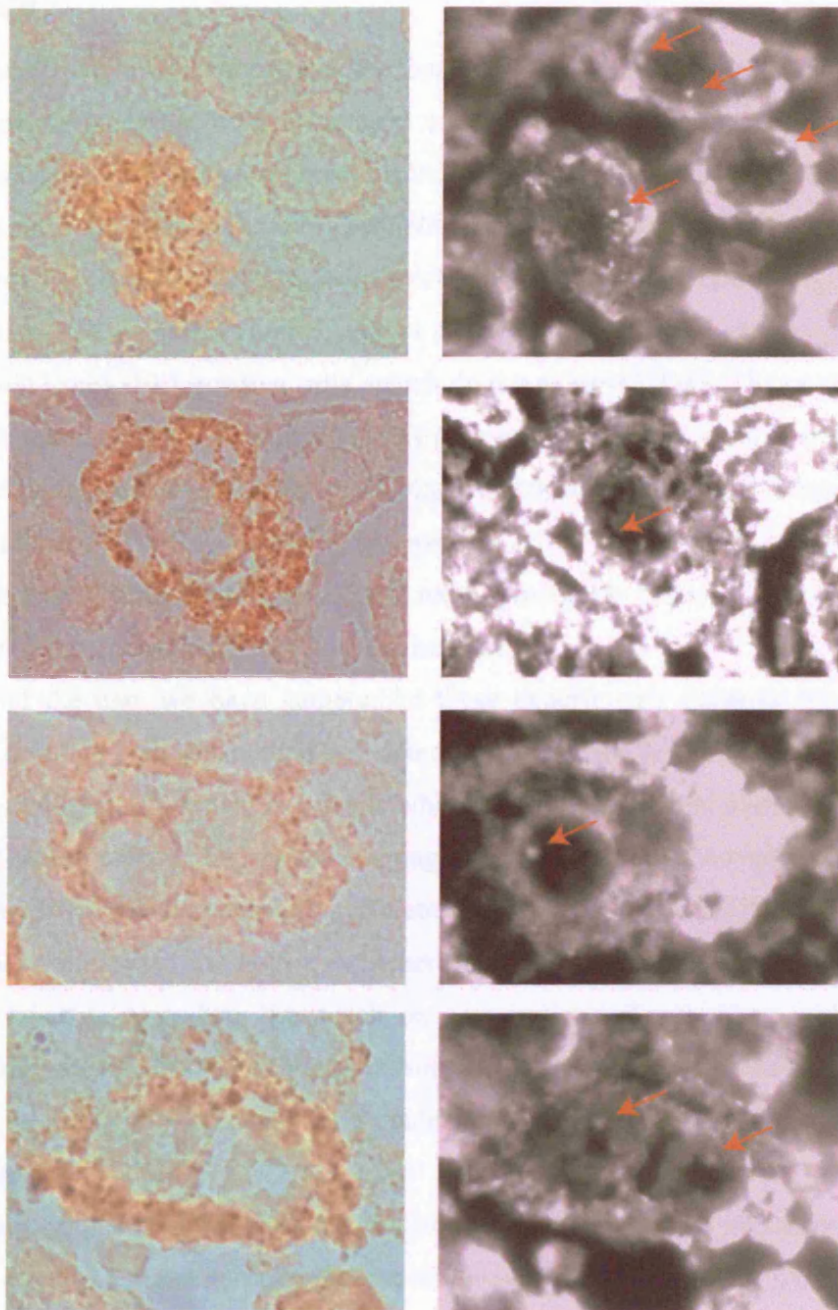
Figure 29 HSA positive cells contain mouse Y chromosomes

Paraffin liver sections were first stained for HSA expression and subsequently FISH for the mouse Y chromosome was performed. HSA staining was captured in bright-field (left panels) while fluorescence of the FITC probe was captured using the appropriate filter setup showing only the green fluorescence in greyscale (right panels). In the top panels three cell nuclei contain Y-FISH spots (red arrows), two not stained by HSA and one stained by HSA. Three more cells from two different slides are shown.

Summary

In this chapter we have demonstrated the detection of HSA positive cells in mice which have received human haematopoietic stem cells. The HSA antibody highlights cells of hepatocyte morphology, located mostly close to vessels. It has been used in previous studies to show apparently trans-differentiated cells (Danet *et al.* 2002; Almeida-Porada *et al.* 2004). Staining for CD45 highlights cells of the haematopoietic lineage present in the liver tissue of transplanted mice, and we have shown that these haematopoietic cells are different to the HSA positive cells, which do not express CD45. The enumeration of these cells revealed that the amount of HSA positive hepatocytes is not correlated to the amount of bone marrow engraftment or to the pre-conditioning given to animals.

We also report that we can detect HSA positive cells in one mouse which has never been transplanted with human cells. Even more remarkably we can show the presence of murine Y chromosome in HSA positive hepatocytes.

Analysis of the data we have gathered in these experiments suggests that the HSA antibody is not a reliable method for detection of human hepatocytes in the mouse model. It highlights a population of cells which in our experiments does not co-express any other human markers by immunostaining and the amount of these cells seems not to be correlated with bone marrow engraftment. The appearance of HSA positive cells in one of our control mice can not be explained easily, especially taking into account that we have failed to reproduce this result on any sections of our other control mouse tissues. The presence of murine Y chromosome in HSA positive hepatocytes excludes a pure human origin for these cells and could only be explained with a cellular fusion mechanism.

In summary, as this antibody does not produce a strong staining on normal human liver tissue, is directed against an unknown protein present only in paraffin fixed tissue and highlights cells of unclear origin we conclude that it is not a suitable means of detection for human cells in a murine model of transdifferentiation.

Chapter 4 Human stem cells transduced with GFP expressing lentivirus

Introduction

The detection of transplanted cells in a transplantation model is one of the challenges in this field of research. In murine studies the availability of genetically marked mouse models like the ROSA26 mouse which expresses β-lactamase under a ubiquitous promoter (Soriano 1999) or the more recently introduced GFP mouse which expresses GFP in all tissues (Okabe *et al.* 1997) allow for a well controlled environment in which the distinction between host and donor cells is clear. Another method often used in murine and also in human studies is FISH analysis after sex-mismatched transplantations. The condensed nature of the Y chromosome makes it an ideal target for these studies and probes for the murine Y chromosome are readily available.

In the human system however, whole chromosome probes which have been optimised for the difficult conditions encountered in the course of this study were not readily available. A further complication is that the gender of the cord blood cells used here was not always known.

To counter all these problems and to establish a method to detect human cells in murine tissues by immunohistochemistry we developed a system in which human stem cells are labelled with GFP. This method utilises a lentiviral construct which is introduced into human stem cells. The protocol involves production of the virus by combined transfection of three plasmids carrying the different parts of the viral chromosome and active reverse transcriptase into a producer cell line. The virus is then harvested from the supernatant of the cells and concentrated by ultracentrifugation and frozen at -80° for future use. Human cord blood stem cells were purified by either lineage depletion or CD34 enrichment and transduced overnight with a multiplicity of infection of 35 in the presence of a cocktail of growth factors. After transduction the expression of GFP was confirmed by fluorescence microscopy and the cells were injected into host animals in aliquots of $\sim 10^5$ cells per animal (in collaboration with a post-doctoral fellow in the laboratory, Dr Elena Siapati). Pre-treatment of NOD/Scid animals was performed by injection of CCl₄ 24 hrs before or on the day of transplantation as well as 375 RAD of gamma irradiation.

Transplantation of human GFP marked haematopoietic stem cells leads to the emergence of GFP positive cells in multiple tissues

8 weeks after the transplantation the animals were sacrificed, bone marrow was harvested and analyzed for engraftment by FACS, and sections of several tissues were prepared for analysis. Detection of GFP expression in various tissues was achieved by immunohistochemistry using a rabbit polyclonal anti-GFP antibody and various secondary antibodies for visualization.

Figure 30 demonstrates several different populations of GFP positive cells seen in organs of these animals. Bone marrow engraftment levels were determined by FACS analysis, and spleen tissue was used for immunohistochemistry. The amount of GFP positive cells in the spleen is directly related to the bone marrow engraftment level. Figure 30a demonstrates a typical example of a spleen section from a mouse with ~10% bone marrow engraftment. Dark stained, GFP positive haematopoietic cells are clearly visible in the tissue.

Another tissue of interest in the lab is the lung, and staining of the lung for GFP positive cells revealed the presence of small single GFP positive cells (Figure 30b). These cells are embedded into the tissue and appear to be part of the lung epithelium. Their exact identity is the subject of a separate project in the lab.

GFP positive cells were also seen in the gut epithelium, demonstrated in Figure 30c. The dark stained GFP positive cells are enterocytes which form the gut epithelium.

In the liver tissue we could find substantial amounts of GFP positive, large cells (Figure 30d-f). These cells are of clear hepatocyte morphology (Figure 30g-i). The GFP positive hepatocytes are clearly distinct from the much smaller haematopoietic cells (Figure 30e, arrow). The whole cytoplasm of these cells is positive for GFP and they are sometimes bi-nucleated. We can detect GFP in these cells with two different antibodies, and used either horseradish peroxidase and DAB for permanent staining, or fluorescence conjugated antibodies for fluorescent imaging (Figure 30g).
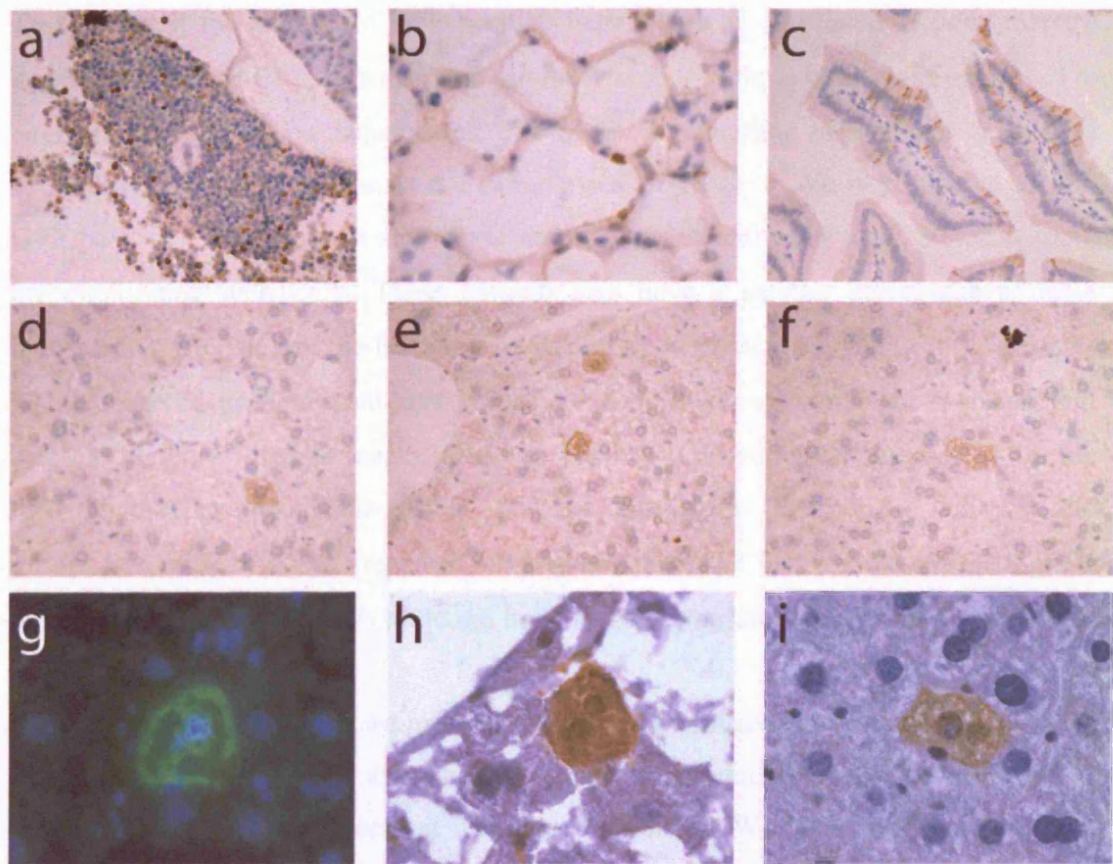
Figure 30 GFP positive cells in tissues of experimental animals

~10^5 lin⁻ or CD34⁺ cells were transplanted into CCl_4 treated, irradiated hosts. After 8 weeks animals were sacrificed and tissue sections were prepared. After staining with αGFP antibody GFP positive cells are visible in several organs. Paraffin sections (a-f,i) or frozen sections (g,h) were stained for GFP with a rabbit polyclonal antibody. Secondary antibodies bearing a horseradish peroxidase were used for DAB visualization (a-f,h,i) a) Small GFP positive cells in the spleen. b) Cells of a morphology reminiscent of lung epithelia in the lung. c) Cells of the mucus layer of the gut epithelia show specific GFP staining. d-f) DAB staining of liver cells with clear hepatocyte morphology. Natural fluorescence of GFP is visible in the fluorescence microscope. (g)

The amount of GFP positive hepatocyte-like cells is correlated to the CCl$_4$ treatment

To find out if the amount of GFP positive hepatocytes is correlated to bone marrow engraftment and/or CCl$_4$ treatment we used the same technique which was employed to enumerate HSA positive hepatocytes. The results of counting hepatocytes from liver slides from 23 different animals are summarised in Table 1. We were unable to find GFP positive hepatocytes in any of the animals which had been transplanted without preconditioning with CCl$_4$. These animals also have a smaller percentage of bone marrow engraftment, but the lentiviral transduction efficiency was high. In the animals which received pre-treatment with 10 or 25μl of CCl$_4$ we could see a substantial increase in bone marrow engraftment as has been described earlier, and also the emergence of small numbers of GFP positive hepatocytes (2-5 per 10^6 cells). In the group of animals which has received the highest dose of CCl$_4$ we could see the highest amount of GFP positive cells although bone marrow engraftment was very variable in this group.

In two separate experiments we injected 1.5x10^5 GFP transduced cells into 6 NOD/Scid animals and sacrificed the animals after 2 weeks to elucidate if the GFP positive hepatocytes are already present at this early time-point. We could not find any GFP positive cells of clear hepatocyte morphology in these animals suggesting that GFP positive cells do not directly home to the liver to give rise to GFP positive hepatocytes but that either bone marrow repopulation is a prerequisite to the colonisation of the liver or the formation of GFP positive hepatocytes is a very slow process.

CCL$_4$ treatment	% human CD45$^+$ cells in bone marrow ± SD	% eGFP$^+$ cells of human CD45$^+$ cells ± SD	eGFP$^+$ hepatocytes per 10^5 cells ± SD
0 µl (n=3)	10.3 ± 1.2	48.7 ± 21.4	0.0
10 µl (n=3)	26.0 ± 18.5	24.9 ± 12.4	0.2 ± 0.4
25 µl (n=6)	44.0 ± 37.3	57.5 ± 20.1	0.5 ± 0.7
40 µl (n=11)	21.2 ± 15.2	50.7 ± 15.1	11.9 ± 8.4

Table 1 Bone marrow and liver engraftment following CCl$_4$ treatment.

Analysis was performed 8-11 weeks post haematopoietic stem cell transplantation Approximately 2x10^5 cells were analyzed for each animal following immunohistochemical staining with anti-eGFP antibody. Two to three slides of different areas of the liver were analyzed. Linear regression analysis reveals weak correlation between CCl$_4$ treatment and number of GFP positive hepatocytes with an R2 value of 0.346 which is due to the few timepoints available. The total liver area on the slide was measured in square millimetres and the number of total hepatocytes occupying the given area was calculated after counting the number of hepatocytes per square millimetre on several different areas of multiple slides.

Potential isolation of GFP positive cells from the liver by FACS sorting

As the amount of GFP positive cells in the liver is very small we attempted to enrich the population of GFP positive hepatocytes by FACS sorting.

To obtain a single cell suspension of liver cells we used the liver perfusion method described by Seglen et al (Seglen 1973) with modifications. Figure 31 depicts the FACS gating strategy used. Figure 31a shows the whole cell population obtained from liver perfusion of an experimental animal. After removal of small dead DAPI positive debris (Figure 31b) we analysed several cell populations present in the plot of GFP versus an empty channel. Two populations (d and g) represent debris in the sample. This is to be expected, as a crude preparation of liver cells was used for analysis. The population shown in Figure 31h most probably represents haematopoietic and other non-parenchymal cells, while the large population of cells in gate e represents the hepatocytes. There are also two populations of cells (f, i) ,which seem to be GFP

positive. While one of these populations (f) is very small and again is most probably debris, the other one (i) is in an area of the side scatter/forward scatter plot where one would expect haematopoietic cells, with a small proportion of cells in the area of hepatocytes. (Figure 31g-i)

The ultimate goal of this protocol was to attempt to sort the GFP positive population of cells from the vast majority of non GFP expressing cells. We attempted to sort GFP positive cells from the original single cell suspension (Figure 31j) on the FACS Vantage Cell Sorting System (BD Biosystems). Cells were sorted in gates similar to Figure 31c and collected the cells directly onto glass slides. After sorting approximately 20 million cells 5000 GFP positive events per slide were examined under the fluorescence microscope. Figure 31k demonstrates the small cell population (gate f), in which we find a substantial amount of hepatocytes with small fluorescent debris and occasional putative haematopoietic cells. The gate described in Figure 31i yielded slightly bigger cells but no visible GFP positive hepatocytes.

Subsequent attempts to perform FISH analysis or immunostaining on these cells failed due to loss of the material from the slide.
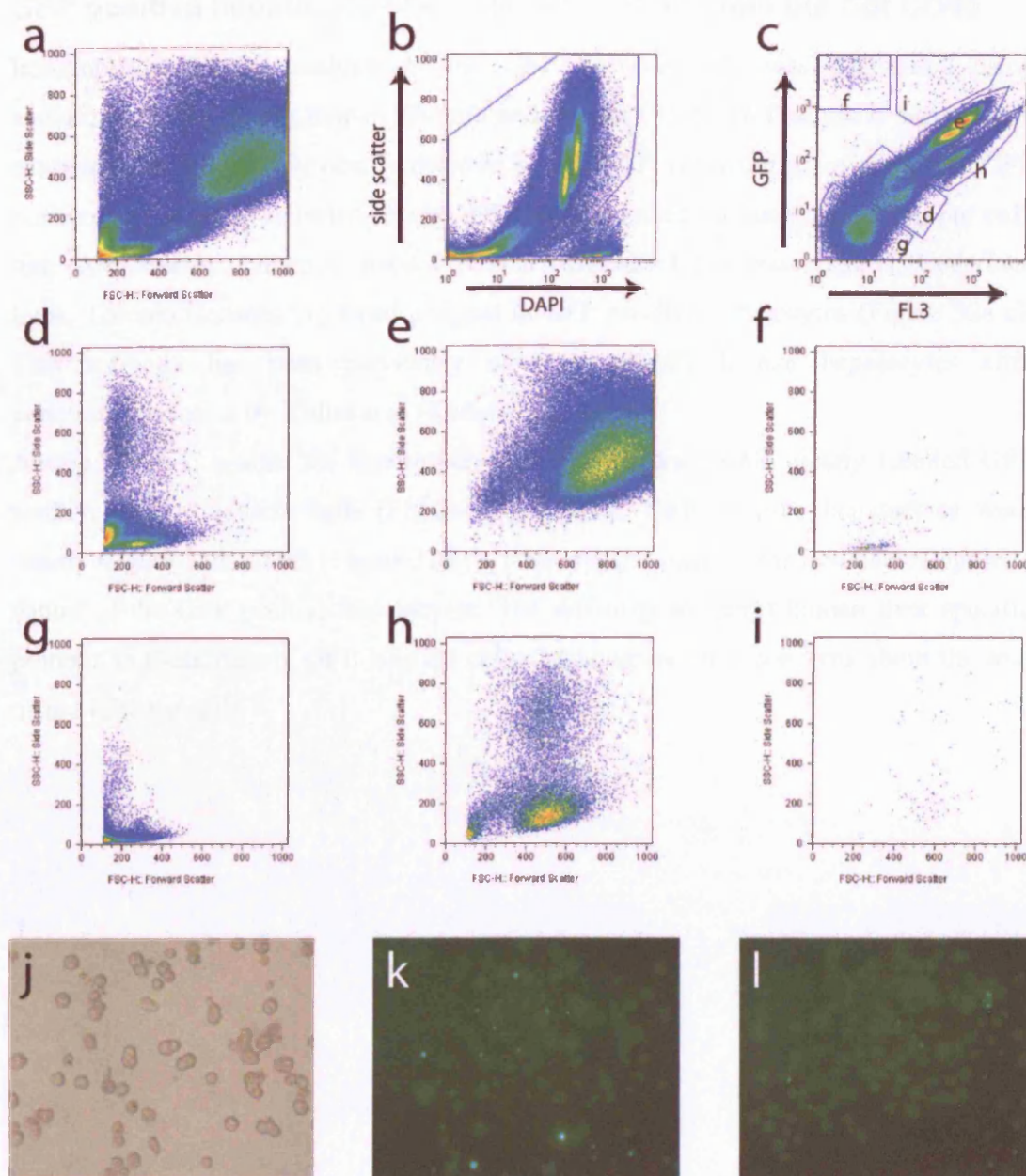
Figure 31 FACS analysis of liver cells

Single cell suspension was obtained from mouse livers of animals transplanted with GFP positive haematopoietic stem cells. FACS plots are side scatter vs. forward scatter unless indicated otherwise. c) Six different populations were analyzed. d,g) Small fragments and cell debris, e,h) hepatocytes and non-parenchymal cells, f,i) putative GFP positive cells. j) Initial cell preparation in bright-field. k,l) Sorted cell populations in GFP fluorescence channel. (k=f, l=i)

GFP positive hepatocyte-like cells express albumin but not CD45

Immunohistochemical analysis of the GFP positive cells was performed using antibodies raised against human albumin and human CD45. To find out if the albumin expression which was previously detected by RT-PCR is having its origin in the GFP positive hepatocytes we tested several different antibodies for human albumin, but only one (Anti-Human Albumin, Ascites (Clone HSA1/25.1.3) (mouse IgG1), Cedarlane Labs, Toronto Canada) produced a signal in GFP positive hepatocytes (Figure 32a-c). This antibody has been previously used to identify human hepatocytes after xenotransplantation by Kollet et al (Kollet *et al.* 2003).

Antibody raised against the human pan-leukocyte marker CD45 clearly labelled GFP positive haematopoietic cells (Figure 32g-i) while GFP positive hepatocytes were clearly negative for CD45 (Figure 32d-f). These results confirm the non-haematopoietic nature of the GFP positive hepatocytes. The difficulty to detect human liver specific proteins in these clearly GFP labelled cells did however raise concerns about the true nature of these cells.
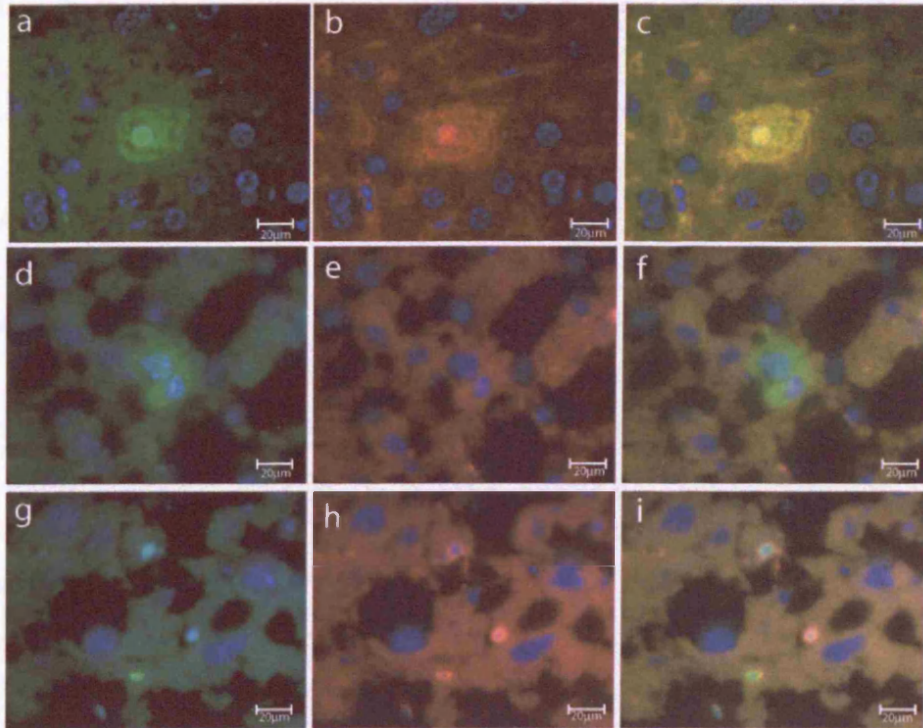
Figure 32 Albumin and CD45 expression on GFP positive cells

Liver sections from transplanted animals were stained with rabbit-anti-GFP antibody (green) and specific antibodies for human albumin and CD45 (red). Hepatocyte like GFP positive cells (a) express albumin (b) yielding yellow in the overlay (c), but do not express CD45 (d-f). Small GFP positive cells are CD45 positive. (g-i)

GFP positive haematopoietic cells but not hepatocytes express human specific marker proteins

The difficulty to stain for cell specific markers in tissues to identify trans-differentiated human cells led us to explore other means for identification of human cells. Immunohistochemistry using two antibodies raised against human nuclear proteins and human mitochondria (Chemicon, Temecula CA) highlight all cells of human origin. The antibody against human mitochondria strongly labelled the cytoplasm of cells in all tissues. The nucleus remained unstained and presented blue DAPI staining. Figure 33a demonstrates staining on frozen human liver sections, whereas staining is completely absent in murine liver (Figure 33e). The second antibody, specific for human nuclear antigens highlighted only the nucleus of human cells, leaving the cytoplasm unstained. Figure 33i demonstrates staining on human liver, Figure 33m on murine liver. The specificity of these antibodies allowed us to do two-colour staining for the human antigen in conjunction with GFP.

As was expected the human specific antibodies clearly labelled all small GFP positive haematopoietic cells. The mitochondrial staining formed a ring of staining in the thin layer of cytoplasm around the nucleus of haematopoietic cells, whereas the nuclear antibody presented clear staining in the centre of the haematopoietic cell. To our surprise the hepatocyte-like cells where not stained by these antibodies. Figure 33b-d and f-h demonstrate GFP (green) and human mitochondrial (red) staining of a haematopoietic and a hepatocytic cell next to each other. It is evident that staining for human mitochondria was absent in the GFP positive hepatocyte and clearly present in the haematopoietic cell. The same pattern of staining was present in Figure 33j-l and n-p which depicts human nuclear staining.

This very clear-cut result raised further doubts about the nature of the GFP positive hepatocytes.
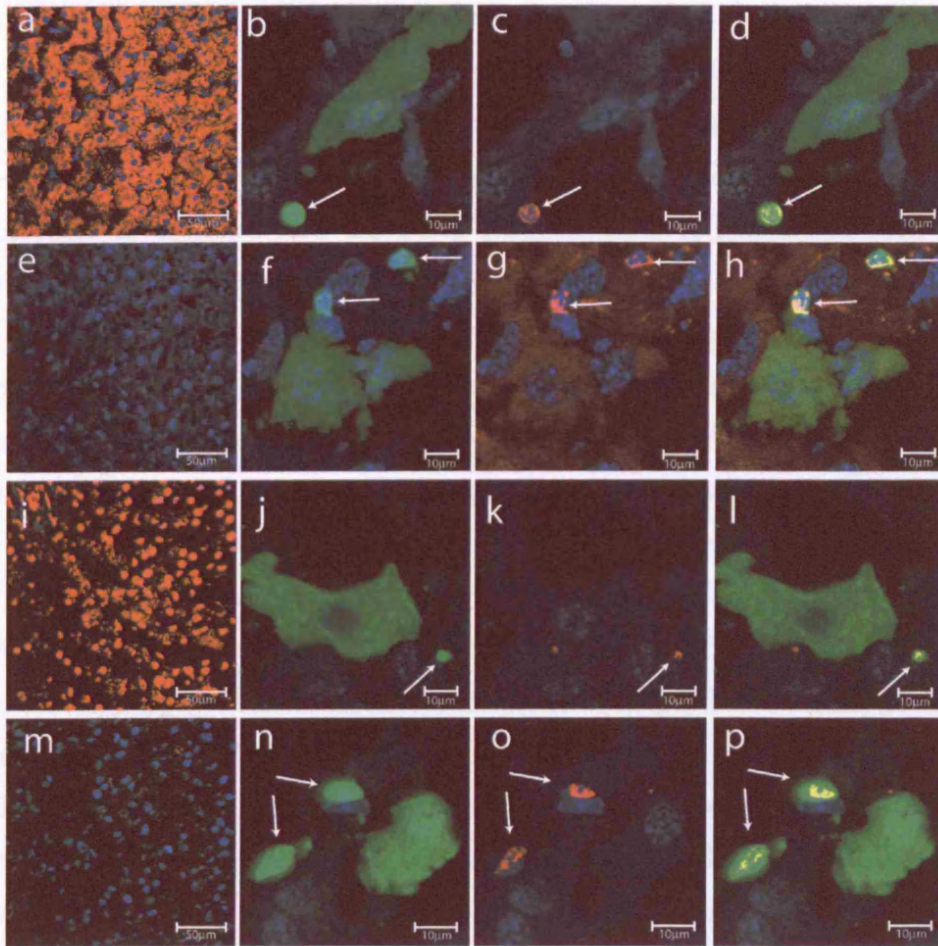
Figure 33 GFP positive hepatocyte-like cells do not stain with anti-human-mitochondria or anti-human-nuclei antibody.

Anti-human-mitochondria antibody highlights human mitochondria in the cytoplasm of human cells (a) but no signal is obtained in mouse liver cells (e). eGFP positive hepatocyte-like cells in the liver of experimental animals (b, f) are negative for human mitochondria (c,g) whereas adjacent haematopoietic cells (arrows) are clearly labelled (d, h merge images) Likewise anti-human-nuclei antibody highlights human nuclei (i) but not mouse liver cell nuclei (m). eGFP positive hepatocyte-like cells (j,n) are negative for anti-human nuclei (k,o) whereas adjacent haematopoietic cells (arrows) are again labelled (l,p merge images).

GFP positive hepatocytes harbour a murine Y chromosome, but no human chromosome I

To clarify the real origin of the GFP positive hepatocytes we performed FISH analysis in conjunction with GFP analysis. As the protease digestion for FISH analysis removes all of the GFP staining in the frozen sections we devised a two stage strategy to produce images of the same cell from GFP fluorescence and FISH staining.

In the first step we took images of GFP positive cells on a Zeiss LSM 510 confocal microscope. We designed software which read the x and y position of each picture taken from the microscope and stored it in digital format. After capturing images of all GFP positive hepatocytes on the slide we then performed the FISH protocol to stain murine Y or human chromosome I. The accompanying protease digestion removes most protein from the slides and leaves only nuclei. After performing the FISH protocol the slides were re-inserted into the fluorescence microscope, and the aforementioned software was used to position the microscope lenses exactly at the same locations where GFP positive hepatocytes had been photographed earlier. We then captured images of the fluorescence signals and produced overlays in Adobe Photoshop. Figure 34 demonstrates images of natural GFP fluorescence (a,d,g), FISH signal (b,e,h) and overlay images (c,f,i). GFP positive hepatocytes contain murine Y chromosomes (red signal) similar to the surrounding murine cells. When we performed dual FISH for murine Y and human chromosome 1 simultaneously we discovered that only the haematopoietic cells (h, lower left arrow) but not the GFP positive hepatocytes contain the human chromosome 1. Vice-versa we could only detect the murine Y chromosome (h, top right arrow) in the green hepatocytes, but not in the haematopoietic cells.

This result was incompatible with a hypothesis of transdifferentiation as the origin of the GFP positive hepatocytes. As we have performed rigorous tests on the lentiviral preparations used for transduction of the original stem cell population we felt confident to exclude the possibility of lentiviral contamination of the host animal.
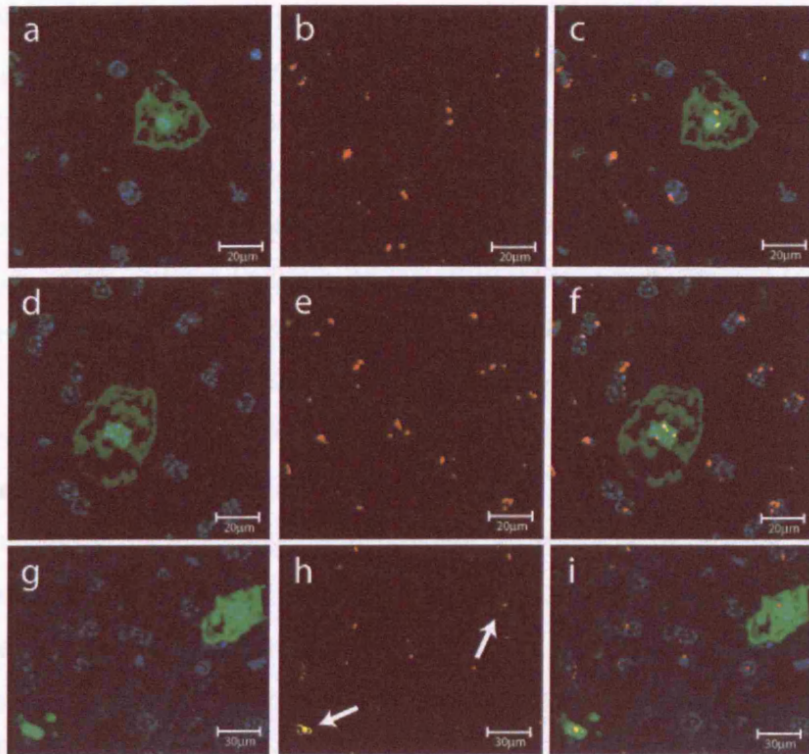
Figure 34 eGFP positive hepatocyte-like cells contain mouse Y and lack human chromosome 1.

eGFP positive cells in liver sections were photographed, and the location of each cell was saved (a, d, native eGFP fluorescence). Subsequently fluorescence in situ hybridization for mouse Y chromosome (red) or human chromosome 1 (yellow) was performed. Pictures corresponding to the same area of the slide as the original eGFP positive cells were taken (b, e). Overlay images (c, f) demonstrate the presence of mouse Y chromosome in eGFP positive hepatocyte-like cells as well as in surrounding eGFP negative cells. Simultaneous detection of mouse Y and human chromosome 1 (h and i: overlay image) reveals absence of human chromosome 1 in eGFP positive hepatocyte-like cells but detection of human chromosome 1 in eGFP-positive haematopoietic donor-derived cells (left arrow image h and overlay image i).

GFP positive cells contain genetic material of human and mouse origin

The difficulties of obtaining human marker staining in the GFP positive hepatocytes by FISH and immunohistochemistry led us to establish another technique in the lab.

Laser capture microdissection and single cell PCR allows us to analyze the genetic content of single cells from tissue sections. The liver parenchyme is well suited for this approach as hepatocytes are large cells with cytoplasm clearly separating the nucleus from the surrounding tissue. Frozen sections of liver tissue were stained for GFP using DAB as the visualising agent. We then used a PALM laser microdissection microscope to cut out single cells and collect them individually in PCR tubes. A typical GFP positive cell as seen in the PALM microscope is depicted in Figure 35a, with a picture of the remaining hole in the tissue after excision of the cell next to it. These images also demonstrate that no surrounding haematopoietic cells could have been inadvertently included into the sample as the GFP positive cell is clearly visible. When cutting the nucleus we also took care to not include surrounding tissue and to cut inside the cell wall of the hepatocyte. The laser pulse vaporises tissue in a trail of approximately 5µm thickness further reducing the possibility of a haematopoietic cell closely associated to the hepatocytes being included in the sample. The single cell DNA in the PCR tube was amplified by random primed PCR and specific PCR for human and murine genomic targets and for GFP was performed. Figure 35b demonstrates that on control tissues from human and murine liver slides we could detect a positive band for the respective genome in ~30% of samples. This is within the expected range taking into account the thickness of our sections (10µm), the size of a hepatocyte (~35µm) and technical limitations of cell capturing and PCR. We did not observe contaminating bands in control tissues or in non-GFP stained hepatocytes from experimental animals.

Figure 35c depicts the PCR result of 24 individual GFP positive hepatocytes in duplicates. We detect GFP in ~30% of samples which is consistent with the genomic locus being present in all the samples. We also were able to detect the murine TNFα locus in 10 of 24 samples which demonstrates that these hepatocytes contain murine DNA in a proportion similar to murine control cells. The human TNFα locus on the other hand was only detected in a small percentage of GFP positive hepatocytes. Nevertheless we could also detect a second human genomic marker, human TCR in sample number 2.

As shown in Figure 35d the proportion of murine DNA in these GFP positive hepatocytes clearly demonstrates a murine origin of the cells. The presence of GFP in all these cells is the result of the selection of cells by GFP expression. The amount of human DNA in these GFP positive hepatocytes is not consistent with a model of fusion with full maintenance of the whole genomic material of the fused human cell.

We speculate that human DNA is introduced into these cells by a mechanism of fusion, but the foreign DNA is then subsequently removed from the cells. This mechanism would also explain the difficulty in finding other human marker in these cells.
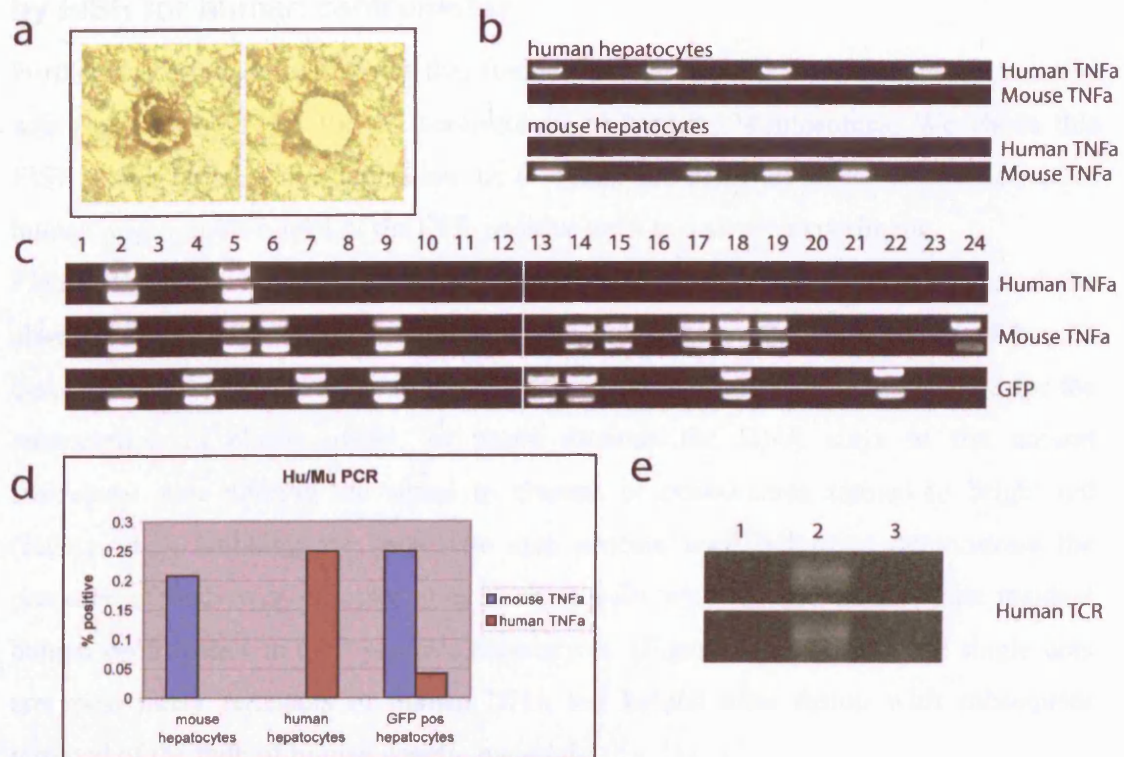
Figure 35 Presence of both human and mouse TNFα in single eGFP positive hepatocyte-like cells after single-cell PCR analysis.

Frozen tissue sections of experimental livers were stained with eGFP antibody. Single eGFP positive hepatocyte-like cells were cut from the section with a PALM laser microdissection microscope (a. before (left) and after (right) dissection) and captured into PCR tubes containing 1x PCR buffer with 0.5% tween. After digestion with proteinase K overnight, 60 cycles of i-PEP PCR were performed (see detailed in methods). 3 μl of this reaction were then used as template in duplicate nested PCR for human TNFα, mouse TNFα and eGFP. Efficiency and specificity of PCR was determined by cutting cells from mouse liver or human liver (b and d: average of 3 experiments). 24 single eGFP positive hepatocyte-like cells were cut out and processed. Human TNFα can only be detected in 2/24 samples, whereas mouse TNFα is present in 10/24 and eGFP in 7/24.(c, panels show duplicate reactions) Cells 2 and 5 are positive for human and mouse TNFα. Samples 1-3 were additionally tested for presence of human TCR locus, which is detected only in sample 2 (e).

Residual human DNA can be detected in GFP positive hepatocytes by FISH for human centromeres

Further proof for the hypothesis that fusion with subsequent loss of genomic material was provided by FISH for the centromeres of human chromosomes. We chose this FISH probe because it would allow us to detect the presence of all chromosomes of human origin in the nuclei of the GFP positive cells in a single experiment.

Figure 36 shows the detection of human chromosomes in human liver (a) and the absence of staining in murine liver (d). The probe stains the centromeres of human chromosomes, and in metaphase spreads of haematopoietic cells it can be used for the enumeration of chromosomes. In tissue sections the DNA stays in the natural condensed state altering the signal to clusters of centromeres stained in bright red (Figure 36a). Utilizing the same two step process used before to demonstrate the presence of murine Y chromosomes in these cells we can here demonstrate residual human centromeres in GFP positive hepatocytes. (Figure 36b-c, e-f) These single dots are most likely remnants of human DNA left behind after fusion with subsequent removal of the bulk of human genetic material.
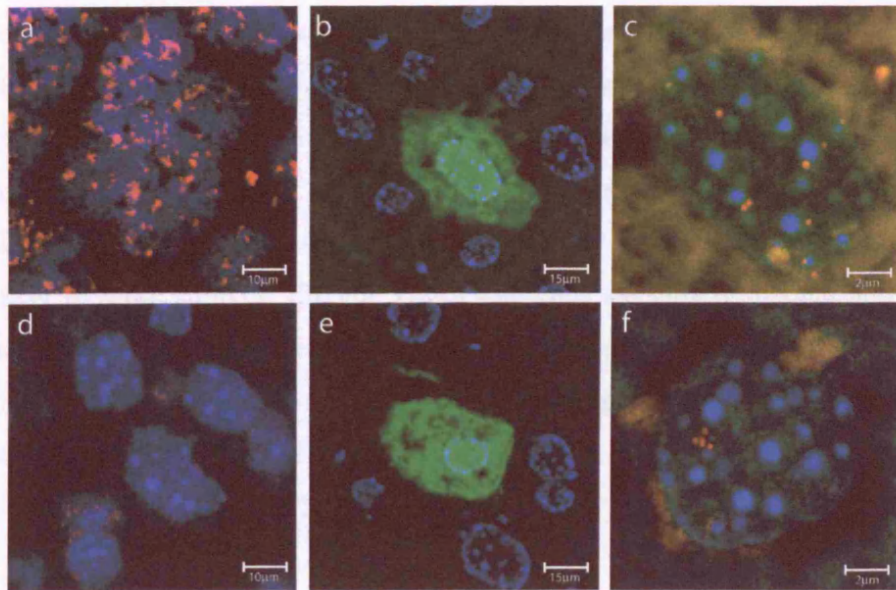
Figure 36 eGFP positive hepatocyte-like cells contain few human centromeres.

FISH for human centromeres highlights multiple spots and clusters (red) in human hepatocytes (a) but not in mouse hepatocytes (d). eGFP positive hepatocyte-like cells in experimental animals (b-f) contain only few human centromeres (c, f: high magnification). Nuclei were counter-stained with DAPI (blue).

GFP positive cells and HSA positive hepatocytes are different populations

The two populations of cells which have been described in this study in detail are HSA positive cells arising in mice which have been transplanted by human lin⁻ stem cells, and GFP positive hepatocytes present in livers of animals transplanted with GFP marked cells. To find out if these two populations are related we performed simultaneous staining for HSA and GFP on livers of animals which had received GFP marked cells. Figure 37 demonstrates that both distinct populations of cells are present in the liver of these animals. (Figure 37a-c) The cells are clearly distinct and no cells expressing both markers are present. The two cells present in Figure 37c (white arrows) are shown in higher magnification in Figure 37d-i. Figure 37d-f demonstrates a HSA positive cell which is not exhibiting any GFP staining, and Figure 37g-i demonstrates the GFP positive cell lacking HSA expression.
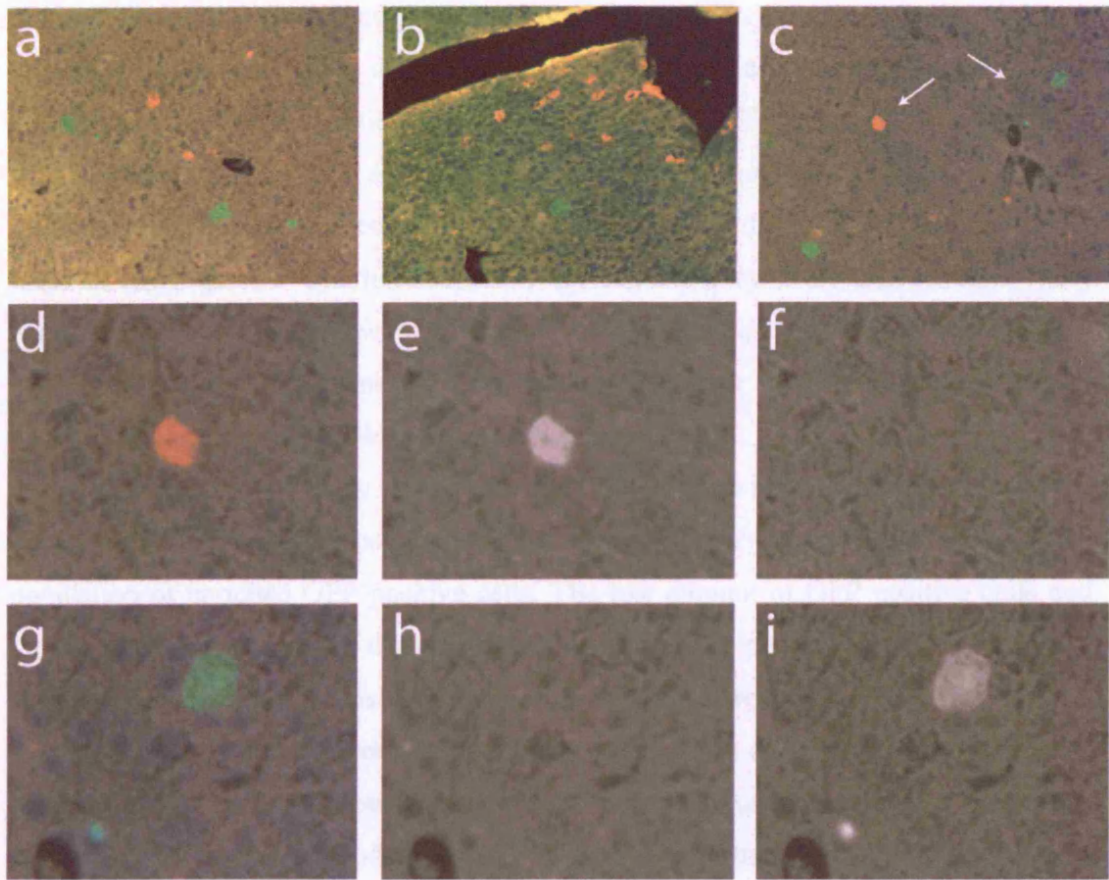
Figure 37 GFP and HSA are mutually exclusive

Liver sections of experimental animals were stained for GFP (green) and HSA (red). a-c) Low magnification images of liver tissue showing that GFP expressing and HSA expressing cells appear next to each other in the same tissue section. The HSA positive cell indicated by the white arrow in panel c demonstrates strong staining for HSA (e) but no staining for GFP (f). The GFP positive cell indicated by the white arrow in panel c does not stain with HSA, but is positive for GFP (i)

Summary

We have demonstrated the occurrence of GFP positive cells of non-haematopoietic morphology in liver, lung and gut tissue in addition to haematopoietic cells visible in the spleen. The enumeration of GFP positive hepatocytes in the livers of these animals allowed us to find a correlation between the number of GFP positive hepatocytes and the pre-treatment with CCl_4. As we have previously demonstrated that CCl_4 also has an influence on bone marrow engraftment we can conclude that the overall engraftment level in bone marrow and liver is positively regulated by CCl_4 intoxication. These results do however not allow us to deduce if the higher percentage of GFP positive hepatocytes in the liver stems from the tissue damage per se, or is a result of higher bone marrow engraftment induced by the CCl_4 intoxication.

In an attempt to more closely characterise the GFP positive hepatocytes we pursued the isolation of GFP positive hepatocytes by FACS sorting, but were unable to obtain a cell population of enriched GFP positive cells. The low amount of GFP positive cells and the technical constraints of the experiment such as liver perfusion, FACS detection, sorting and collection are most likely the cause of this failure.

The expression of human liver specific mRNA in the livers of the experimental animals reported in an earlier chapter of this work prompted us to investigate numerous immunohistochemical methods and antibodies to demonstrate the expression of these proteins in the GFP positive hepatocytes. However we were only able to demonstrate albumin expression in some GFP positive hepatocytes. The lack of strong human antigen expression raised doubts about the true nature of these cells. These doubts were even more reinforced by the observation that these cells lack expression of pan-human immunological markers which are usually present on all cells of human origin.

FISH analysis is a powerful tool to show the genetic content of cells. It is however also very difficult to achieve reliable FISH results on whole tissue sections. Nevertheless, the presence of murine Y chromosome in the GFP positive hepatocytes is a clear indicator of the non-human nature of these cells. When we probed for the presence of chromosome 1, the largest human chromosome, we could not find any staining in the GFP positive hepatocytes while it was clearly present in haematopoietic cells.

Individual single chromosome paints displayed a very diverse efficiency on liver sections, so we turned to microdissection and single cell PCR. With this technique we can show the presence of human and murine genetic material in GFP positive

hepatocytes. The murine genetic material is present at the rate of detection in control tissues, while the human genetic material is clearly underrepresented.

We utilised the staining for the centrosomes of all human chromosomes to find out if residual human DNA is present in the GFP positive hepatocytes and can demonstrate single dispersed human centromeric fragments in the nuclei of these cells.

These results suggest a mechanism which has already been proposed by Wang et al (Wang *et al.* 2003) in the murine model. The fusion of resident hepatocytes with donor derived haematopoietic cells produces hybrid cells with an unstable genome. Over time non-essential genetic material from the donor is removed leaving an incoherent genotype in the hybrid cells. This incoherent genotype could be the reason for the poor expression of human antigens by the cell hybrids.

Chapter 5 Other models of transdifferentiation

Introduction

Although the focus of this study was placed on the possible transdifferentiation of human cord blood progenitor cells into functional liver cells in the NOD/Scid mouse model we additionally investigated several other possible systems which could be used in this research.

The transdifferentiation of haematopoietic cells to hepatocytes was at the focus of this study, but nevertheless the close developmental relationship between the haematopoietic system and the liver made it conceivable that cells from the liver could also give rise to haematopoietic cells. To test if human liver cells can give rise to blood cells in our model we obtained human liver tissue from surgical liver resections and transplanted these cells into NOD/Scid mice to see if bone marrow engraftment can originate from a liver cell population.

One well known model of liver disease is the alb-uPA model (Sandgren *et al.* 1991). These transgenic mice over-express the urokinase plasminogen activator (uPA) under the control of the albumin (Alb) promoter. The animals die of liver failure unless rare hepatocytes excise the transgene. These wild-type hepatocytes then proliferate, and they regenerate the entire liver within 8 weeks. During this interval the Alb-uPA mouse suffers chronic liver damage and long-term regeneration. The Alb-uPA mouse was back-crossed onto the RAG2$^{-/-}$ background to allow for the transplantation of xenogeneic cells (Petersen *et al.* 1998). We collaborated with the laboratory of Dr. Petersen at the Heinrich-Pette-Institute in Hamburg, Germany to conduct an experiment using human cord blood cells and RAG$^{-/-}$Alb-uPA mice (RAG2-uPA).

The NOD/Scid model allows introduction of human cells into a murine environment without the adverse immune reaction associated with xenotransplantation. It is an efficient host for haematopoietic cell transplants that mimic a human bone marrow transplantation. In this study however the focus was on liver regeneration, and the NOD/Scid model does not allow for any selection specific for human liver cells per se.

To overcome this limitation we have back-crossed the metallothionein knockout mouse (Masters *et al.* 1994) onto the NOD/Scid background as described in materials and methods and in chapter 1. We have then performed bone marrow transplantation, and multiple rounds of cadmium intoxication in these mice to specifically destroy host hepatocytes and give a selective advantage to prospective human transdifferentiated hepatocytes.

One of the main problems in cell replacement treatments is to obtain sufficient numbers of cells for transplantation. As non autologous cord blood stem cells can not be expanded *in vitro* and are not immunologically matched to prospective human recipients of cell transplants, much effort has been directed at finding other sources of cells capable of transdifferentiation. One of the most promising populations isolated to date are mesenchymal stem cells. These cells seem to be capable of differentiation along lines of all three germ layers (Pittenger *et al.* 1999; Jiang *et al.* 2002; Anjos-Afonso *et al.* 2004) and can be expanded *in vitro*. We tested if murine mesenchymal stem cells which had been pre-differentiated with conditions favouring the development of hepatocytes are able to integrate into the NOD/Scid liver and give rise to functional hepatocytes.

Human liver cells do not give rise to hematopoietic cell engraftment

The close relationship of liver and haematopoietic system during development prompted us to investigate the developmental potential of human hepatocytes in the NOD/Scid xenotransplantation model. We obtained human hepatocytes from the UK human tissue bank and transplanted 2×10^6 human hepatocytes into 8 recipient mice. Of these animals 4 had received 10µl CCl_4 2 days before transplantation and all animals received 375 RAD irradiation on the day before transplantation. After 14 weeks the animals were sacrificed and bone marrow was harvested for FACS analysis. Figure 38a demonstrates a typical FACS plot from these animals showing no engraftment in the myeloid or lymphoid lineage. Figure 38d depicts an engrafted animal from a different experiment for comparison. None of the 8 animals in this experiment showed any human cells in the bone marrow. A repetition of this experiment with another set of 6 animals demonstrated the same result.

Many HSA positive, only few FISH positive hepatocytes after transplantation of human hepatocytes

In the livers of the animals that had been treated with CCl_4 we could readily detect HSA positive hepatocytes. (Figure 38b,e) To confirm the human origin of these hepatocytes we performed FISH analysis for the human chromosome 1 on frozen sections, and can detect positive staining in large nuclei of hepatocyte morphology. However, the number of FISH positive cells present in the liver is much smaller than the number of HSA positive cells. Due to technical difficulties in performing human chromosome FISH and HSA staining on the same section we can not provide evidence that these two methods highlight the same cells.
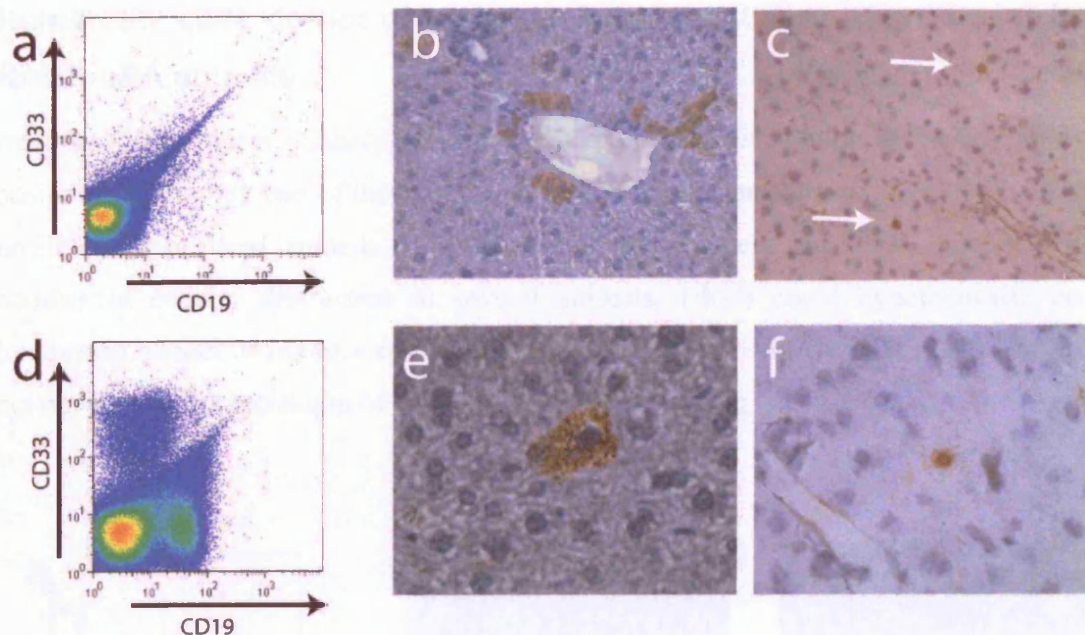
Figure 38 Engraftment from human hepatocytes

Transplantation of $2x10^6$ human hepatocytes did not lead to significant haematopoietic engraftment a) FACS plot of a mouse transplanted with 10^6 human hepatocytes after irradiation and CCl_4 treatment, b,e) HSA staining of liver from the same animal, c,f) FISH for human chromosome 1. (positive nuclei marked by white arrows) d) FACS plot of a mouse transplanted with 10^5 lin⁻ cord blood cells.

Human cord blood stem cells do not engraft in the bone marrow of RAG2-uPA animals

RAG2-uPA animals are a model for the engraftment of xenogeneic liver cells. To test the possibility of trans-differentiation of human haematopoietic progenitors in these animals we transplanted 12 animals with 10^5 human lin⁻ cord blood cells after pre-treatment of half of the animals with 350 RAD irradiation. The animals were sacrificed at 6 and 12 weeks after transplantation, and bone marrow and livers were harvested for analysis. Analysis of the bone marrow by FACS revealed a complete absence of human cells in the bone marrow of these animals regardless of the timepoint and the pre-treatment. Figure 39a demonstrates FACS analysis of one of these animals.

Human lin⁻ cells do not give rise to substantial liver engraftment in RAG2-uPA animals

Analysis of the livers of these animals revealed a small population of weakly HSA positive cells in only two of the animals. Figure 39b,c demonstrate some of these HSA positive cells in these animals. In addition to these few cells we could also observe nodules of cellular destruction in several animals, which could hypothetically be interpreted as loci of immune response to lodging human cells. (Figure 39d-f) We do not have any other indication of human cells in these animals.
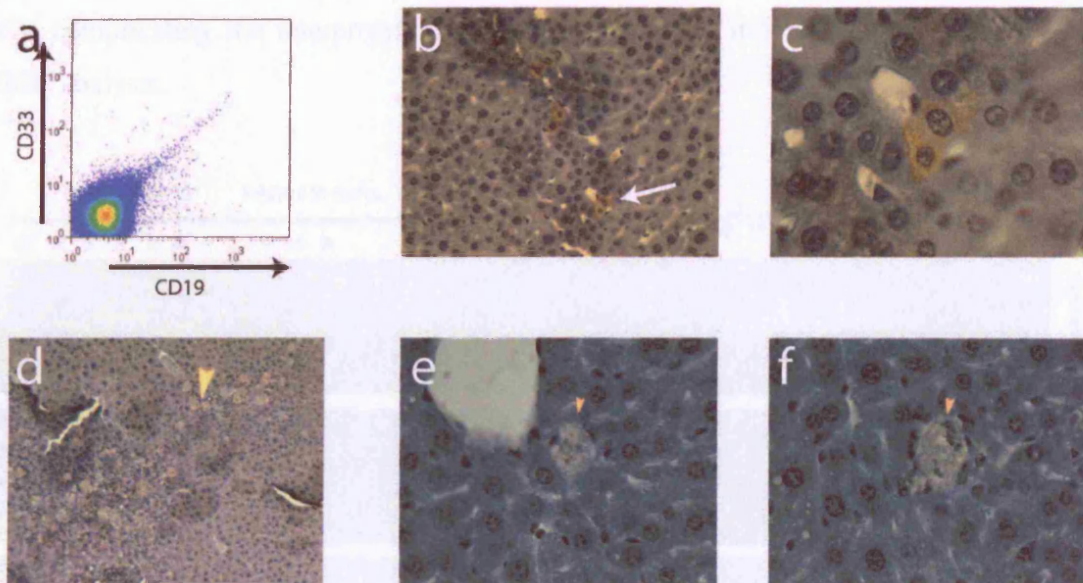
Figure 39 Transplantation of human cells into RAG2-uPA animals

Animals were transplanted with 2×10^5 human cord blood lin⁻ cells. After 6 or 12 weeks animals were sacrificed. Absence of cells positive for the human CD19 or CD33 antigen establishes that there is no engraftment in the bone marrow (a). Paraffin sections were stained with the HSA antibody and developed with DAB. Weakly HSA positive cells are visible in the liver (b,c). Nodules of debris possibly the remainder of tissue necrosis are present in several animals. (d-f)

No Expression of human mRNA in livers of NOD/Scid animals transplanted with human hepatocytes or RAG2-uPA animals transplanted with human haematopoietic cells

We performed RT-PCR for human specific mRNA on livers of NOD/Scid animals that had been transplanted with human liver cells and also from livers of RAG2-uPA animals transplanted with human cord blood lin⁻ cells. As demonstrated in Figure 40 we could not detect any human albumin mRNA in any of the animals of both sets of experiments. Furthermore we were unable to detect any human β-Actin mRNA. PCR for GAPDH which is not species specific demonstrates the presence of sufficient amounts of RNA in the samples. Although this result could be due to sensitivity issues it is complicating the interpretation of data gained from immunohistochemistry and FISH analysis.
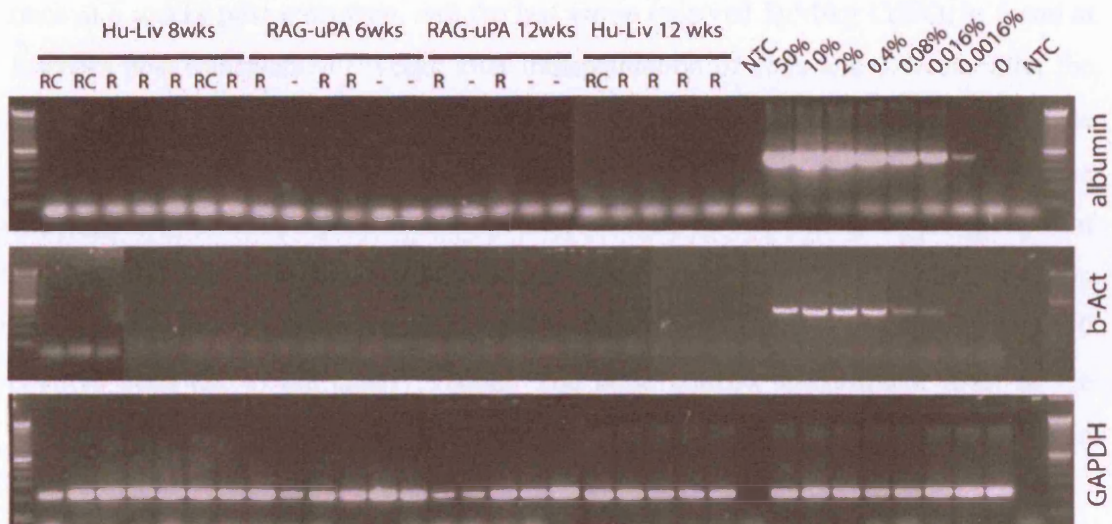
Figure 40 No human mRNA expression in experimental animals

RNA was extracted from the liver of experimental animals which had been transplanted with human haematopoietic cells (RAG2-uPA) or human liver cells (NOD/Scid) Control samples consist of RNA extracted from human hepatocytes mixed with murine liver cells. 3µg RNA were reverse transcribed, and 10% of that reaction were used for PCR.
Mice were either pretreated with 350 RAD irradiation (R) and/or 25µl CCl₄ (C) or left without pre-treatment (-).

Cadmium treatment after bone marrow transplantation induces altered liver morphology in NOD/Scid/met animals

The metallothionein knockout model was established to give a selective growth advantage to transplanted cells by making the host cells vulnerable to cadmium intoxication.

Female NOD/Scid/met mice (n=20) were transplanted with 3×10^5 human lin- cord blood hematopoietic stem cells after receiving 375 RAD irradiation as pre-treatment. We did not use CCl_4 in these experiments as we did not have enough mice to test the effect of CCl_4, and did not want to risk loosing mice. We also used only female mice to avoid problems associated with the extensive tissue destruction seen in the testis of males after cadmium treatment. The engraftment of the hematopoietic cells was allowed to proceed for 6 weeks, after which the animals were divided into three groups. The first group received mock injections of PBS, the second group received 5µM/kg $CdSO_4$ once at 6 weeks post transplant, and the last group received 5µM/kg $CdSO_4$ at 6 and at 8 weeks post transplant. 11 weeks after transplantation of cells and 3 weeks after the last $CdSO_4$ injection the animals were sacrificed and tissue samples were taken. The bone marrow of the animals was harvested and analyzed by FACS analysis. Figure 41a demonstrates the FACS profile of bone marrow cells of one animal of the group that showed 28% bone marrow engraftment and had received two injections of cadmium. The two populations of myeloid CD33 positive cells (3.6%) and lymphoid CD19 positive cells (22%) are clearly visible. The bone marrow engraftment level of the animals in this experiment was very variable from 0 to 46% with no significant bias in any of the three treatment groups.

Upon extraction of the murine livers we immediately noticed strong morphological abnormalities of the livers, relative to the cadmium dose received by the animals. While the livers of animals without cadmium looked normal, albeit a bit pale, the livers of animals that had received cadmium were hard, rigid, pale and had outgrowths on the outside of the lobes. Figure 41b demonstrates macroscopic images of a normal liver (left) and the liver of animal 25.14, the same animal used in the bone marrow analysis in Figure 41a. It is clearly visible that the liver is grossly abnormal, and protrusions are visible from the upper side shown in the middle of Figure 41b, and also on the underside of the liver shown on the right. These morphological changes were seen in

varying degree, being stronger in the mice that had received cadmium twice like this animal.

Hematoxylin and eosin staining of liver sections from these animals revealed the presence of large amounts of small cells. These small cells seem to present in a variety of shapes from very small and longitudinal to larger and round cells. Of special interest is that we can also see a large proportion of cells with clear hepatocyte morphology, albeit much smaller than normal hepatocytes. This is highly reminiscent of reports by Gordon et. al. about small hepatocyte progenitors emerging in livers after retrorsine treatment (Gordon *et al.* 2000). Although these cells could not be maintained in culture after isolation they nevertheless created fully functional hepatocytes when transplanted into recipient animals (Gordon *et al.* 2002). Figure 41c shows an hematoxylin/eosin staining of the protrusion of the liver indicated in Figure 41b. In the higher magnification we can clearly see many small cells occupying the space between the hepatocytes. In comparison to an animal that has not received cadmium (Figure 41f) the liver of animal 20.14 which had received two doses of cadmium contains two additional cell populations. One is a population of small cells of non-hepatocyte morphology with elongated features reminiscent of inflammatory infiltration. However, the second population consists of hepatocyte-like cells which do exhibit clear hepatocyte features including large cytoplasm and large round nuclei with clearly visible nucleoli, but are much smaller than normal residual hepatocytes in the surrounding parenchyme. Although we have no data to support this hypothesis it is intriguing to speculate that the two populations represent two different stages of regeneration as a result of the two cadmium treatments.
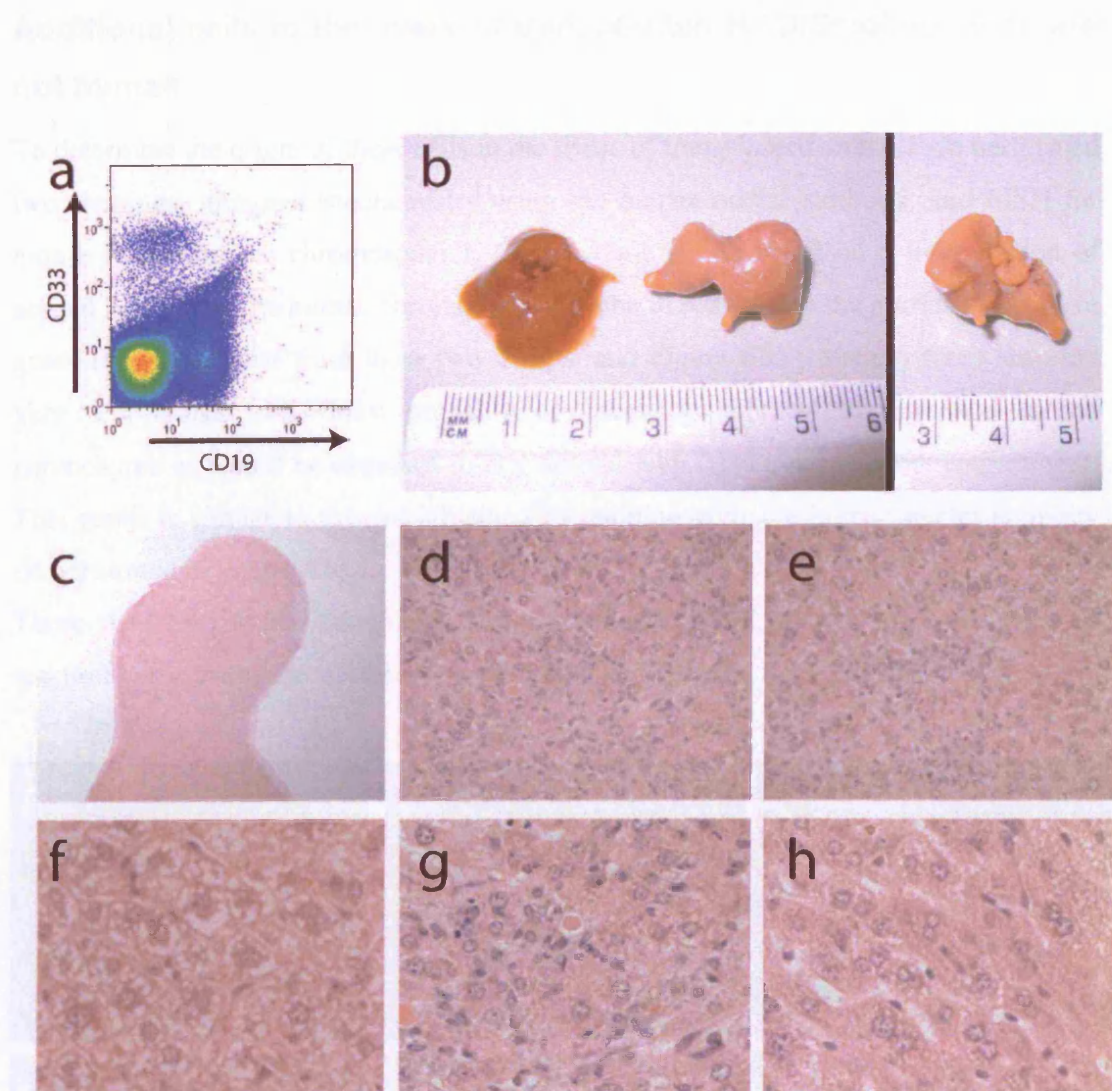
Figure 41 Bone marrow engraftment and liver morphology of NOD/Scid/met mice

Bone marrow of a NOD/Scid/met animal transplanted with 10^5 lin⁻ cells. The animal was pretreated with 350 RAD irradiation and was given 2 injections of 5 µmol/kg $CdSO_4$ 6 and 8 weeks after transplantation. Analysis was performed after 10 weeks. Engraftment of this animal was 28.2% (a). The liver of the same animal demonstrates gross macroscopic abnormality (b). H&E staining of the liver at low (c) and higher magnification (d,e) reveals abnormal cell growth. In comparison to normal liver (f) the liver of experimental animals contains additional small cells of haematopoietic morphology (g) and small hepatocyte like cells (h).

Additional cells in the livers of transplanted NOD/Scid/met mice are not human

To determine the origin of these cells in the livers of transplanted animals we performed two stainings, immunohistochemistry using the human-nuclei antibody, and FISH for mouse X and human chromosome 1. Figure 42a-c shows FISH on a liver section of animal 21.14 with the human chromosome 1 probe in red (a) and the murine X probe in green (b). As is clear from these two images and Figure 42c (overlay) there are only very few human cells most probably of haematopoietic origin dispersed in the parenchyme as would be expected in any animal with 23% bone marrow engraftment. This result is similar to the one obtained by staining with the human-nuclei antibody demonstrated in Figure 42d-f.

These data lead to the conclusion that the abnormal cell growth in these livers in reaction to the cadmium treatment originates solely from the host cells.
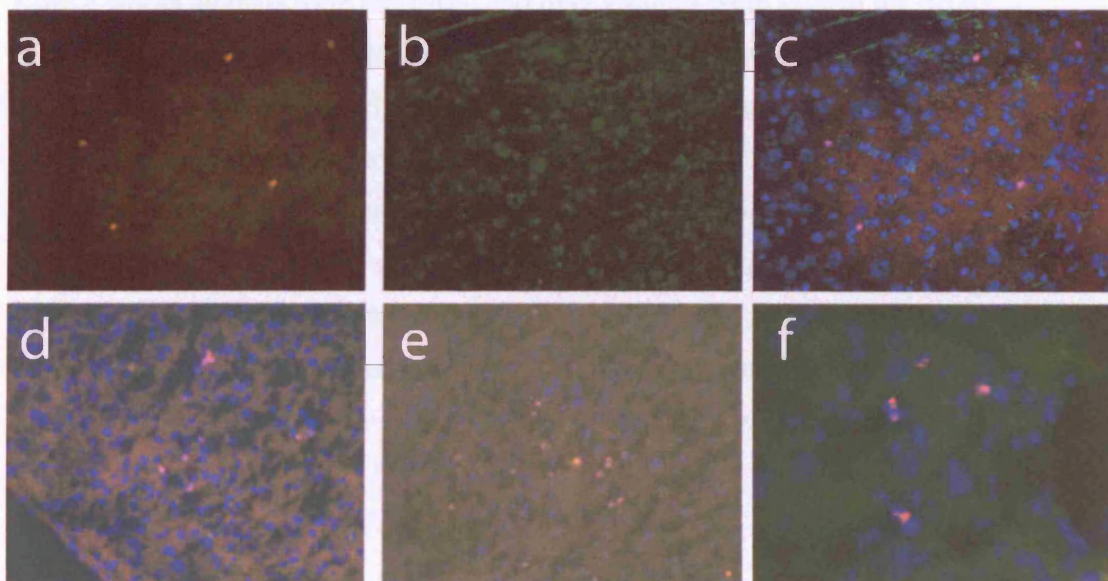
Figure 42 Few human cells in livers of transplanted NOD/Scid/met animals

Frozen sections from the same liver as in Figure 41. FISH for human chromosome 1 (a, red) and mouse chromosome X (b, green) reveals the presence of only few single human cells (c, overlay) with a nuclear morphology of haematopoietic cells. Staining with human nuclei antibody (red, d,e low magnification, f high magnification) reveals the same low number of human cells consistent with the presence of haematopoietic cells after bone marrow engraftment.

Possible engraftment of murine Mesenchymal Stem Cells in the mouse liver

In collaboration with Fernando Afonso, a colleague in the lab, murine mesenchymal stem cells were *in vitro* differentiated into the hepatocyte lineage, labelled with BrDU and introduced into NOD/Scid animals.

MSC were isolated from murine bone marrow of unspecified gender and grown in culture (Anjos-Afonso *et al.* 2004). After two doublings the cells were introduced into 12 well plates at a density of 200-3000 cells/cm^2 and labelled with BrDU by incubation with 10μM BrDU for 48 hours. FACS analysis reveals that about 30% of the cells are efficiently BrDU labelled after this procedure. The cells were then induced to differentiate along the hepatocyte lineage by switching the medium to DMEM 2%FCS supplemented with 10ng/ml fibroblast growth factor 4 (FGF4) and 20μg/ml hepatocyte growth factor (HGF) changing medium every three days. After 7 and 14 days one million cells was transplanted into mice treated with CCL$_4$ (n=3) or without CCl$_4$ (n=3). After 4 weeks animals were sacrificed and liver sections were stained for BrDU.

Figure 43a depicts a low magnification image of a liver section stained for BrDU with one hepatocyte nucleus clearly labelled. In the higher magnification (Figure 43b) it is evident that the nucleus is dark and the morphology of the cell is that of a hepatocytes. Several of these cells could be found in liver sections of mice treated with CCl$_4$ but we were unable to detect any in mice not pre-treated with CCl$_4$. A more thorough analysis of these samples could provide more information about the amount of cells but was not conducted due to time constraints. We also had to consider that a repetition of this experiment using GFP positive or ROSA26 MSC would make analysis of the results more efficient and reliable.
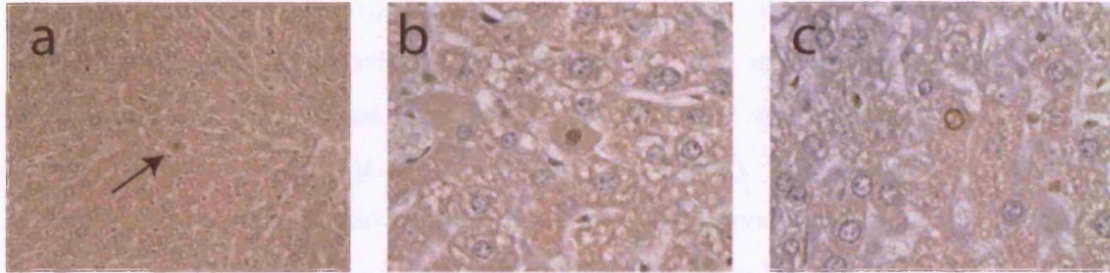
Figure 43 BrDU staining of MSC in NOD/Scid animals

MSC differentiated along the hepatocytic lineage and labelled by BrDU were introduced into mice treated with CCl_4. Staining with rat-anti-BrDU antibody reveals several hepatocytes with dark, stained nuclei presumably originating from the transplanted population of MSC. a) low magnification showing single positive cell (arrow), b) the same cell in higher magnification c) another BrDU positive cell

Summary

We have investigated several alternative directions of research into transdifferentiation in this chapter. The first approach was to investigate the possible reversal of the transdifferentiation seen in our model, i.e. the conversion of a cell of liver origin into a haematopoietic cell. We have introduced human hepatocytes into mice half of which were pretreated with CCl4. All animals have received preparatory total body irradiation, a prerequisite for bone marrow engraftment. In our experimental setup which encompassed 14 transplanted animals we could not find any human haematopoietic engraftment during the time span examined (12 weeks). This result indicates that mature human hepatocytes do not have the capability to give rise to bone marrow cells in this model. Despite the lack of bone marrow integration we can detect hepatocytes which are positive for the HSA antigen, and also some hepatocytes with apparent human genome by FISH analysis.

Another approach taken was the introduction of human haematopoietic stem cells into a well characterised model of liver damage and regeneration, the RAG2-uPA model. After transplantation of human stem cells we could not see any bone marrow engraftment in any of the experimental animals. This is most likely explained by the residual components of the immune system in the RAG2 knockout mice. In HSA stained liver sections we could detect several single HSA positive cells with hepatocyte morphology, and nodules of cellular destruction were apparent.

RNA analysis of several animals from the experiments involving human hepatocyte transplantation or the RAG2-uPA model revealed no significant expression of human mRNA in any of the samples. This result demonstrates that human hepatocytes do not give rise to haematopoietic engraftment in our model, and that the RAG2-uPA model does not support the haematopoietic to hepatocytic conversion of human haematopoietic stem cells.

The new model of hepatocyte damage established with the NOD/Scid/met animals opens very interesting possibilities in liver regeneration research. The specificity of the acute cadmium intoxication for the liver tissue allows the discrimination of host and donor cells inside the regenerating organ. In contrast to the RAG2-uPA model excision of the transgene is not possible, and in contrast to the FAH$^{-/-}$ model the mutation is not lethal and the strain supports xenogeneic cell engraftment. In our first experiments we could induce a severe liver defect during the course of the study. The occurrence of

small cells of both hepatocyte and non hepatocyte morphology indicates the utilization of a regenerative pathway different to the traditional regeneration by division of mature hepatocytes seen in the CCl_4 damage model. Although in our preliminary experiments the regenerative tissue in this liver was constituted only of murine host cells the use of different xenobiotic cell sources may make this inducible damage model a valuable contribution to the scientific community.

The acquisition of sufficient amounts of cells for transplantation remains a challenge in the field of stem cell transplantation. One of the most promising populations of cells currently under investigation is the mesenchymal stem cell pool. We attempted to transplant cells which had been differentiated *in vitro* along the hepatocytic lineage to investigate the possibility of liver integration of these cells. Due to experimental constraints we had to resort to a labelling strategy to allow detection of MSC progeny in the murine organism. Although we could find several hepatocytes with apparent BrDU labelling in the nucleus we are unable to investigate these samples any further as we can not distinguish between host and donor cells other than by the BrDU label. Future experiments will use a genetically distinguishable source of murine MSC cells or human MSCs to allow for careful analysis of the capabilities of MSC in the damaged liver.

Discussion

We have studied the capabilities of human haematopoietic stem cells to give rise to hepatocytes in a murine xenotransplantation model. To improve engraftment we have studied a variety of damage models in the NOD/Scid mouse strain. Only the CCl_4 intoxication was capable of producing large scale tissue destruction in the liver (Figure 14, 15) so it became the focus of our investigation. We tested the efficiency of retrorsine to inhibit hepatocyte regrowth in our animal model but found it to be inefficient. Additionally we established first dose-response data for a new model of liver damage, the metallothionein knockout mouse strain NOD/Scid/met. (Figure 18)

After the initial report by Danet et al (Danet *et al.* 2002) about the occurrence of apparent human hepatocytes in transplantation studies without extensive tissue damage we attempted to find a good animal model that would allow us to investigate this result in more detail. We tried to establish a model that would allow us to study the influence of tissue damage on the quantity and quality of liver engraftment. The CCl_4 model of tissue damage is an ideal tool for this as it induces acute liver damage and a controlled, well characterised repair mechanism. In addition to an acute damage model we also wanted to establish a model in which we could confer a selective advantage to the transdifferentiated human cells so an expansion would occur. Although this has been described to be the case with retrorsine in the rat model (Laconi *et al.* 1998; Laconi *et al.* 2001) we have unfortunately been unable to see a similar effect of retrorsine in our mouse model. This and the unavailability of retrorsine from the supplier for the larger part of this study led us to develop a new mouse model system. In the NOD/Scid/met model a selective advantage can be conferred to xenobiotic hepatocytes by selectively destroying the native host hepatocytes with cadmium intoxication.

The homing of stem cells to the site of engraftment has received much attention recently (Lapidot *et al.* 2002; Kollet *et al.* 2003). We investigated if tissue damage influences homing of human haematopoietic progenitors by utilizing the CCl_4 damage model. In concordance with earlier reports we can detect a higher level of liver homing in animals which have received liver damage, which is also accompanied with larger amounts of cells homing to the bone marrow. (Figure 20) This unexpected result

highlights that even though the damage induced by CCl_4 is tissue specific, the effects of the damage are noticeable in the whole animal organism.

After the initial homing phase human hematopoietic cells engraft primarily into the bone marrow and give rise to sustained multi-lineage engraftment. (Figure 21) The amount of bone marrow engraftment is greatly influenced by CCl_4 intoxication, consistent with a late effect of the homing advantage. (Figure 22) We then went to investigate human mRNA expression and could show detection of RNA for human Albumin, alpha-Anti-Trypsin and human beta-Actin. Animals transplanted with lin⁻, CD34⁺, CD34⁺CD38⁻ and even CD34⁻CD38⁻ cells displayed expression of human albumin at very low levels. (Figure 25) We then report the detection of HSA positive cells in several of the experimental animals. HSA has been used in three other publications (Danet *et al.* 2002; Almeida-Porada *et al.* 2004; Kogler *et al.* 2004) to detect hepatocytes of human origin. We demonstrate that we can see distinct typical HSA staining on a murine tissue sample of an animal that has not been transplanted with any human cells. (Figure 28) We also demonstrate that the HSA positive cells found in our experimental animals contain a murine Y chromosome (Figure 29). Although the murine Y chromosome in the HSA positive cells can theoretically be explained by a fusion event we have no explanation for the occurrence of HSA positive cells in one of our control mice. Based on these data we conclude that the HSA antibody is an unreliable tool for detection of human cells in a murine environment.

Genetically marked human primary cells are a powerful tool in elucidating the possibilities behind stem cell transplants. We used GFP marked human haematopoietic cells in transplantation experiments which allowed reliable detection of cells of human origin in several organs of the experimental animals. (Figure 30) We demonstrate the detection of GFP positive hepatocytes, and show the correlation between CCl_4 treatment and amount of GFP positive hepatocytes. (Table 1) Using immunohistochemistry we can show that GFP positive hepatocytes are CD45 negative, and express albumin, in line with RT-PCR results. (Figures 32 and 25) Closer inspection of the GFP positive hepatocytes did reveal that they were missing several other human antigens, like human-mitochondria and human-nuclei. (Figure 33) Using FISH analysis we show the lack of human chromosome 1 in GFP positive hepatocytes, although it is present in human derived haematopoietic cells. Single cell PCR analysis also paints a complex picture of the genetic composition of the GFP positive hepatocytes indicating that they are hybrid cells containing genomic material from both

murine and human cells. (Figures 34,35 and 36) In summary we can conclude that these GFP positive cells are most likely derived from a fusion of a resident hepatocyte with a human haematopoietic cell which are abundant in highly engrafted animals. This mechanism has been described before (Vassilopoulos et al. 2003; Wang et al. 2003), and has also been shown in in vitro experiments (Terada et al. 2002; Ying et al. 2002). The hybrid cells have a selective advantage in the FAH$^{-/-}$ model by rescuing the biochemical pathway that splits fumarylacetoacetate into fumarate and acetoacetate so they expand and make up a large percentage of the liver mass. In our model the fused cells do not have a selective advantage so no expansion occurs. The loss of human genetic material in our model is also well explained by a lack of selection for human genes and has also been described before in the murine FAH model. While our results are well in line with earlier reports of fusion mechanisms in some animal models there are still two major publications which remain unchallenged. Jang et al demonstrated the generation of hepatocytes from a very specific population of haematopoietic stem cells without any signs of fusion both in vitro and in vivo (Jang et al. 2004) and Harris et al demonstrate the lack of fusion by using a Cre-Lox recombination system which should detect the occurrence of fusion in vivo (Harris et al. 2004).

In the final chapter we conducted experiments utilizing other murine models for xenotransplantation. We can show that human haematopoietic cells are not engrafting in the bone marrow or the hepatic parenchyme of RAG2-uPA animals. The murine metallothionein deficiency model NOD/Scid/met allows us to put selective pressure on host cells without detrimental effects on transplanted donor cells. Although we could not see any evidence of transdifferentiation of human cells in this model we could observe a strong regenerative stimulus exerted by the cadmium treatment in these animals. The lack of human hepatocytic transdifferentiation in these experiments could well be explained by an inability of the transplanted haematopoietic stem cell population to give rise to hepatocytes rendering the selective advantage ineffective.

A reversal of our approach of generating hepatocytes from haematopoietic cells was attempted in experiments where we used human hepatocyte infusion to see if functional haematopoietic engraftment can be achieved. However, in none of the experimental animals could we detect any human bone marrow engraftment. Additionally we can again detect abundant HSA positive cells but no accompanying liver specific RNA expression further reinforcing the difficulties encountered with this antibody. The amount of hepatocyte like cells which are positive for human chromosome 1 FISH is

very low in these animals, and might well be below the detection threshold of the RT-PCR.

The versatility of the mesenchymal stem cell populations prompted us to conduct preliminary experiments to investigate the potential of pre-differentiated MSC to engraft in the rodent liver. Although we do find cells of apparent donor origin, the technical details of the preliminary experiments do not allow a full characterization of these cells and further experiments will be necessary.

In conclusion in this work we have demonstrated the ability of human haematopoietic cells to fuse with murine resident hepatocytes to give rise to unstable heterokaryons. Although this result diminishes the possible use of haematopoietic stem cell transplantation for the treatment of diseases other than haematological disorders it is an important step forward in defining the capabilities of haematopoietic cell transplants. As it seems unlikely that haematopoietic stem cells can be therapeutically used for non-haematological disorders more research needs to be focused into alternative cell populations like MSC or tissue stem cells.

Future work

The apparent inability of haematopoietic cells to give rise to hepatocytes by real transdifferentiation without fusion makes therapeutic use of HSC for treatment of liver diseases unlikely. In our experiments we do not only see cells with human or GFP markers in the liver but also in other tissues, namely the kidneys and the lungs. Especially the cells incorporated into the parenchyme of the lung appear to have non-haematopoietic morphology and are also consistently present in several experiments. Elucidating the true nature of these cells, and conditions enhancing engraftment of these cells in the lung tissue is work currently progressing in the lab. While there is evidence that bone marrow to lung transdifferentiation is possible both in humans (Spencer *et al.* 2005) and in animal experiments (Kotton *et al.* 2001; Krause *et al.* 2001; Theise *et al.* 2002; Anjos-Afonso *et al.* 2004; Harris *et al.* 2004; Krause 2005) we have to keep in mind that more recent research is more cautious on this subject (Beckett *et al.* 2005; Chang *et al.* 2005; Kotton *et al.* 2005).

All of the work presented in this study was done with human haematopoietic stem cells purified from cord blood. As the results indicate, the transdifferentiation potential of this cell population is limited. An investigation of the transdifferentiative potential of MSC is under way in the lab (Anjos-Afonso *et al.* 2004). The advantage of MSC are mainly that this population of cells can be derived from adult bone marrow, expanded *in vitro* and differentiation into several cell types has been shown reliably *in vitro*.

The NOD/Scid/met mouse model provides us with an entirely new environment in which to test the transdifferentiation capabilities of stem cells as well as the capabilities of pre-differentiated cells or even hepatic progenitor cell populations. It is one of the very few systems which allow transplantation of xenogeneic, human cells while at the same time allowing selection for transplanted hepatocytes. We need to further define the damage-repair pathway initiated in this model by cadmium administration as it seems to be different to the repair in partial hepatectomy or CCl_4 damage models. We also should test the possibilities of hepatocytes of murine and human origin to integrate and repopulate the liver of these animals to have a benchmark of engraftment against which we can then compare other cell populations. Hepatic progenitor cells have been

studied extensively in murine models, using the NOD/Scid/met model we can now employ a xenotransplantation model to define hepatic stem cells in the human liver. A study into the ability of MSC which have been pre-differentiated into hepatocytes *in vitro* to integrate into the liver of NOD/Scid/met animals is currently under way in the lab.

References

Almeida-Porada, G., C. Porada, et al. (2004). "Plasticity of human stem cells in the fetal sheep model of human stem cell transplantation." Int J Hematol 79(1): 1-6.

Almeida-Porada, G., C. D. Porada, et al. (2004). "Formation of human hepatocytes by human hematopoietic stem cells in sheep." Blood 104(8): 2582-90.

Anjos-Afonso, F., E. K. Siapati, et al. (2004). "In vivo contribution of murine mesenchymal stem cells into multiple cell-types under minimal damage conditions." J Cell Sci 117(Pt 23): 5655-64.

Arai, F., A. Hirao, et al. (2004). "Tie2/angiopoietin-1 signaling regulates hematopoietic stem cell quiescence in the bone marrow niche." Cell 118(2): 149-61.

Arai, F., O. Ohneda, et al. (2002). "Mesenchymal stem cells in perichondrium express activated leukocyte cell adhesion molecule and participate in bone marrow formation." J Exp Med 195(12): 1549-63.

Avril, A., V. Pichard, et al. (2004). "Mature hepatocytes are the source of small hepatocyte-like progenitor cells in the retrorsine model of liver injury." J Hepatol 41(5): 737-43.

Baum, C. M., I. L. Weissman, et al. (1992). "Isolation of a candidate human hematopoietic stem-cell population." Proc Natl Acad Sci U S A 89(7): 2804-8.

Beckett, T., R. Loi, et al. (2005). "Acute lung injury with endotoxin or NO2 does not enhance development of airway epithelium from bone marrow." Mol Ther 12(4): 680-6.

Berenson, R. J., R. G. Andrews, et al. (1988). "Antigen CD34+ marrow cells engraft lethally irradiated baboons." J Clin Invest 81(3): 951-5.

Bhatia, M., D. Bonnet, et al. (1998). "A newly discovered class of human hematopoietic cells with SCID-repopulating activity." Nat Med 4(9): 1038-45.

Bhatia, M., J. C. Wang, et al. (1997). "Purification of primitive human hematopoietic cells capable of repopulating immune-deficient mice." Proc Natl Acad Sci U S A 94(10): 5320-5.

Bonilla, S., P. Alarcon, et al. (2002). "Haematopoietic progenitor cells from adult bone marrow differentiate into cells that express oligodendroglial antigens in the neonatal mouse brain." Eur J Neurosci 15(3): 575-82.

Bosma, G. C., R. P. Custer, et al. (1983). "A severe combined immunodeficiency mutation in the mouse." Nature 301(5900): 527-30.

Braer F, L. D., Spector I, Vermihlen D, Wisse E. (2001). Endothelial and pit cells. The Liver: Biology and Pathobiology. B. J. Arias I, Chisari F, Fausto N, Schachter D, Shafritz D. Philadelphia PA, Lippincott, Williams & Wilkins: 437-453.

Brittan, M., K. M. Braun, et al. (2005). "Bone marrow cells engraft within the epidermis and proliferate in vivo with no evidence of cell fusion." J Pathol 205(1): 1-13.

Brittan, M., T. Hunt, et al. (2002). "Bone marrow derivation of pericryptal myofibroblasts in the mouse and human small intestine and colon." Gut 50(6): 752-7.

Bull, L. B. and A. T. Dick (1959). "The chronic pathological effects on the liver of the rat of the pyrrolizidine alkaloids heliotrine, lasiocarpine, and their N-oxides." J Pathol Bacteriol 78: 483-502.

Calvi, L. M., G. B. Adams, et al. (2003). "Osteoblastic cells regulate the haematopoietic stem cell niche." Nature 425(6960): 841-6.

Camargo, F. D., M. Finegold, et al. (2004). "Hematopoietic myelomonocytic cells are the major source of hepatocyte fusion partners." J Clin Invest 113(9): 1266-70.

Camargo, F. D., R. Green, et al. (2003). "Single hematopoietic stem cells generate skeletal muscle through myeloid intermediates." Nat Med 9(12): 1520-7.

Campagnoli, C., I. A. Roberts, et al. (2001). "Identification of mesenchymal stem/progenitor cells in human first-trimester fetal blood, liver, and bone marrow." Blood 98(8): 2396-402.

Chalmers, A. D. and J. M. Slack (2000). "The Xenopus tadpole gut: fate maps and morphogenetic movements." Development 127(2): 381-92.

Chang, J. C., R. Summer, et al. (2005). "Evidence that bone marrow cells do not contribute to the alveolar epithelium." Am J Respir Cell Mol Biol 33(4): 335-42.

Chen, J., K. Singh, et al. (1993). "Developmental expression of osteopontin (OPN) mRNA in rat tissues: evidence for a role for OPN in bone formation and resorption." Matrix 13(2): 113-23.

Cheng, J., S. Baumhueter, et al. (1996). "Hematopoietic defects in mice lacking the sialomucin CD34." Blood 87(2): 479-90.

Choi, K., M. Kennedy, et al. (1998). "A common precursor for hematopoietic and endothelial cells." Development 125(4): 725-32.

Civin, C. I., L. C. Strauss, et al. (1984). "Antigenic analysis of hematopoiesis. III. A hematopoietic progenitor cell surface antigen defined by a monoclonal antibody raised against KG-1a cells." J Immunol 133(1): 157-65.

Civin, C. I., T. Trischmann, et al. (1996). "Highly purified CD34-positive cells reconstitute hematopoiesis." J Clin Oncol 14(8): 2224-33.

Colter, D. C., R. Class, et al. (2000). "Rapid expansion of recycling stem cells in cultures of plastic-adherent cells from human bone marrow." Proc Natl Acad Sci U S A 97(7): 3213-8.

Corti, S., F. Locatelli, et al. (2002). "Neuroectodermal and microglial differentiation of bone marrow cells in the mouse spinal cord and sensory ganglia." J Neurosci Res 70(6): 721-33.

Danet, G. H., J. L. Luongo, et al. (2002). "C1qRp defines a new human stem cell population with hematopoietic and hepatic potential." Proc Natl Acad Sci U S A 99(16): 10441-5.

de Bruijn, M. F., X. Ma, et al. (2002). "Hematopoietic stem cells localize to the endothelial cell layer in the midgestation mouse aorta." Immunity 16(5): 673-83.

Deutsch, G., J. Jung, et al. (2001). "A bipotential precursor population for pancreas and liver within the embryonic endoderm." Development 128(6): 871-81.

Dexter, T. M., T. D. Allen, et al. (1977). "Conditions controlling the proliferation of haemopoietic stem cells in vitro." J Cell Physiol 91(3): 335-44.

D'Ippolito, G., S. Diabira, et al. (2004). "Marrow-isolated adult multilineage inducible (MIAMI) cells, a unique population of postnatal young and old human cells with extensive expansion and differentiation potential." J Cell Sci 117(Pt 14): 2971-81.

Du, Y., M. L. Funderburgh, et al. (2005). "Multipotent Stem Cells in Human Corneal Stroma." Stem Cells.

Eaves, C. J., H. J. Sutherland, et al. (1992). "The human hematopoietic stem cell in vitro and in vivo." Blood Cells 18(2): 301-7.

Eguchi, G. and R. Kodama (1993). "Transdifferentiation." Curr Opin Cell Biol 5(6): 1023-8.

Fausto, N. and J. S. Campbell (2003). "The role of hepatocytes and oval cells in liver regeneration and repopulation." Mech Dev 120(1): 117-30.

Fernandes, K. J., I. A. McKenzie, et al. (2004). "A dermal niche for multipotent adult skin-derived precursor cells." Nat Cell Biol 6(11): 1082-93.

Ferrari, G., G. Cusella-De Angelis, et al. (1998). "Muscle regeneration by bone marrow-derived myogenic progenitors." Science 279(5356): 1528-30.

Feuring-Buske, M., B. Gerhard, et al. (2003). "Improved engraftment of human acute myeloid leukemia progenitor cells in beta 2-microglobulin-deficient NOD/SCID mice and in NOD/SCID mice transgenic for human growth factors." Leukemia 17(4): 760-3.

Field, H. A., E. A. Ober, et al. (2003). "Formation of the digestive system in zebrafish. I. Liver morphogenesis." Dev Biol 253(2): 279-90.

Flake, A. W., M. R. Harrison, et al. (1986). "Transplantation of fetal hematopoietic stem cells in utero: the creation of hematopoietic chimeras." Science 233(4765): 776-8.

Friedenstein, A. J., U. F. Deriglasova, et al. (1974). "Precursors for fibroblasts in different populations of hematopoietic cells as detected by the in vitro colony assay method." Exp Hematol 2(2): 83-92.

Friedrich, G. and P. Soriano (1991). "Promoter traps in embryonic stem cells: a genetic screen to identify and mutate developmental genes in mice." Genes Dev 5(9): 1513-23.

Fuchs, E., T. Tumbar, et al. (2004). "Socializing with the neighbors: stem cells and their niche." Cell 116(6): 769-78.

Fujisaki, T., M. G. Berger, et al. (1999). "Rapid differentiation of a rare subset of adult human lin(-)CD34(-)CD38(-) cells stimulated by multiple growth factors in vitro." Blood 94(6): 1926-32.

Goodell, M. A., K. Brose, et al. (1996). "Isolation and functional properties of murine hematopoietic stem cells that are replicating in vivo." J Exp Med 183(4): 1797-806.

Goodell, M. A., M. Rosenzweig, et al. (1997). "Dye efflux studies suggest that hematopoietic stem cells expressing low or undetectable levels of CD34 antigen exist in multiple species." Nat Med 3(12): 1337-45.

Gordon, G. J., G. M. Butz, et al. (2002). "Isolation, short-term culture, and transplantation of small hepatocyte-like progenitor cells from retrorsine-exposed rats." Transplantation 73(8): 1236-43.

Gordon, G. J., W. B. Coleman, et al. (2000). "Liver regeneration in rats with retrorsine-induced hepatocellular injury proceeds through a novel cellular response." Am J Pathol 156(2): 607-19.

Gouysse, G., A. Couvelard, et al. (2002). "Relationship between vascular development and vascular differentiation during liver organogenesis in humans." J Hepatol 37(6): 730-40.

Greiner, D. L., L. D. Shultz, et al. (1995). "Improved engraftment of human spleen cells in NOD/LtSz-scid/scid mice as compared with C.B-17-scid/scid mice." Am J Pathol 146(4): 888-902.

Grisham, J. W. (1962). "A morphologic study of deoxyribonucleic acid synthesis and cell proliferation in regenerating rat liver; autoradiography with thymidine-H3." Cancer Res 22: 842-9.

Grompe, M. (2001). "Mouse liver goes human: a new tool in experimental hepatology." Hepatology 33(4): 1005-6.

Guenechea, G., O. I. Gan, et al. (2001). "Distinct classes of human stem cells that differ in proliferative and self-renewal potential." Nat Immunol 2(1): 75-82.

Gussoni, E., Y. Soneoka, et al. (1999). "Dystrophin expression in the mdx mouse restored by stem cell transplantation." Nature 401(6751): 390-4.

Habeebu, S. S., J. Liu, et al. (2000). "Metallothionein-null mice are more sensitive than wild-type mice to liver injury induced by repeated exposure to cadmium." Toxicol Sci 55(1): 223-32.

Hao, Q. L., A. J. Shah, et al. (1995). "A functional comparison of CD34 + CD38- cells in cord blood and bone marrow." Blood 86(10): 3745-53.

Harris, R. G., E. L. Herzog, et al. (2004). "Lack of a fusion requirement for development of bone marrow-derived epithelia." Science 305(5680): 90-3.

Hayes, M. A., E. Roberts, et al. (1985). "Initiation and selection of resistant hepatocyte nodules in rats given the pyrrolizidine alkaloids lasiocarpine and senecionine." Cancer Res 45(8): 3726-34.

Hess, D. A., T. E. Meyerrose, et al. (2004). "Functional characterization of highly purified human hematopoietic repopulating cells isolated according to aldehyde dehydrogenase activity." Blood 104(6): 1648-55.

Hirschmann-Jax, C., A. E. Foster, et al. (2004). "A distinct "side population" of cells with high drug efflux capacity in human tumor cells." Proc Natl Acad Sci U S A 101(39): 14228-33.

Ianus, A., G. G. Holz, et al. (2003). "In vivo derivation of glucose-competent pancreatic endocrine cells from bone marrow without evidence of cell fusion." J Clin Invest 111(6): 843-50.

Jackson, K. A., S. M. Majka, et al. (2001). "Regeneration of ischemic cardiac muscle and vascular endothelium by adult stem cells." J Clin Invest 107(11): 1395-402.

Jago, M. V. (1969). "The development of the hepatic megalocytosis of chronic pyrrolizidine alkaloid poisoning." Am J Pathol 56(3): 405-21.

Jang, Y. Y., M. I. Collector, et al. (2004). "Hematopoietic stem cells convert into liver cells within days without fusion." Nat Cell Biol 6(6): 532-9.

Jiang, Y., D. Henderson, et al. (2003). "Neuroectodermal differentiation from mouse multipotent adult progenitor cells." Proc Natl Acad Sci U S A 100 Suppl 1: 11854-60.

Jiang, Y., B. N. Jahagirdar, et al. (2002). "Pluripotency of mesenchymal stem cells derived from adult marrow." Nature 418(6893): 41-49.

Jung, J., M. Zheng, et al. (1999). "Initiation of mammalian liver development from endoderm by fibroblast growth factors." Science 284(5422): 1998-2003.

Kagi, J. H. and Y. Kojima (1987). "Chemistry and biochemistry of metallothionein." Experientia Suppl 52: 25-61.

Kogler, G., S. Sensken, et al. (2004). "A new human somatic stem cell from placental cord blood with intrinsic pluripotent differentiation potential." J Exp Med 200(2): 123-35.

Kollet, O., A. Peled, et al. (2000). "beta2 microglobulin-deficient (B2m(null)) NOD/SCID mice are excellent recipients for studying human stem cell function." Blood 95(10): 3102-5.

Kollet, O., S. Shivtiel, et al. (2003). "HGF, SDF-1, and MMP-9 are involved in stress-induced human CD34+ stem cell recruitment to the liver." J Clin Invest 112(2): 160-9.

Kopen, G. C., D. J. Prockop, et al. (1999). "Marrow stromal cells migrate throughout forebrain and cerebellum, and they differentiate into astrocytes after injection into neonatal mouse brains." Proc Natl Acad Sci U S A 96(19): 10711-6.

Kotton, D. N., A. J. Fabian, et al. (2005). "Failure of bone marrow to reconstitute lung epithelium." Am J Respir Cell Mol Biol 33(4): 328-34.

Kotton, D. N., B. Y. Ma, et al. (2001). "Bone marrow-derived cells as progenitors of lung alveolar epithelium." Development 128(24): 5181-8.

Krause, D. S. (2005). "Engraftment of bone marrow-derived epithelial cells." Ann N Y Acad Sci 1044: 117-24.

Krause, D. S., T. Ito, et al. (1994). "Characterization of murine CD34, a marker for hematopoietic progenitor and stem cells." Blood 84(3): 691-701.

Krause, D. S., N. D. Theise, et al. (2001). "Multi-organ, multi-lineage engraftment by a single bone marrow-derived stem cell." Cell 105(3): 369-77.

Kucia, M., J. Ratajczak, et al. (2005). "Bone marrow as a source of circulating CXCR4(+) tissue-committed stem cells." Biol Cell 97(2): 133-46.

LaBarge, M. A. and H. M. Blau (2002). "Biological progression from adult bone marrow to mononucleate muscle stem cell to multinucleate muscle fiber in response to injury." Cell 111(4): 589-601.

Laconi, E., R. Oren, et al. (1998). "Long-term, near-total liver replacement by transplantation of isolated hepatocytes in rats treated with retrorsine." Am J Pathol 153(1): 319-29.

Laconi, S., S. Pillai, et al. (2001). "Massive liver replacement by transplanted hepatocytes in the absence of exogenous growth stimuli in rats treated with retrorsine." Am J Pathol 158(2): 771-7.

Lagasse, E., H. Connors, et al. (2000). "Purified hematopoietic stem cells can differentiate into hepatocytes in vivo." Nat Med 6(11): 1229-34.

Lamps, L. W. and A. L. Folpe (2003). "The diagnostic value of hepatocyte paraffin antibody 1 in differentiating hepatocellular neoplasms from nonhepatic tumors: a review." Adv Anat Pathol 10(1): 39-43.

Lapidot, T. and I. Petit (2002). "Current understanding of stem cell mobilization: the roles of chemokines, proteolytic enzymes, adhesion molecules, cytokines, and stromal cells." Exp Hematol 30(9): 973-81.

Larochelle, A., J. Vormoor, et al. (1996). "Identification of primitive human hematopoietic cells capable of repopulating NOD/SCID mouse bone marrow: implications for gene therapy." Nat Med 2(12): 1329-37.

Link, H., L. Arseniev, et al. (1996). "Transplantation of allogeneic CD34+ blood cells." Blood 87(11): 4903-9.

Liu, Y., J. Liu, et al. (2000). "Metallothionein-I/II null mice are sensitive to chronic oral cadmium-induced nephrotoxicity." Toxicol Sci 57(1): 167-76.

Lowry, P. A., L. D. Shultz, et al. (1996). "Improved engraftment of human cord blood stem cells in NOD/LtSz-scid/scid mice after irradiation or multiple-day injections into unirradiated recipients." Biol Blood Marrow Transplant 2(1): 15-23.

Majka, S., M. A. Beutz, et al. (2005). "Identification of Novel Resident Pulmonary Stem Cells: Form & Function of the Lung Side Population." Stem Cells.

Makin, A. and R. Williams (1994). "The current management of paracetamol overdosage." Br J Clin Pract 48(3): 144-8.

Mardiney, M., 3rd and H. L. Malech (1996). "Enhanced engraftment of hematopoietic progenitor cells in mice treated with granulocyte colony-stimulating factor before low-dose irradiation: implications for gene therapy." Blood 87(10): 4049-56.

Masters, B. A., E. J. Kelly, et al. (1994). "Targeted disruption of metallothionein I and II genes increases sensitivity to cadmium." Proc Natl Acad Sci U S A 91(2): 584-8.

Menthena, A., N. Deb, et al. (2004). "Bone marrow progenitors are not the source of expanding oval cells in injured liver." Stem Cells 22(6): 1049-61.

Moore, M. A. and D. Metcalf (1970). "Ontogeny of the haemopoietic system: yolk sac origin of in vivo and in vitro colony forming cells in the developing mouse embryo." Br J Haematol 18(3): 279-96.

Morel, F., S. J. Szilvassy, et al. (1996). "Primitive hematopoietic cells in murine bone marrow express the CD34 antigen." Blood 88(10): 3774-84.

Mosier, D. E., R. J. Gulizia, et al. (1988). "Transfer of a functional human immune system to mice with severe combined immunodeficiency." Nature 335(6187): 256-9.

Nagasawa, T., S. Hirota, et al. (1996). "Defects of B-cell lymphopoiesis and bone-marrow myelopoiesis in mice lacking the CXC chemokine PBSF/SDF-1." Nature 382(6592): 635-8.

Nakamura, Y., K. Ando, et al. (1999). "Ex vivo generation of CD34(+) cells from CD34(-) hematopoietic cells." Blood 94(12): 4053-9.

Okabe, M., M. Ikawa, et al. (1997). "'Green mice' as a source of ubiquitous green cells." FEBS Lett 407(3): 313-9.

Osawa, M., K. Hanada, et al. (1996). "Long-term lymphohematopoietic reconstitution by a single CD34-low/negative hematopoietic stem cell." Science 273(5272): 242-5.

Ottersbach, K. and E. Dzierzak (2005). "The murine placenta contains hematopoietic stem cells within the vascular labyrinth region." Dev Cell 8(3): 377-87.

Overturf, K., M. al-Dhalimy, et al. (1997). "Serial transplantation reveals the stem-cell-like regenerative potential of adult mouse hepatocytes." Am J Pathol 151(5): 1273-80.

Oz, H. S., C. J. McClain, et al. (2004). "Diverse antioxidants protect against acetaminophen hepatotoxicity." J Biochem Mol Toxicol 18(6): 361-8.

Patrawala, L., T. Calhoun, et al. (2005). "Side population is enriched in tumorigenic, stem-like cancer cells, whereas ABCG2+ and ABCG2- cancer cells are similarly tumorigenic." Cancer Res 65(14): 6207-19.

Pearce, D. J., C. M. Ridler, et al. (2004). "Multiparameter analysis of murine bone marrow side population cells." Blood 103(7): 2541-6.

Pearce, D. J., D. Taussig, et al. (2005). "Characterization of cells with a high aldehyde dehydrogenase activity from cord blood and acute myeloid leukemia samples." Stem Cells 23(6): 752-60.

Petersen, B. E., W. C. Bowen, et al. (1999). "Bone marrow as a potential source of hepatic oval cells." Science 284(5417): 1168-70.

Petersen, J., M. Dandri, et al. (1998). "Liver repopulation with xenogenic hepatocytes in B and T cell-deficient mice leads to chronic hepadnavirus infection and clonal growth of hepatocellular carcinoma." Proc Natl Acad Sci U S A 95(1): 310-5.

Pittenger, M. F., A. M. Mackay, et al. (1999). "Multilineage potential of adult human mesenchymal stem cells." Science 284(5411): 143-7.

Pittenger, M. F., J. D. Mosca, et al. (2000). "Human mesenchymal stem cells: progenitor cells for cartilage, bone, fat and stroma." Curr Top Microbiol Immunol 251: 3-11.

Ploemacher, R. E., J. P. van der Sluijs, et al. (1991). "Use of limiting-dilution type long-term marrow cultures in frequency analysis of marrow-repopulating and spleen colony-forming hematopoietic stem cells in the mouse." Blood 78(10): 2527-33.

Puri, M. C. and A. Bernstein (2003). "Requirement for the TIE family of receptor tyrosine kinases in adult but not fetal hematopoiesis." Proc Natl Acad Sci U S A 100(22): 12753-8.

Rafii, S., D. Lyden, et al. (2002). "Vascular and haematopoietic stem cells: novel targets for anti-angiogenesis therapy?" Nat Rev Cancer 2(11): 826-35.

Ratajczak, M. Z., M. Kucia, et al. (2004). "Stem cell plasticity revisited: CXCR4-positive cells expressing mRNA for early muscle, liver and neural cells 'hide out' in the bone marrow." Leukemia 18(1): 29-40.

Ratajczak, M. Z., M. Majka, et al. (2003). "Expression of functional CXCR4 by muscle satellite cells and secretion of SDF-1 by muscle-derived fibroblasts is associated with the presence of both muscle progenitors in bone marrow and hematopoietic stem/progenitor cells in muscles." Stem Cells 21(3): 363-71.

Sandgren, E. P., R. D. Palmiter, et al. (1991). "Complete hepatic regeneration after somatic deletion of an albumin-plasminogen activator transgene." Cell 66(2): 245-56.

Sato, T., J. H. Laver, et al. (1999). "Reversible expression of CD34 by murine hematopoietic stem cells." Blood 94(8): 2548-54.

Scarpelli, D. G. and M. S. Rao (1981). "Differentiation of regenerating pancreatic cells into hepatocyte-like cells." Proc Natl Acad Sci U S A 78(4): 2577-81.

Schoental, R. and P. N. Magee (1959). "Further observations on the subacute and chronic liver changes in rats after a single dose of various pyrrolizidine (Senecio) alkaloids." J Pathol Bacteriol 78: 471-82.

Schofield, R. (1978). "The relationship between the spleen colony-forming cell and the haemopoietic stem cell." Blood Cells 4(1-2): 7-25.

Schwartz, R. E., M. Reyes, et al. (2002). "Multipotent adult progenitor cells from bone marrow differentiate into functional hepatocyte-like cells." J Clin Invest 109(10): 1291-302.

Seglen, P. O. (1973). "Preparation of rat liver cells. 3. Enzymatic requirements for tissue dispersion." Exp Cell Res 82(2): 391-8.

Sell, S., H. L. Leffert, et al. (1981). "Rapid development of large numbers of alpha-fetoprotein-containing "oval" cells in the liver of rats fed N-2-fluorenylacetamide in a choline-devoid diet." Gann 72(4): 479-87.

Shafritz, D. A. and M. D. Dabeva (2002). "Liver stem cells and model systems for liver repopulation." J Hepatol 36(4): 552-64.

Shi, D., H. Reinecke, et al. (2004). "Myogenic fusion of human bone marrow stromal cells, but not hematopoietic cells." Blood 104(1): 290-4.

Shultz, L. D., P. A. Schweitzer, et al. (1995). "Multiple defects in innate and adaptive immunologic function in NOD/LtSz-scid mice." J Immunol 154(1): 180-91.

Simpson, G. E. and E. S. Finckh (1963). "The Pattern of Regeneration of Rat Liver after Repeated Partial Hepatectomies." J Pathol Bacteriol 86: 361-70.

Smith, L. G., I. L. Weissman, et al. (1991). "Clonal analysis of hematopoietic stem-cell differentiation in vivo." Proc Natl Acad Sci U S A 88(7): 2788-92.

Soriano, P. (1999). "Generalized lacZ expression with the ROSA26 Cre reporter strain." Nat Genet 21(1): 70-1.

Sosa-Pineda, B., J. T. Wigle, et al. (2000). "Hepatocyte migration during liver development requires Prox1." Nat Genet 25(3): 254-5.

Spees, J. L., S. D. Olson, et al. (2003). "Differentiation, cell fusion, and nuclear fusion during ex vivo repair of epithelium by human adult stem cells from bone marrow stroma." Proc Natl Acad Sci U S A 100(5): 2397-402.

Spencer, H., D. Rampling, et al. (2005). "Transbronchial biopsies provide longitudinal evidence for epithelial chimerism in children following sex mismatched lung transplantation." Thorax 60(1): 60-2.

Spradling, A., D. Drummond-Barbosa, et al. (2001). "Stem cells find their niche." Nature 414(6859): 98-104.

Srour, E. F., E. D. Zanjani, et al. (1992). "Sustained human hematopoiesis in sheep transplanted in utero during early gestation with fractionated adult human bone marrow cells." Blood 79(6): 1404-12.

Srour, E. F., E. D. Zanjani, et al. (1993). "Persistence of human multilineage, self-renewing lymphohematopoietic stem cells in chimeric sheep." Blood 82(11): 3333-42.

Stadtfeld, M. and T. Graf (2005). "Assessing the role of hematopoietic plasticity for endothelial and hepatocyte development by non-invasive lineage tracing." Development 132(1): 203-13.

Sutherland, H. J., C. J. Eaves, et al. (1989). "Characterization and partial purification of human marrow cells capable of initiating long-term hematopoiesis in vitro." Blood 74(5): 1563-70.

Tavian, M., L. Coulombel, et al. (1996). "Aorta-associated CD34+ hematopoietic cells in the early human embryo." Blood 87(1): 67-72.

Tavian, M., M. F. Hallais, et al. (1999). "Emergence of intraembryonic hematopoietic precursors in the pre-liver human embryo." Development 126(4): 793-803.

Terada, N., T. Hamazaki, et al. (2002). "Bone marrow cells adopt the phenotype of other cells by spontaneous cell fusion." Nature 416(6880): 542-5.

Theise, N. D., O. Henegariu, et al. (2002). "Radiation pneumonitis in mice: a severe injury model for pneumocyte engraftment from bone marrow." Exp Hematol 30(11): 1333-8.

Theise, N. D., R. Saxena, et al. (1999). "The canals of Hering and hepatic stem cells in humans." Hepatology 30(6): 1425-33.

Tokoyoda, K., T. Egawa, et al. (2004). "Cellular niches controlling B lymphocyte behavior within bone marrow during development." Immunity 20(6): 707-18.

Tosh, D., C. N. Shen, et al. (2002). "Conversion of pancreatic cells to hepatocytes." Biochem Soc Trans 30(2): 51-5.

Uchida, N., T. Fujisaki, et al. (2001). "Transplantable hematopoietic stem cells in human fetal liver have a CD34(+) side population (SP)phenotype." J Clin Invest 108(7): 1071-7.

Uchida, N. and I. L. Weissman (1992). "Searching for hematopoietic stem cells: evidence that Thy-1.1lo Lin- Sca-1+ cells are the only stem cells in C57BL/Ka-Thy-1.1 bone marrow." J Exp Med 175(1): 175-84.

Vassilopoulos, G., P. R. Wang, et al. (2003). "Transplanted bone marrow regenerates liver by cell fusion." Nature 422(6934): 901-4.

Wang, X., H. Willenbring, et al. (2003). "Cell fusion is the principal source of bone-marrow-derived hepatocytes." Nature 422(6934): 897-901.

Weglarz, T. C., J. L. Degen, et al. (2000). "Hepatocyte transplantation into diseased mouse liver. Kinetics of parenchymal repopulation and identification of the proliferative capacity of tetraploid and octaploid hepatocytes." Am J Pathol 157(6): 1963-74.

Weimann, J. M., C. B. Johansson, et al. (2003). "Stable reprogrammed heterokaryons form spontaneously in Purkinje neurons after bone marrow transplant." Nat Cell Biol 5(11): 959-66.

Willenbring, H., A. S. Bailey, et al. (2004). "Myelomonocytic cells are sufficient for therapeutic cell fusion in liver." Nat Med 10(7): 744-8.

Wulf, G. G., R. Y. Wang, et al. (2001). "A leukemic stem cell with intrinsic drug efflux capacity in acute myeloid leukemia." Blood 98(4): 1166-73.

Yang, L., S. Li, et al. (2002). "In vitro trans-differentiation of adult hepatic stem cells into pancreatic endocrine hormone-producing cells." Proc Natl Acad Sci U S A 99(12): 8078-83.

Yano, S., Y. Ito, et al. (2005). "Characterization and localization of side population cells in mouse skin." Stem Cells 23(6): 834-41.

Yasuda, H., N. Shima, et al. (1998). "Osteoclast differentiation factor is a ligand for osteoprotegerin/osteoclastogenesis-inhibitory factor and is identical to TRANCE/RANKL." Proc Natl Acad Sci U S A 95(7): 3597-602.

Ying, Q. L., J. Nichols, et al. (2002). "Changing potency by spontaneous fusion." Nature 416(6880): 545-8.

Zanjani, E. D., G. Almeida-Porada, et al. (1998). "Human bone marrow CD34- cells engraft in vivo and undergo multilineage expression that includes giving rise to CD34+ cells." Exp Hematol 26(4): 353-60.

Zanjani, E. D., G. Almeida-Porada, et al. (2003). "Reversible expression of CD34 by adult human bone marrow long-term engrafting hematopoietic stem cells." Exp Hematol 31(5): 406-12.

Zhang, J., C. Niu, et al. (2003). "Identification of the haematopoietic stem cell niche and control of the niche size." Nature 425(6960): 836-41.

Zhao, R. and S. A. Duncan (2005). "Embryonic development of the liver." Hepatology 41(5): 956-67.

Zon, L. I. (1995). "Developmental biology of hematopoiesis." Blood 86(8): 2876-91.